US005354376A

United States Patent [19]

Aidun

[11] Patent Number: 5,354,376

[45] Date of Patent: Oct. 11, 1994

[54] FLOTATION COATING DEVICE FOR TRAVELING WEBS

[75] Inventor: **Cyrus K. Aidun**, Marietta, Ga.

[73] Assignee: **Institute of Paper Science and Technology**, Atlanta, Ga.

[21] Appl. No.: **137,957**

[22] Filed: **Oct. 15, 1993**

Related U.S. Application Data

[63] Continuation-in-part of Ser. No. 881,512, May 12, 1992, which is a continuation-in-part of Ser. No. 849,530, Mar. 11, 1992, abandoned.

[51] **Int. Cl.**[5] **B05C 5/00**

[52] **U.S. Cl.** **118/410**; 118/419; 118/411

[58] **Field of Search** 427/434.3, 434.5, 439, 427/595, 598; 118/411, 410, 412, 419

[56] **References Cited**

U.S. PATENT DOCUMENTS

3,083,685	4/1963	Colgan	118/410
3,113,884	12/1963	Kohler	117/37
3,418,970	12/1968	Phelps et al.	118/410
3,690,917	9/1972	Hershoff et al.	117/34
4,102,299	7/1978	Wallsten	118/50
4,250,211	2/1981	Damrau et al.	427/356
4,369,731	1/1983	Damrau	118/410
4,387,663	6/1983	Alheid	118/413
4,452,833	6/1984	Holt	427/356
4,643,127	2/1987	Wanke	118/413
4,688,516	8/1987	Sommer	118/410
4,834,018	5/1989	Sollinger et al.	118/410
4,836,134	6/1989	Knop	118/413
4,839,201	6/1989	Rantanen et al.	427/355
4,858,553	8/1989	Westergard et al.	118/126
4,873,939	10/1989	Eskelinen	118/410
4,920,913	5/1990	Knop et al.	118/410
4,945,855	8/1990	Eklund et al.	118/407
5,173,120	12/1992	Suzumura et al.	118/410

OTHER PUBLICATIONS

Rudolf Beisswanger and Dr. Ing. Hans-Peter Sollinger, "Coating Paper and Board, Practical Experience with the SDTA and LDTA," from *TAPPI Seminar Notes,* 1986 Blade Coating, pp. 137-142.

E. W. Wight, "Modern Coating Application and Blade Metering Systems," from *TAPPI Seminar Notes,* 1986 Blade Coating, pp. 105-108.

Herbert Sommer, "Applicating Systems for Coating ULWC and MFP Papers," from *TAPPI Proceedings,* 1988 Coating Conference, pp. 131-137.

(List continued on next page.)

Primary Examiner—W. Gary Jones
Assistant Examiner—Brenda Lamb
Attorney, Agent, or Firm—Fitch, Even, Tabin & Flannery

[57] **ABSTRACT**

A coating applicator for application of coating material to the surface of a web or a flexible substrate. The coating device contains a walled application chamber where a flowing stream of the coating liquid first comes into contact with the substrate. The coating liquid enters a channel of the application chamber at the upstream side and wets the substrate as it flows in the same direction as the substrate. A doctor element is positioned at the downstream side of the channel where the excess coating in the channel follows the contour of the boundary formed by the doctor element and leaves the channel. One of the applicator walls is designed to be a floating or moving wall or belt. The floating applicator wall and geometry of the streamlined boundaries of the coating device eliminates the formation of recirculating eddies or vortices. The elimination of vortices eliminates flow instability due to centrifugal forces and removes harmful pressure fluctuations which could result in coatweight nonuniformities.

18 Claims, 44 Drawing Sheets

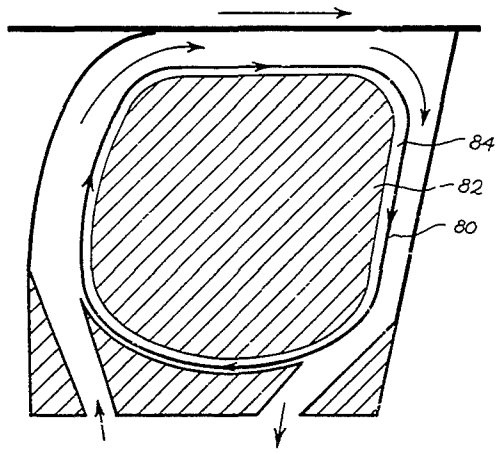

OTHER PUBLICATIONS

F. R. Pranckh and L. E. Scriven, "Elastohydrodynamics of Blade Coating," *AIChE Journal,* vol. 36, No. 4, pp. 587–597, Apr. 1990, (best copy).

N. G. Triantafillopoulos and C. K. Aidun, "Relationship between flow instability in short-dwell ponds and cross directional coat weight nonuniformities,"reprinted from *Tappi Journal,* vol. 73, No. 6, pp. 127–136, Jun. 1990.

Cyrus K. Aidun, "Principles of Hydrodynamic Instability: Application on Coating Systems; Part 1. Background," reprinted from *Tappi Journal,* vol. 74, No. 2, pp. 213–219, Feb. 1991.

Cyrus K. Aidun, "Principles of Hydrodynamic Instability: Application on Coating Systems; Part 2. Examples of flow instability," reprinted from *Tappi Journal,* vol. 74, No. 3, pp. 213–220, Mar. 1991.

Cyrus K. Aidun, "Principles of Hydrodynamic Instability: Application on Coating Systems; Part 3. A generalized view of instability and bifurcation," reprinted from *Tappi Journal,* vol. 74, No. 4, pp. 209–213, Apr. 1991.

C. K. Aidun, N. G. Triantafillopoulos and J. D. Benson "Global stability of a lid-driven cavity with throughflow: Flow visualization studies," *Phys. Fluids A* vol. 3, No. 9, American Institute of Physics, pp. 2081–2091, Sep. 1991.

J. D. Benson and C. K. Aidun, "Transition to unsteady nonperiodic state in a through-flow lid-driven cavity", *Phys. Fluids A,* (Brief Communications) vol. 4, No. 10, American Institute of Physics, pp. 2316–2319, Oct. 1992.

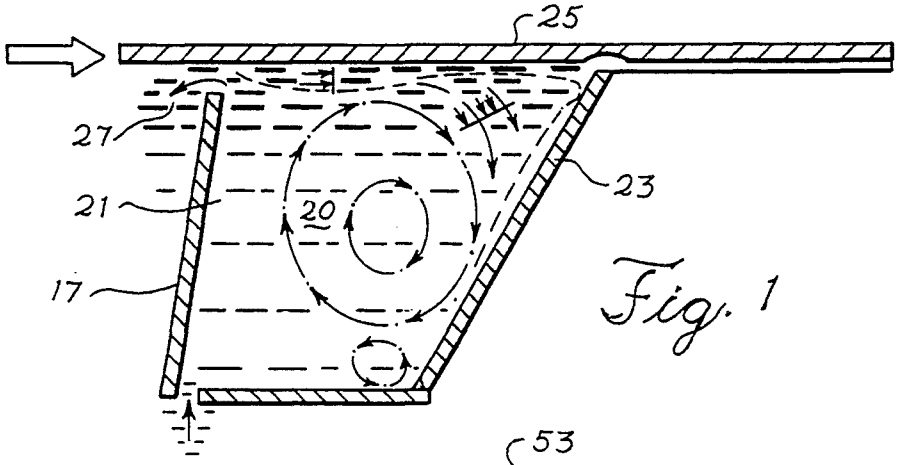

Fig. 1

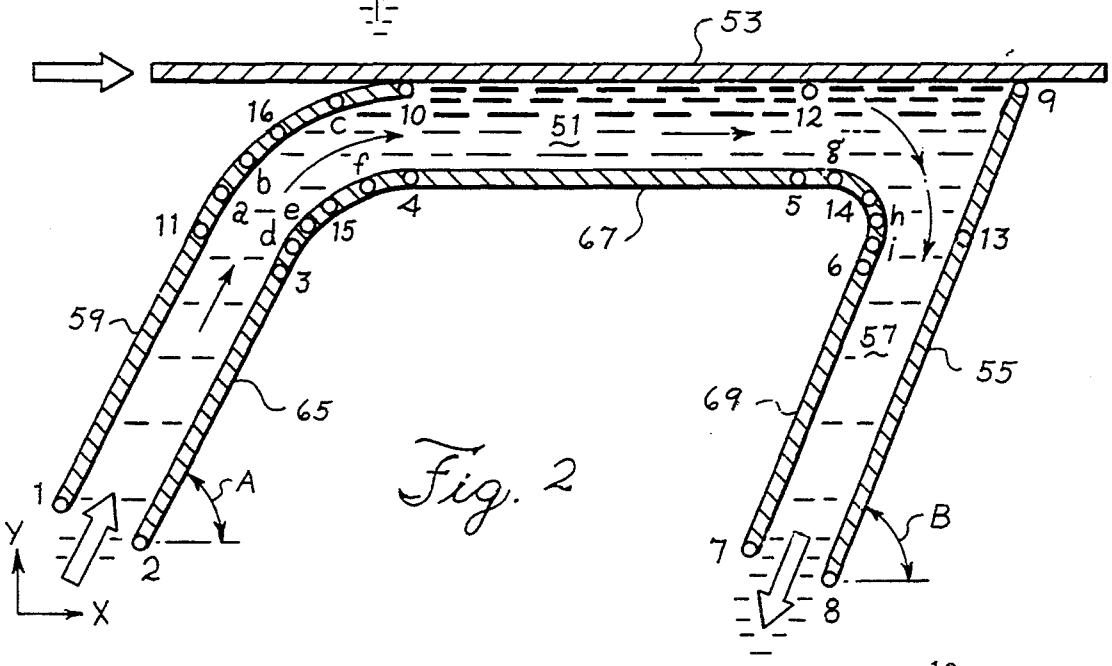

Fig. 2

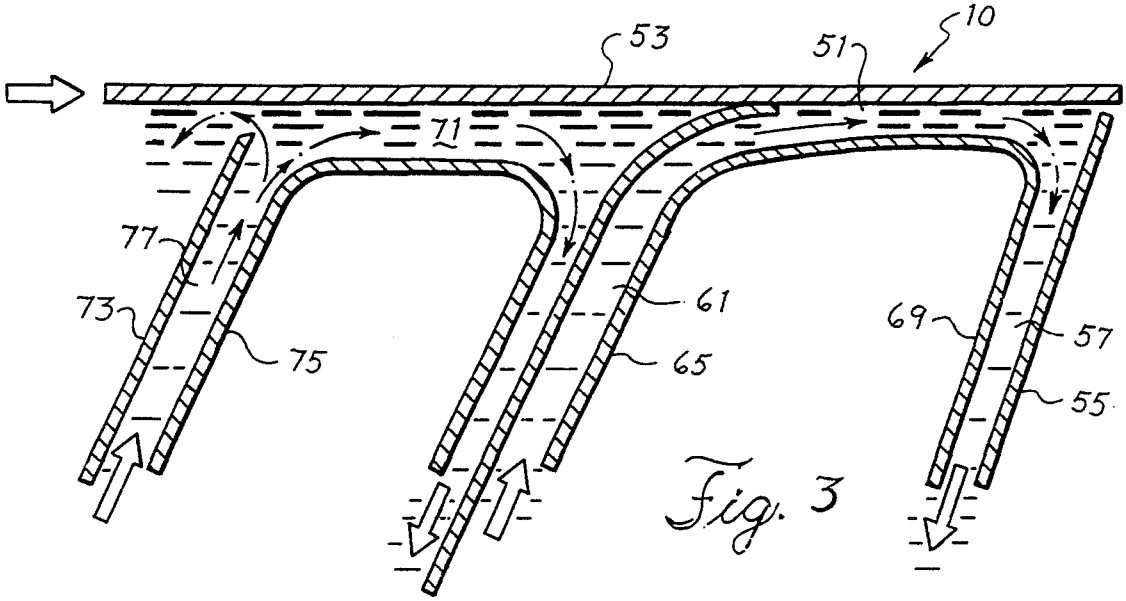

Fig. 3

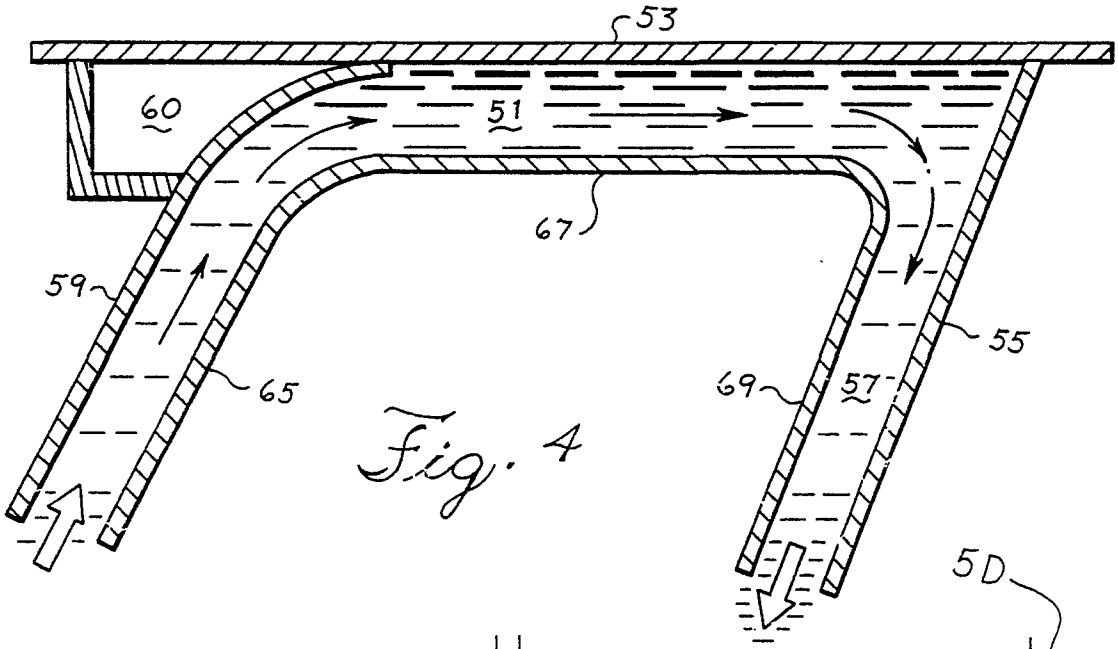

Fig. 4

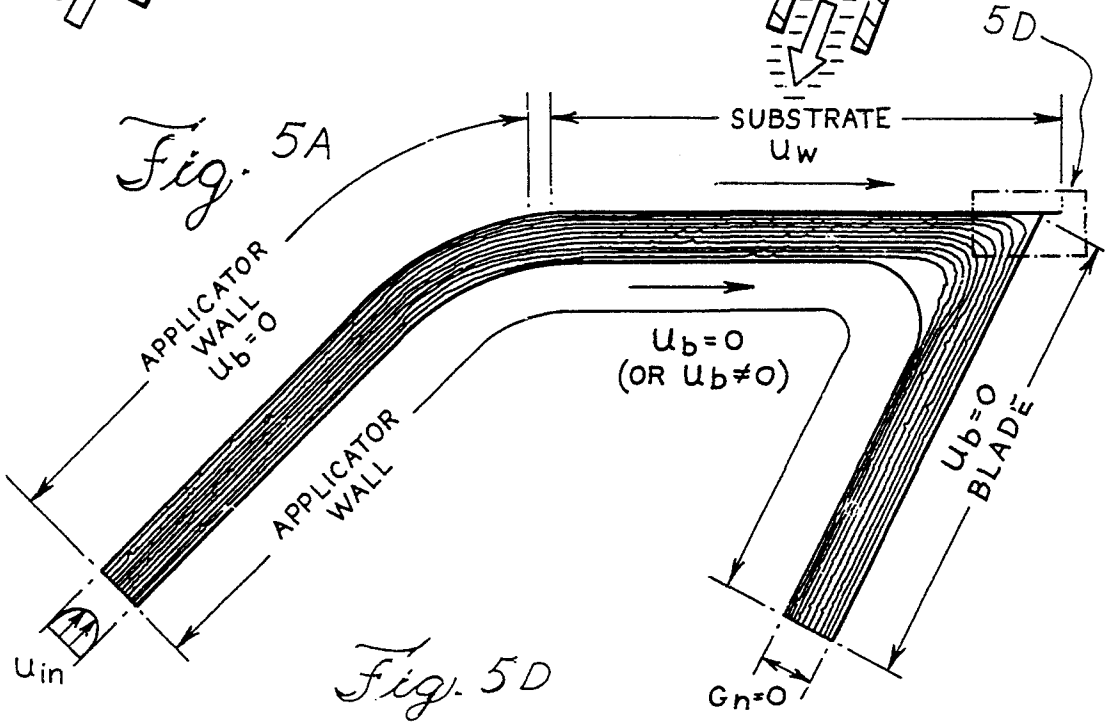

Fig. 5A

Fig. 5D

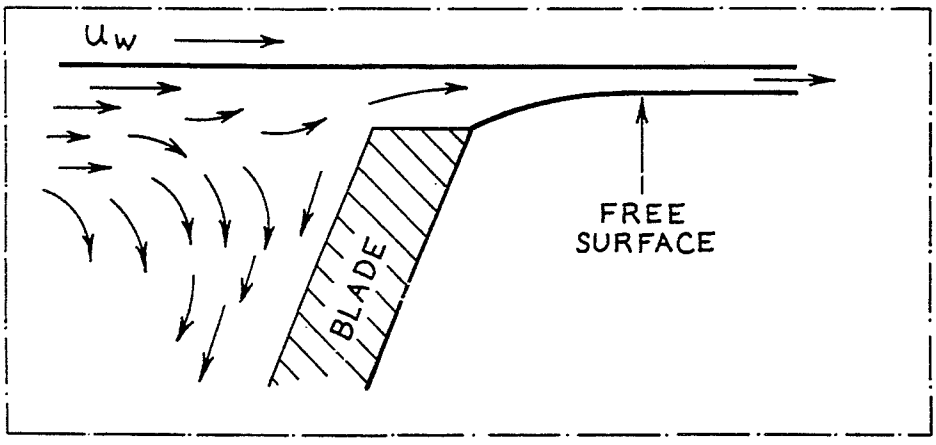

Fig. 5B

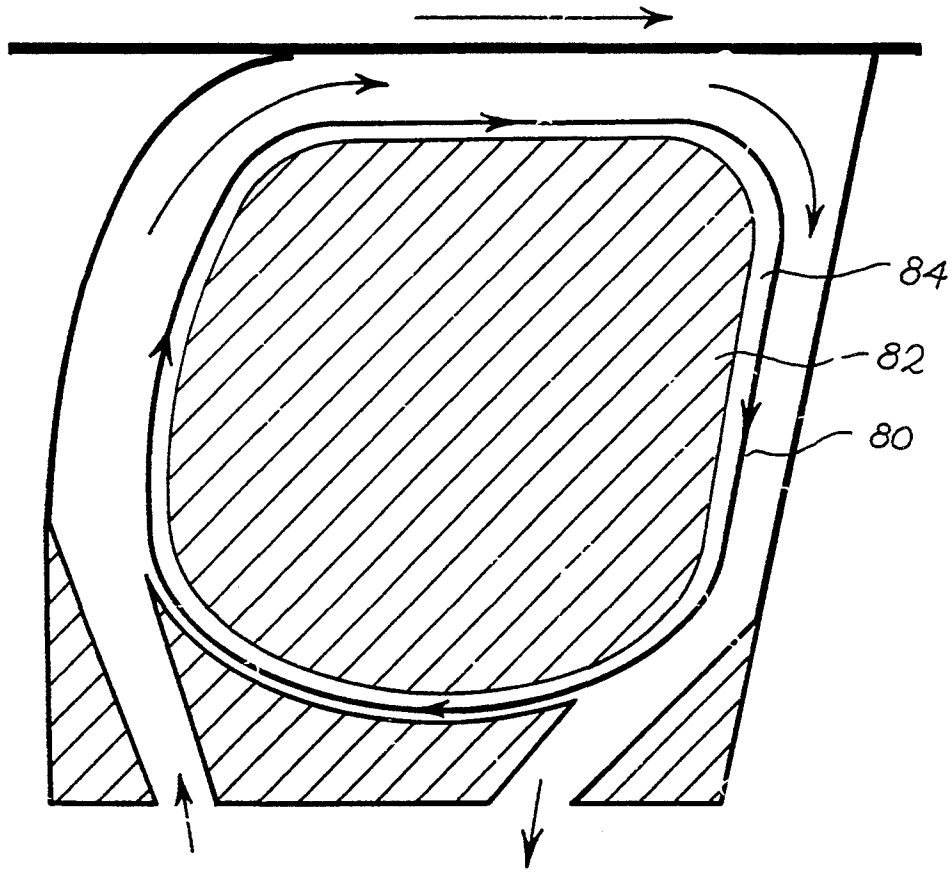

Fig. 5C

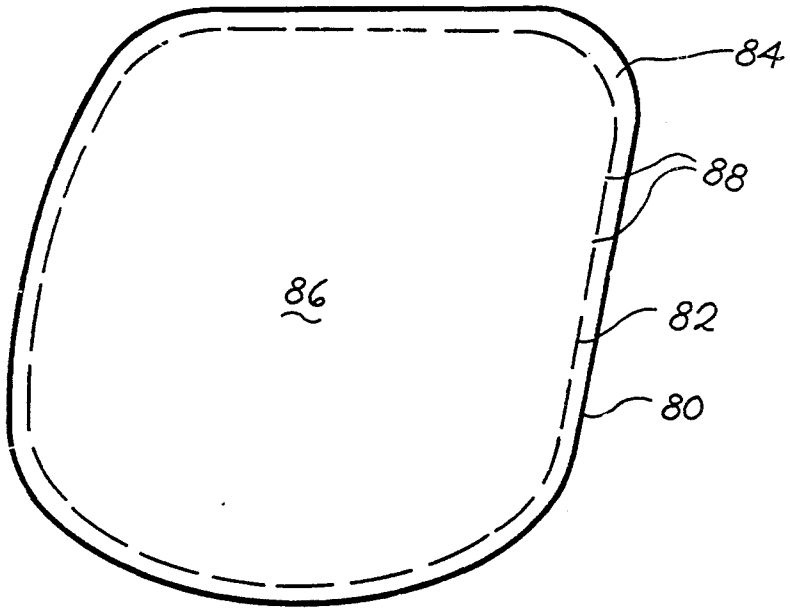

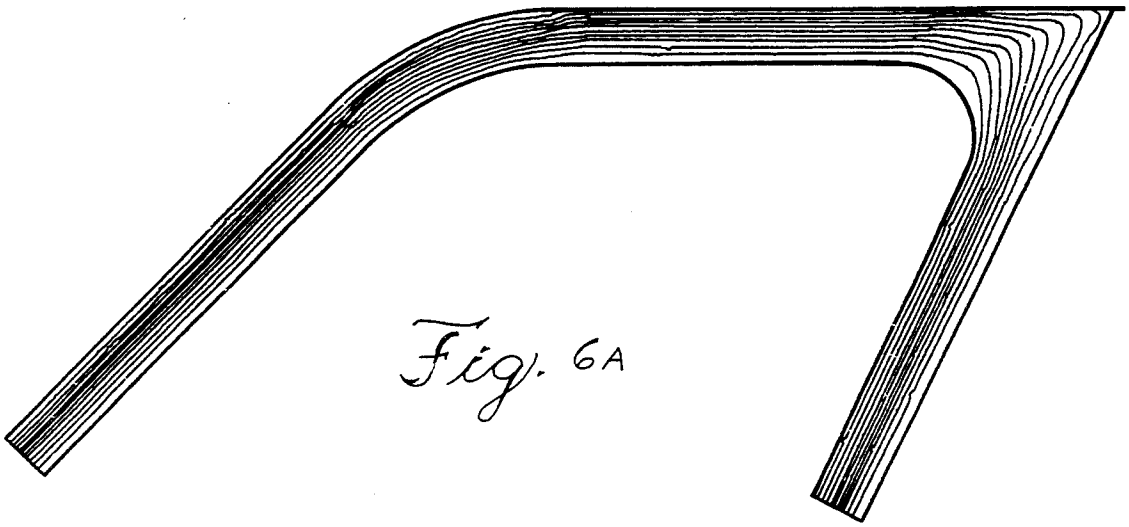

Fig. 6A

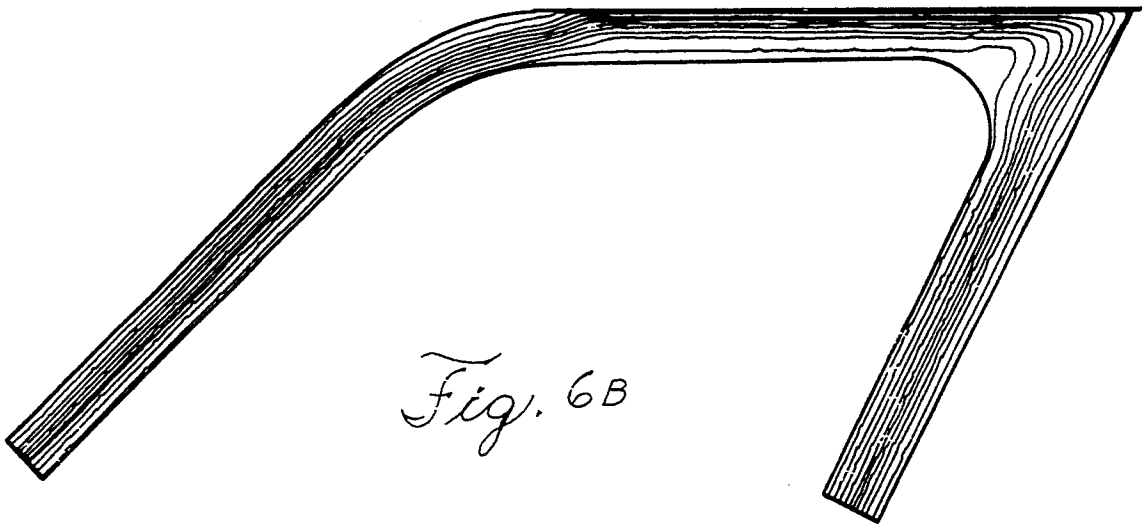

Fig. 6B

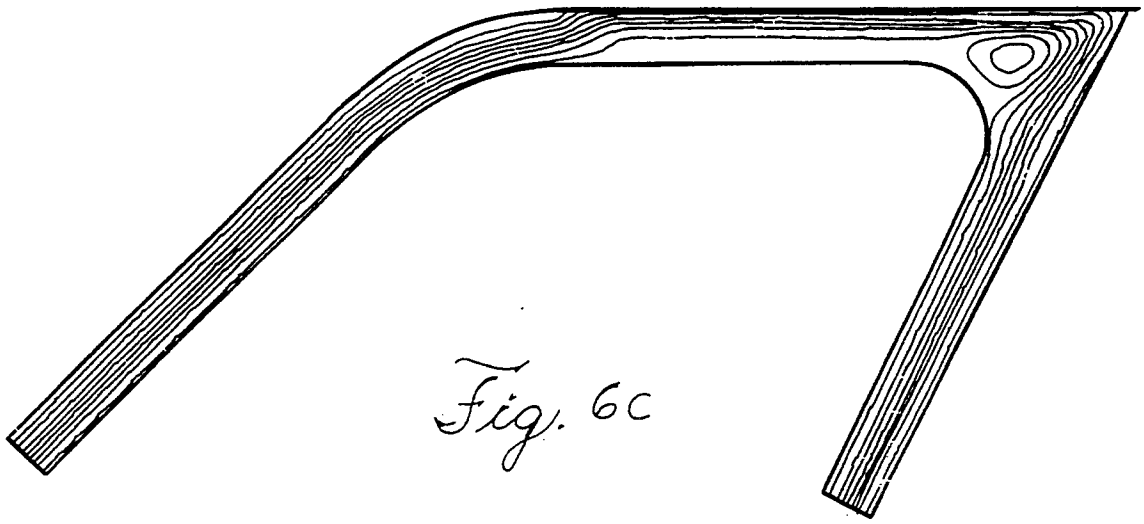

Fig. 6C

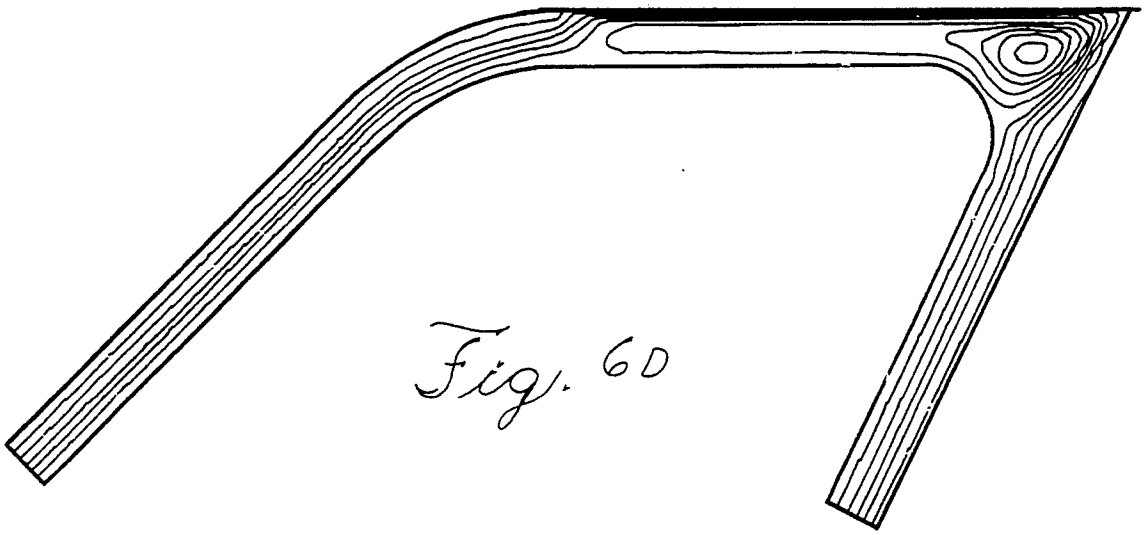

Fig. 6D

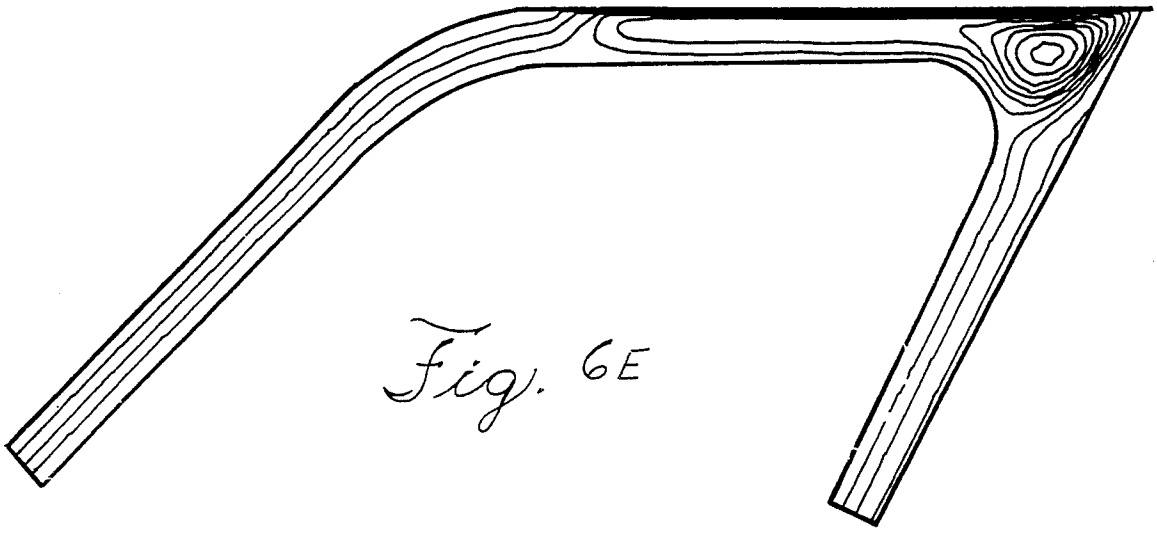

Fig. 6E

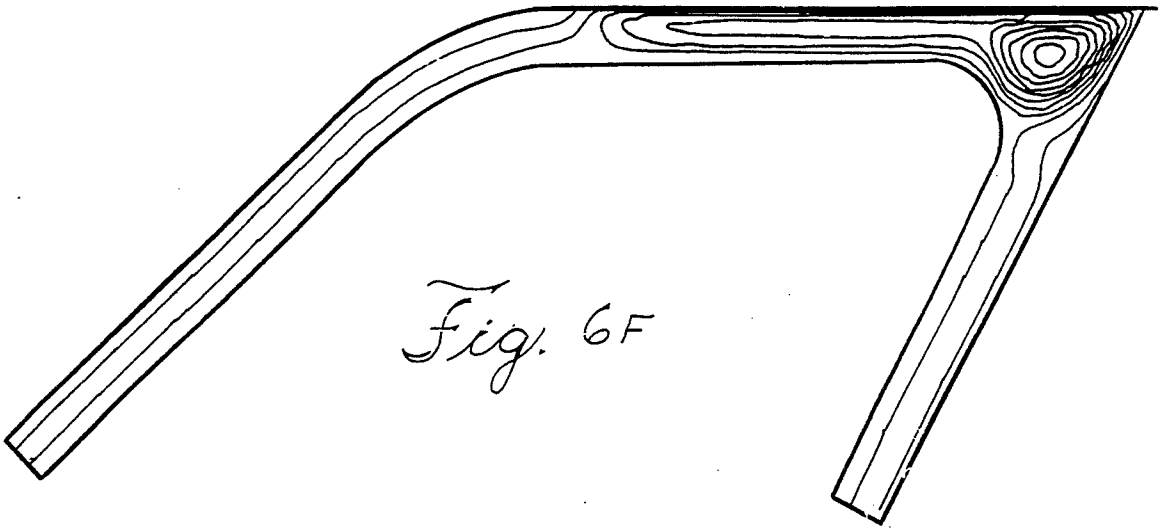

Fig. 6F

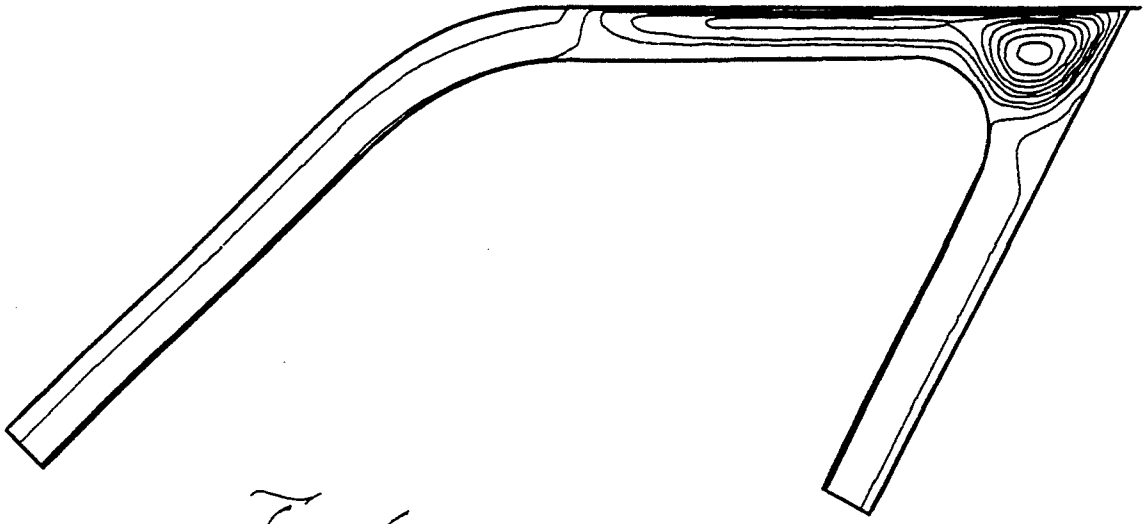

Fig. 6G

Fig. 7A

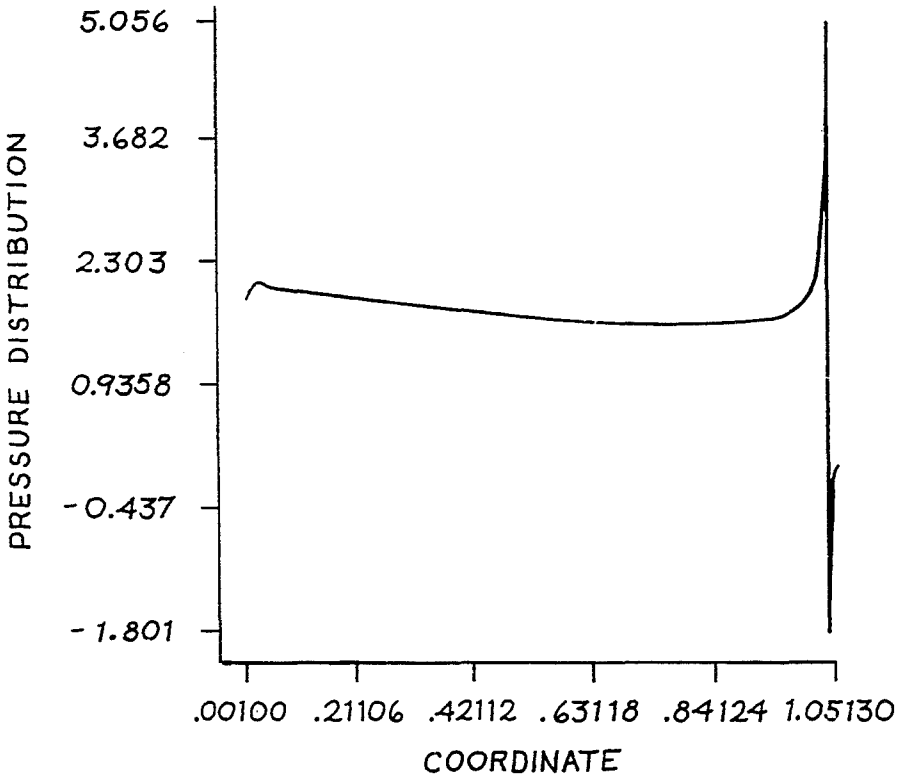
5.056
3.682
2.303
0.9358
-0.437
-1.801
PRESSURE DISTRIBUTION
.00100
.21106
.42112
.63118
.84124
1.05130
COORDINATE

Fig. 7B

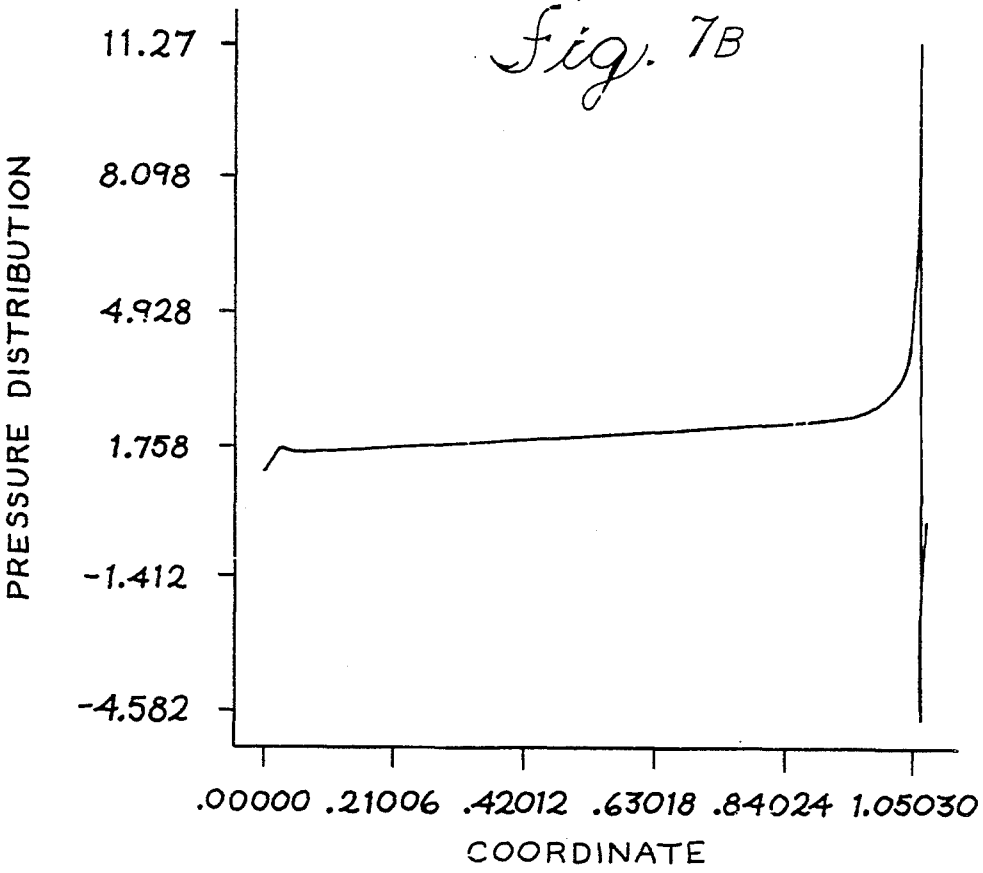
11.27
8.098
4.928
1.758
-1.412
-4.582
PRESSURE DISTRIBUTION
.00000 .21006 .42012 .63018 .84024 1.05030
COORDINATE

Fig. 7C

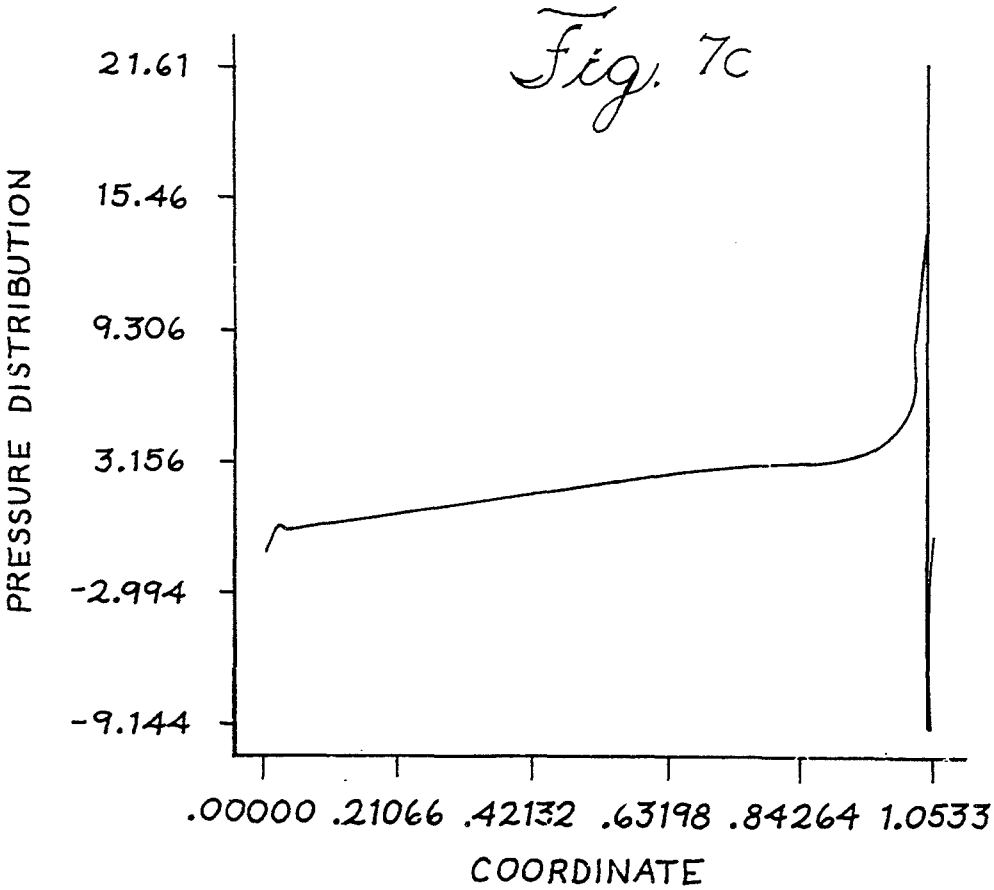
21.61
15.46
9.306
3.156
-2.994
-9.144
PRESSURE DISTRIBUTION
.00000 .21066 .42132 .63198 .84264 1.0533
COORDINATE

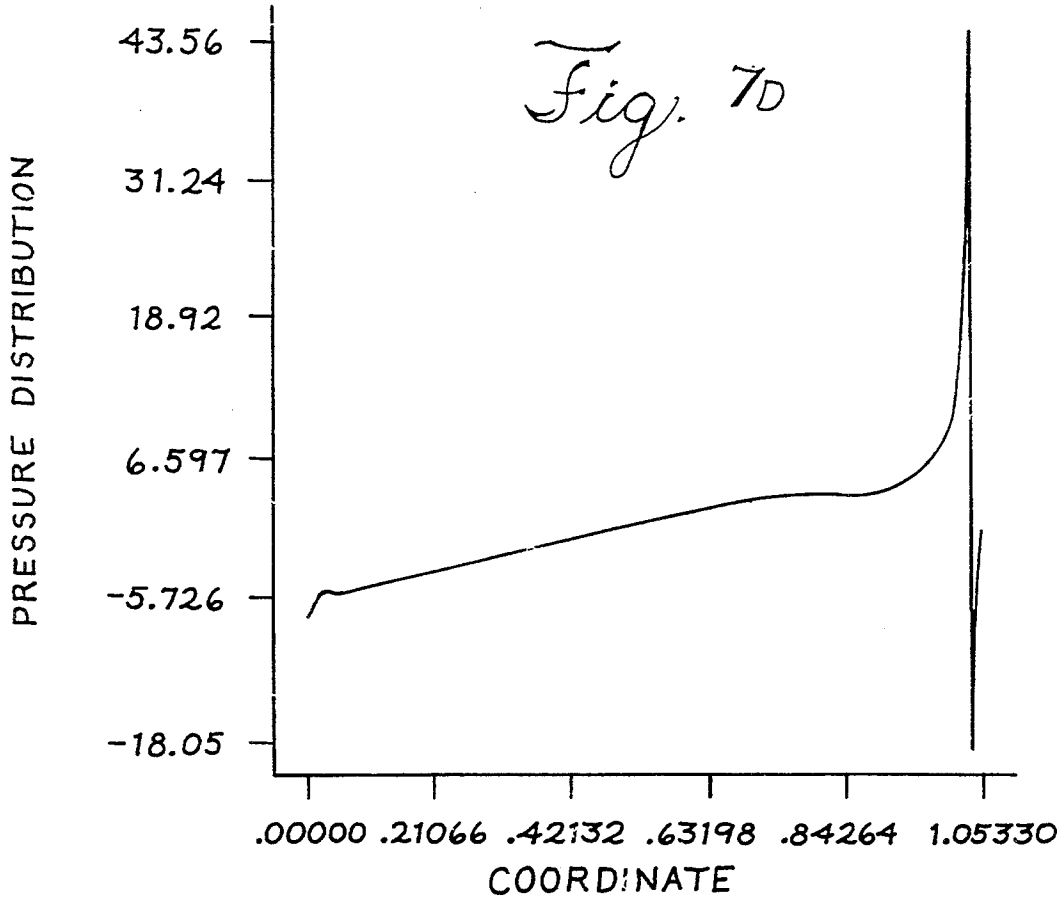
43.56
31.24
18.92
6.597
-5.726
-18.05
PRESSURE DISTRIBUTION
.00000 .21066 .42132 .63198 .84264 1.05330
COORDINATE

Fig. 7D

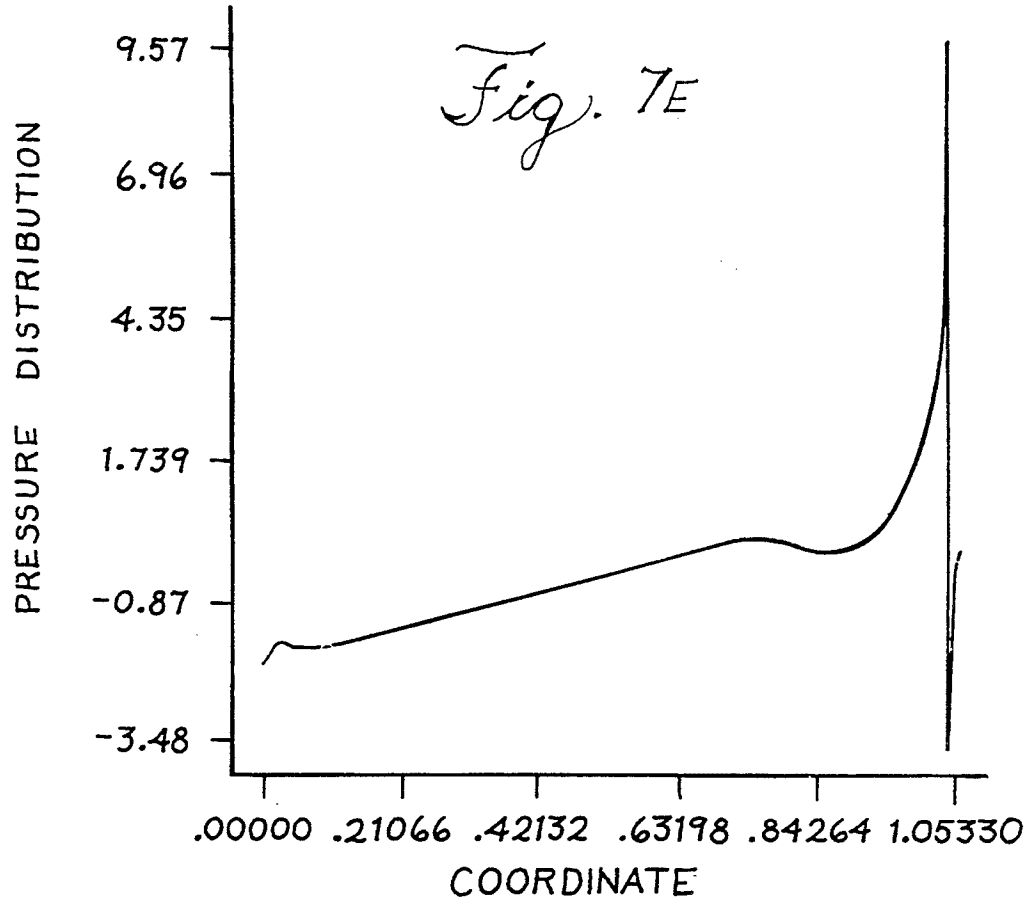
9.57
6.96
4.35
1.739
-0.87
-3.48
PRESSURE DISTRIBUTION
.00000 .21066 .42132 .63198 .84264 1.05330
COORDINATE

Fig. 7E

Fig. 7F

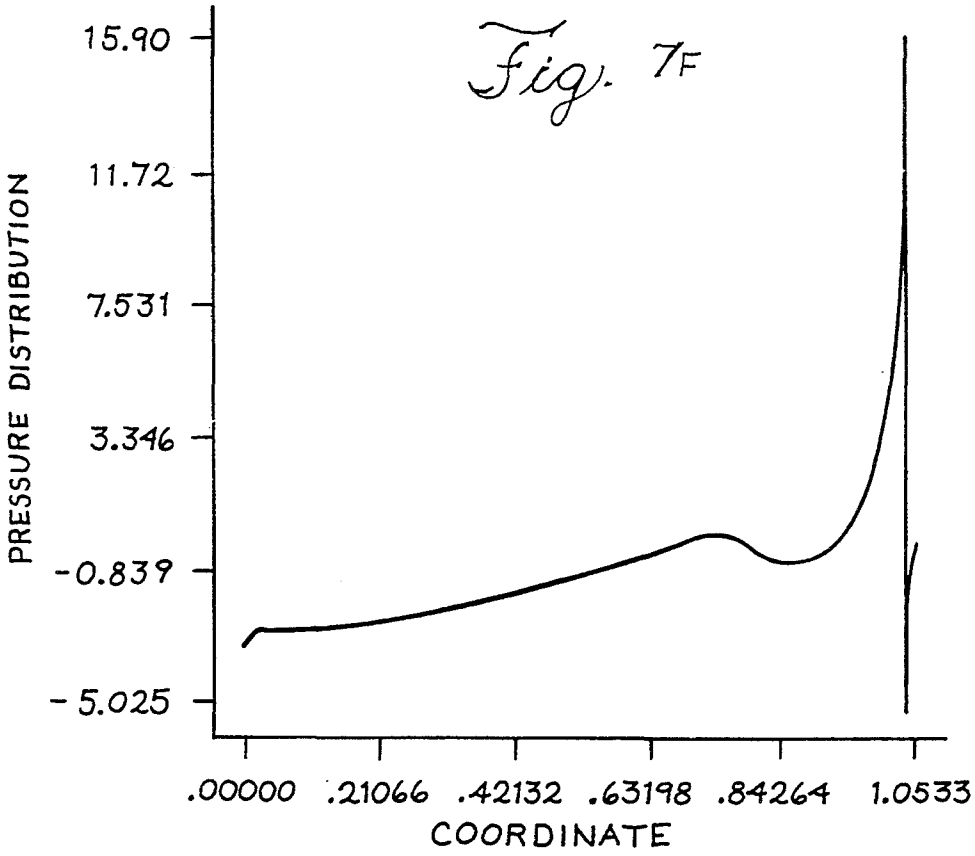
15.90
11.72
7.531
3.346
-0.839
-5.025
PRESSURE DISTRIBUTION
.00000
.21066
.42132
.63198
.84264
1.0533
COORDINATE

Fig. 7G

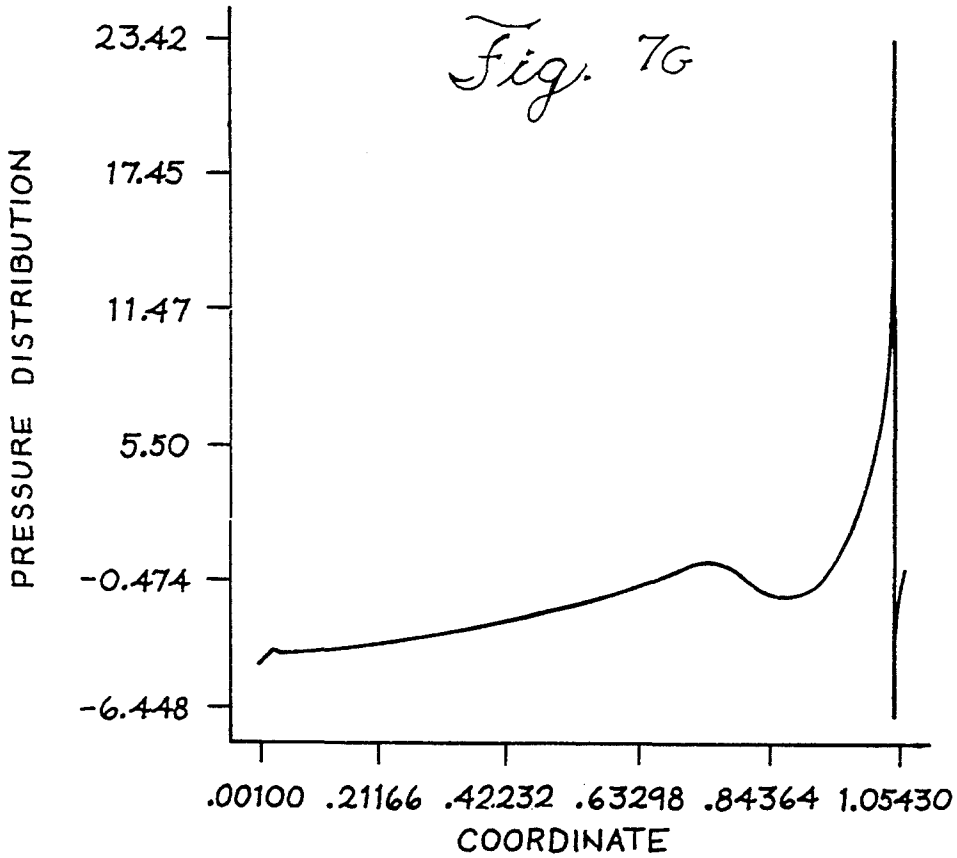
23.42
17.45
11.47
5.50
-0.474
-6.448
PRESSURE DISTRIBUTION
.00100
.21166
.42232
.63298
.84364
1.05430
COORDINATE

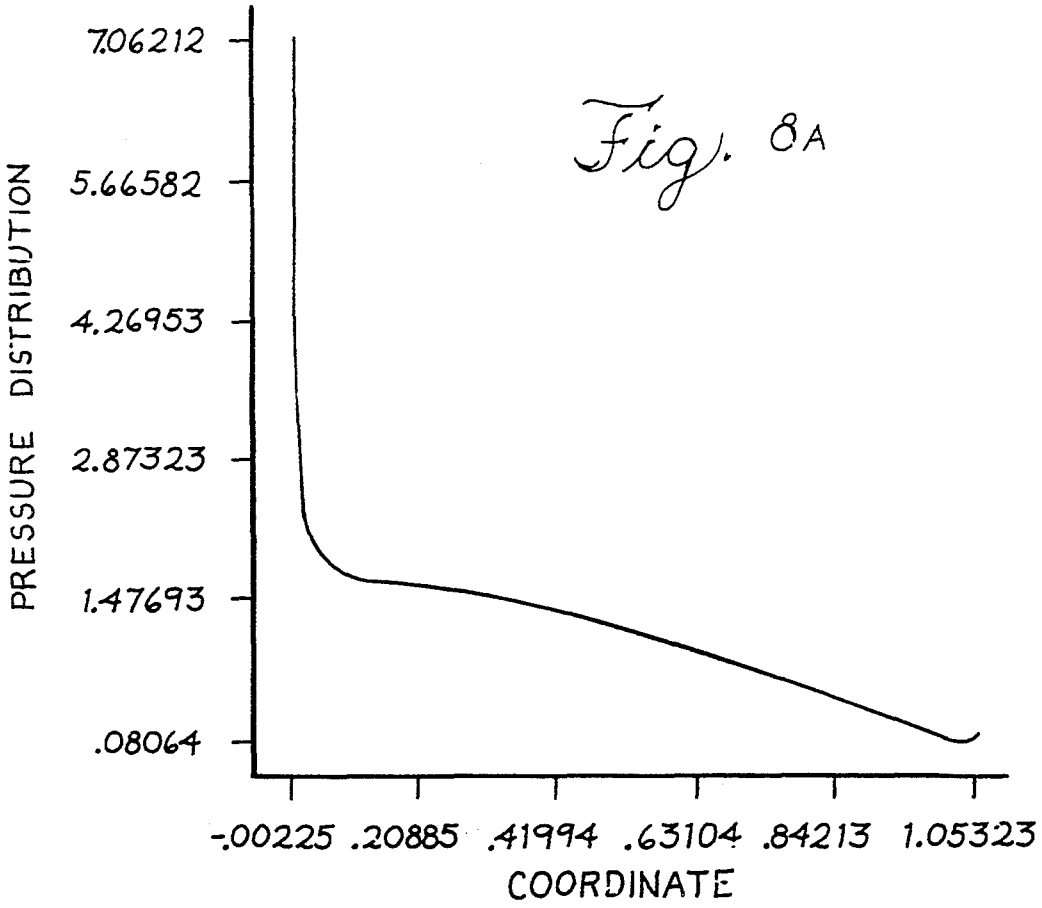
7.06212
5.66582
4.26953
2.87323
1.47693
.08064
PRESSURE DISTRIBUTION
-.00225 .20885 .41994 .63104 .84213 1.05323
COORDINATE

Fig. 8A

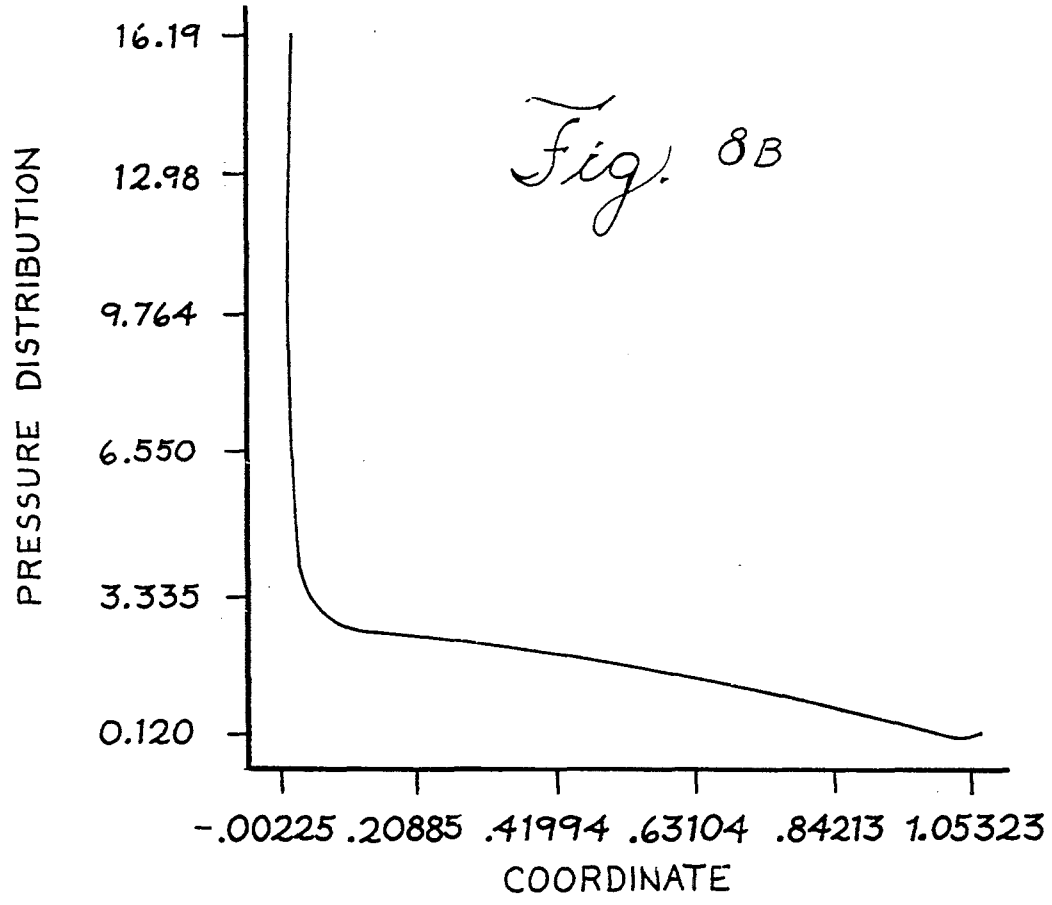
16.19
12.98
9.764
6.550
3.335
0.120
PRESSURE DISTRIBUTION
-.00225 .20885 .41994 .63104 .84213 1.05323
COORDINATE

Fig. 8B

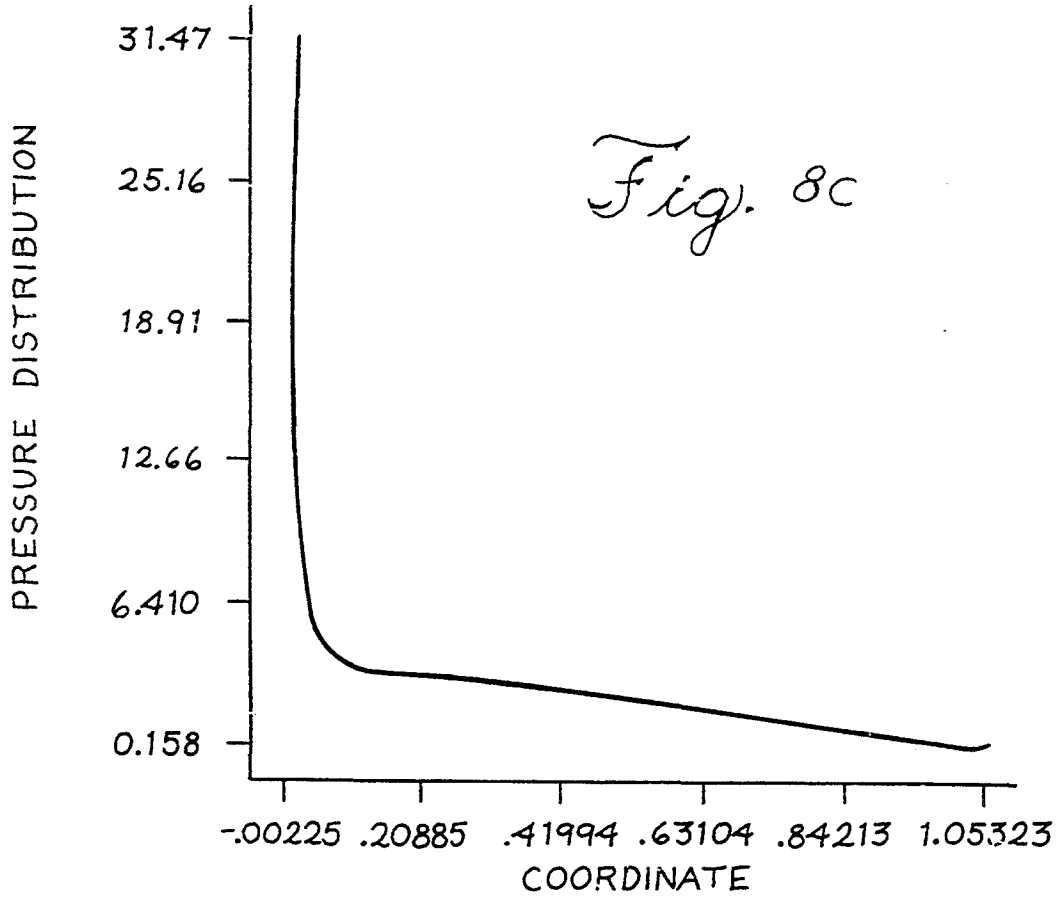
31.47
25.16
18.91
12.66
6.410
0.158
PRESSURE DISTRIBUTION
-.00225 .20885 .41994 .63104 .84213 1.05323
COORDINATE

Fig. 8C

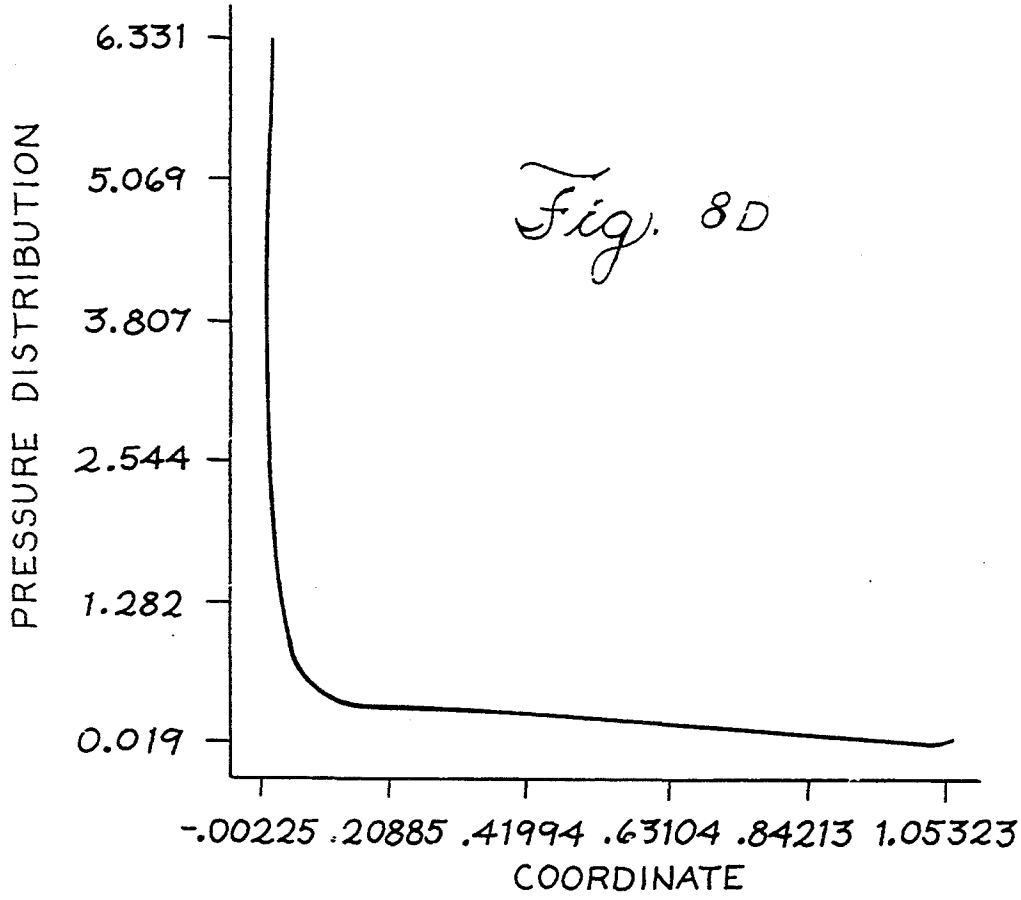
6.331
5.069
3.807
2.544
1.282
0.019
PRESSURE DISTRIBUTION
-.00225 .20885 .41994 .63104 .84213 1.05323
COORDINATE

Fig. 8D

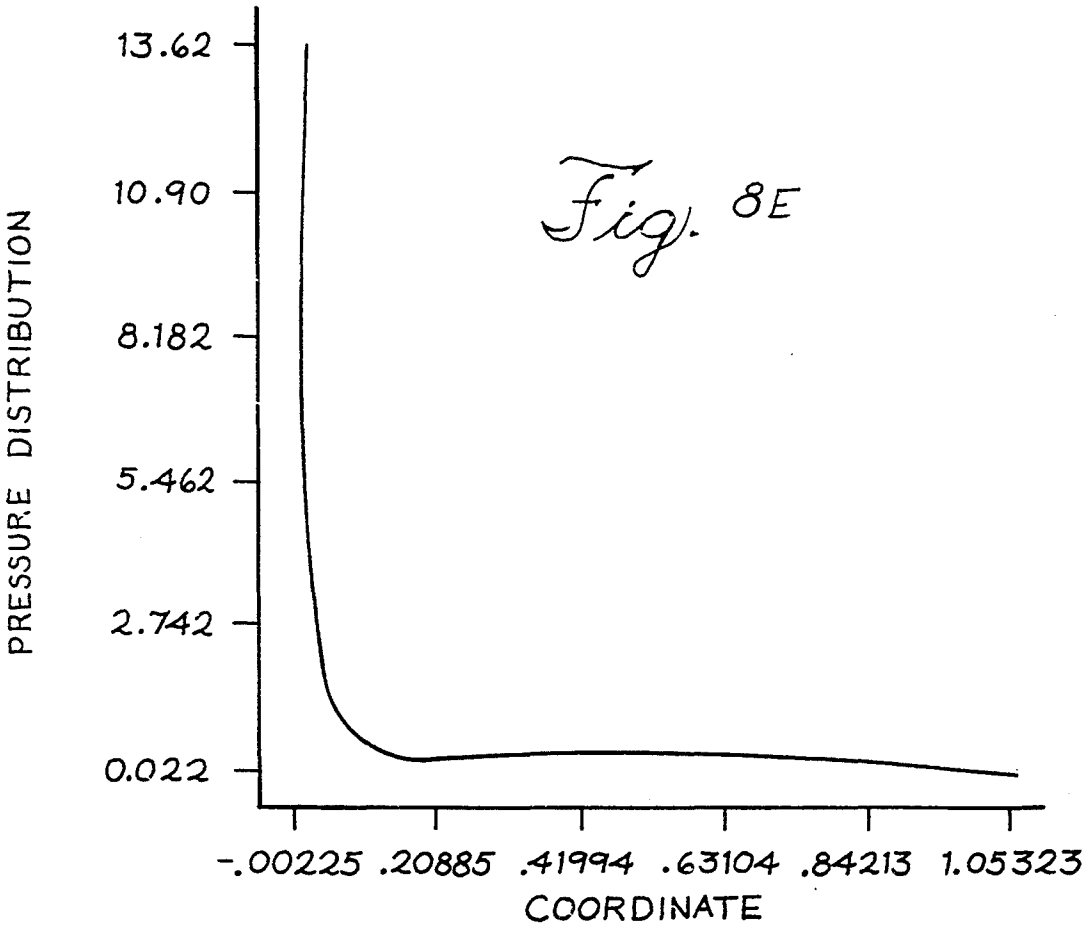
13.62
10.90
8.182
5.462
2.742
0.022
PRESSURE DISTRIBUTION
-.00225 .20885 .41994 .63104 .84213 1.05323
COORDINATE

Fig. 8E

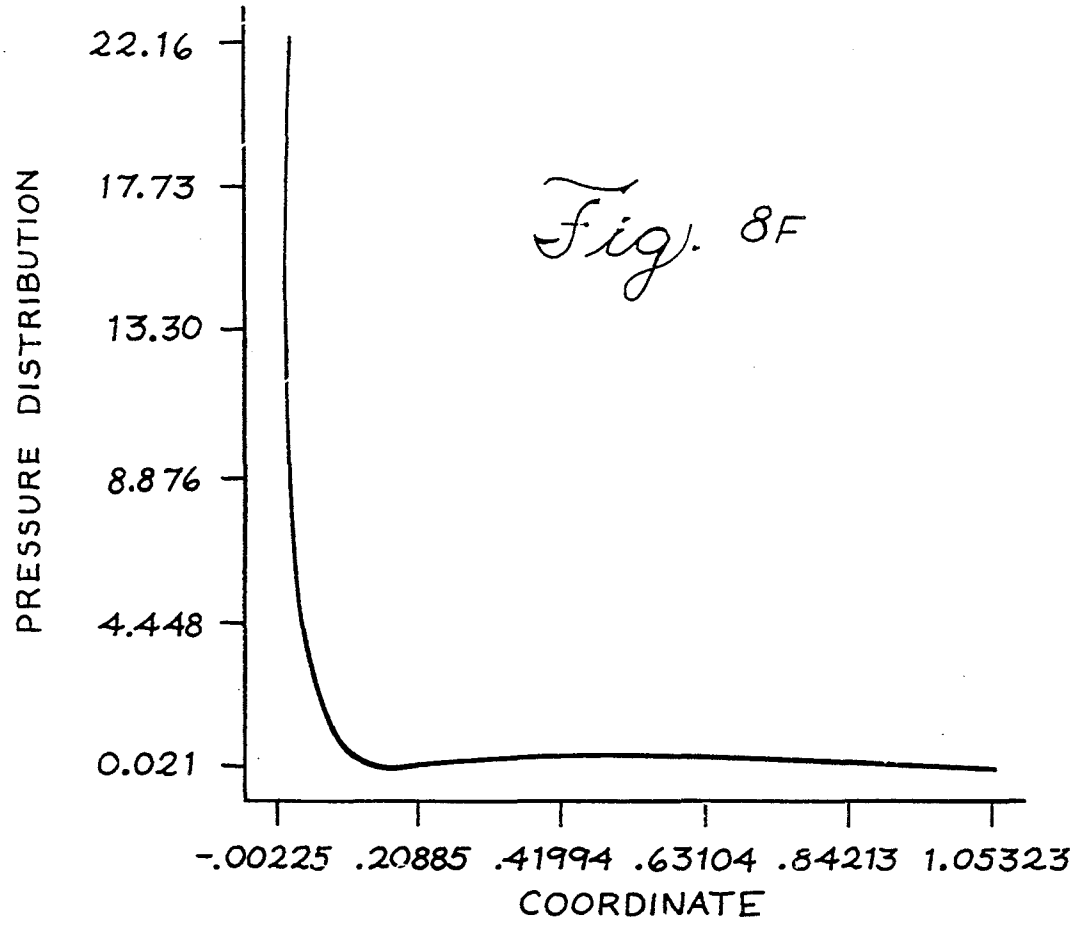
22.16
17.73
13.30
8.876
4.448
0.021
PRESSURE DISTRIBUTION
-.00225 .20885 .41994 .63104 .84213 1.05323
COORDINATE

Fig. 8F

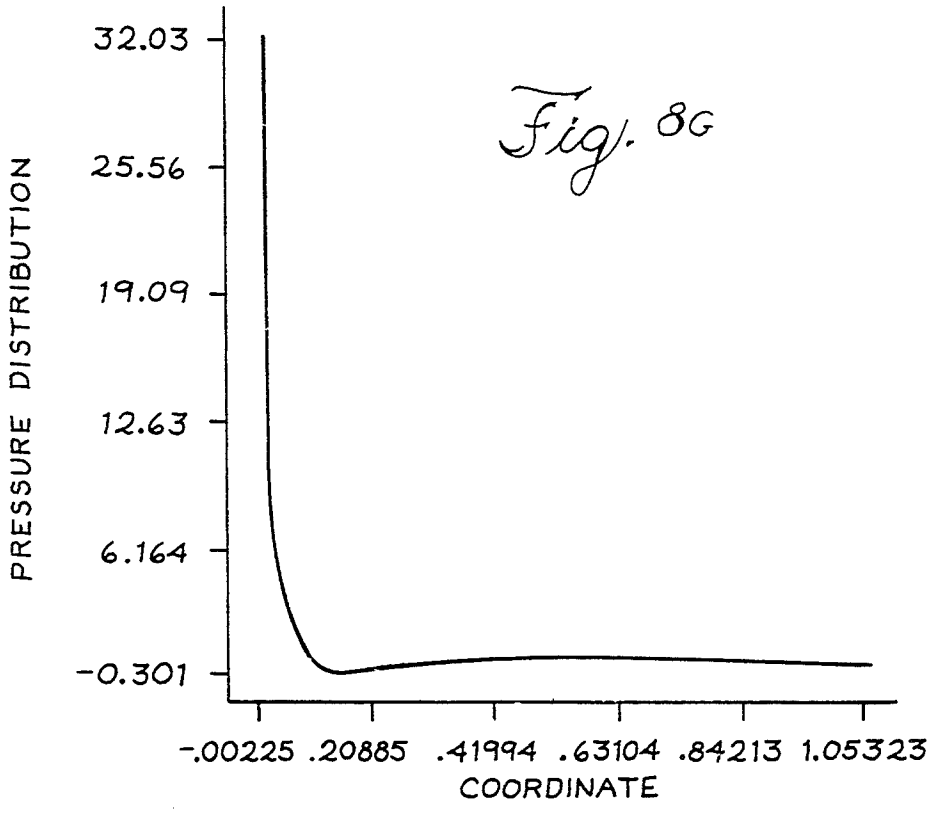
32.03
25.56
19.09
12.63
6.164
-0.301
PRESSURE DISTRIBUTION
-.00225 .20885 .41994 .63104 .84213 1.05323
COORDINATE

Fig. 8G

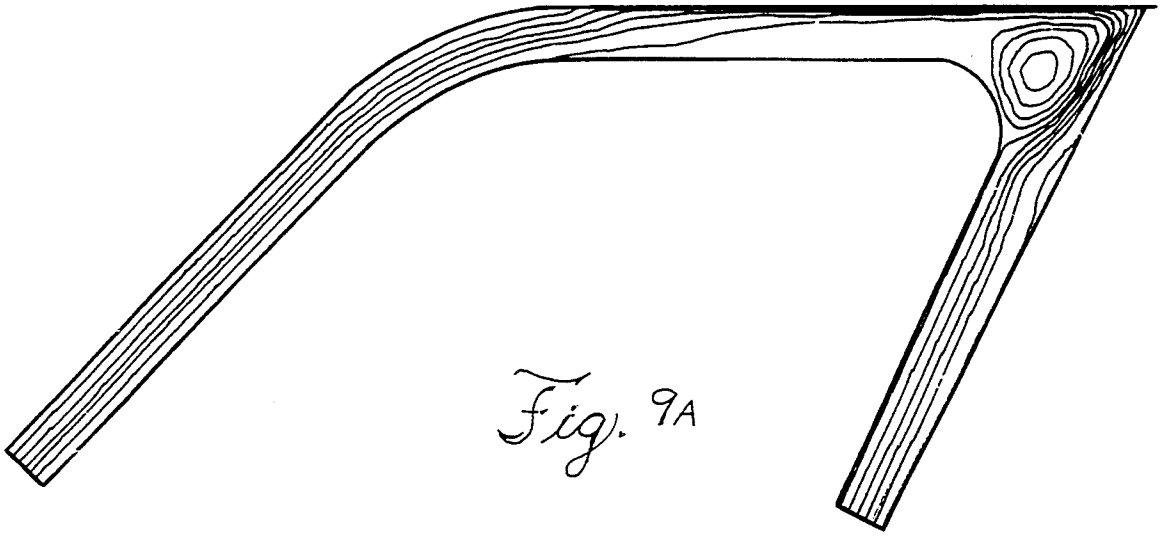

Fig. 9A

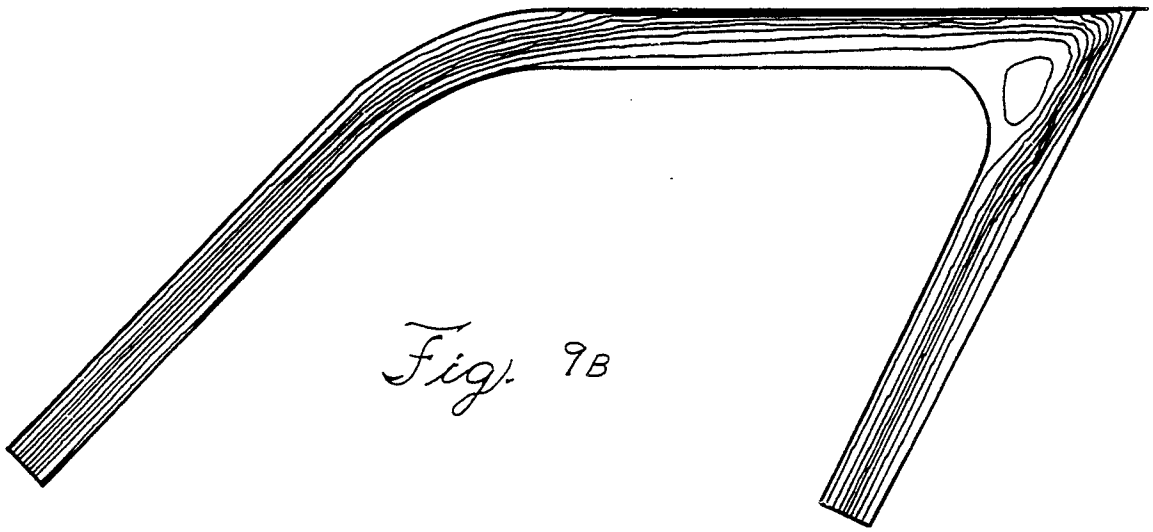

Fig. 9B

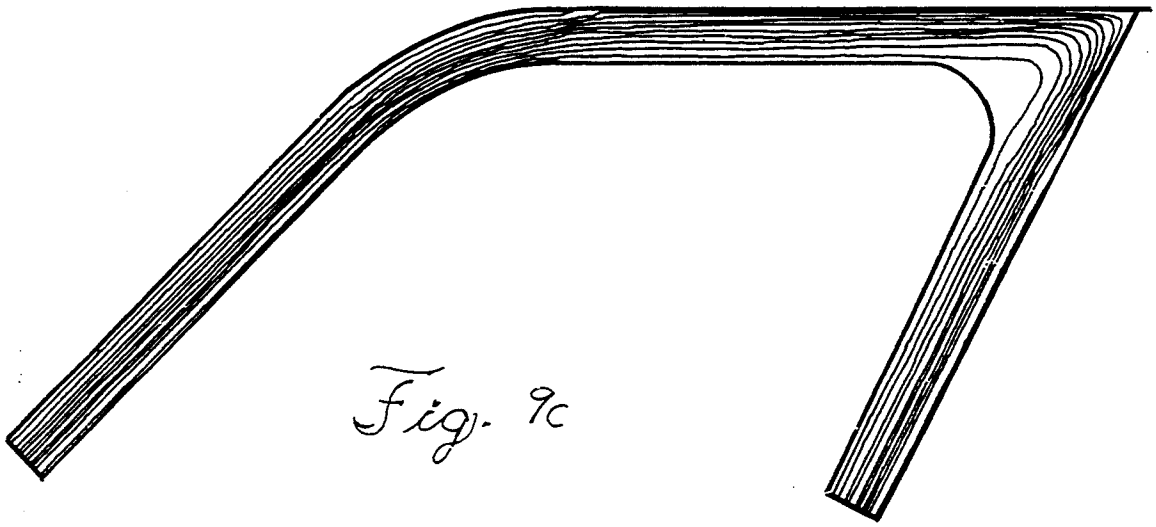

Fig. 9C

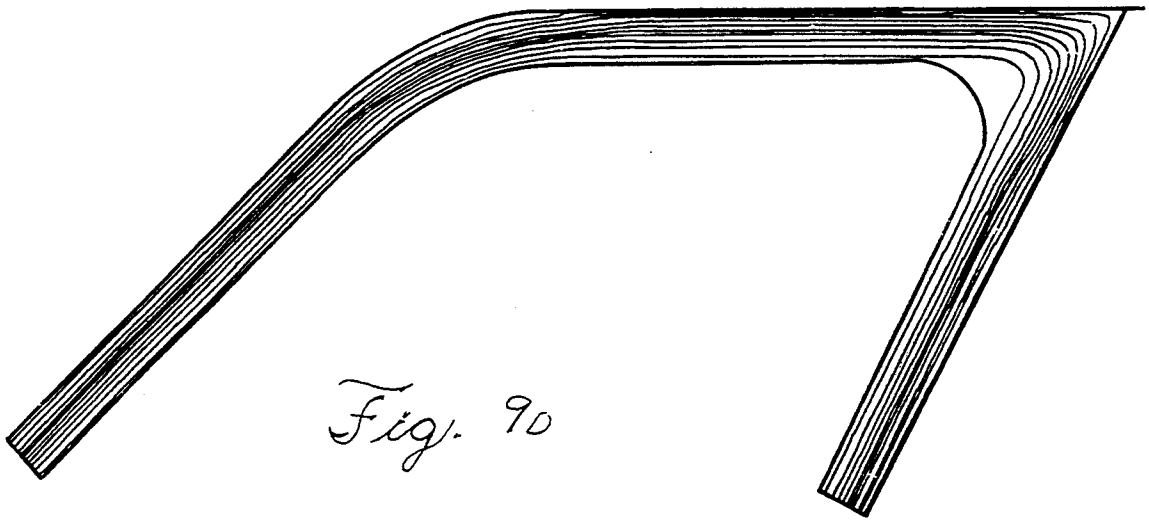

Fig. 9D

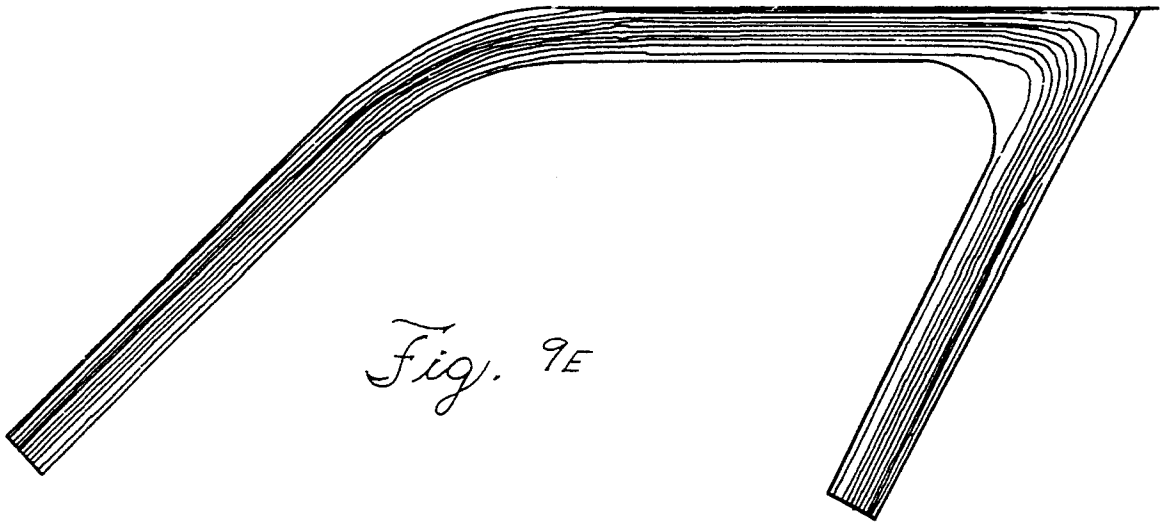

Fig. 9E

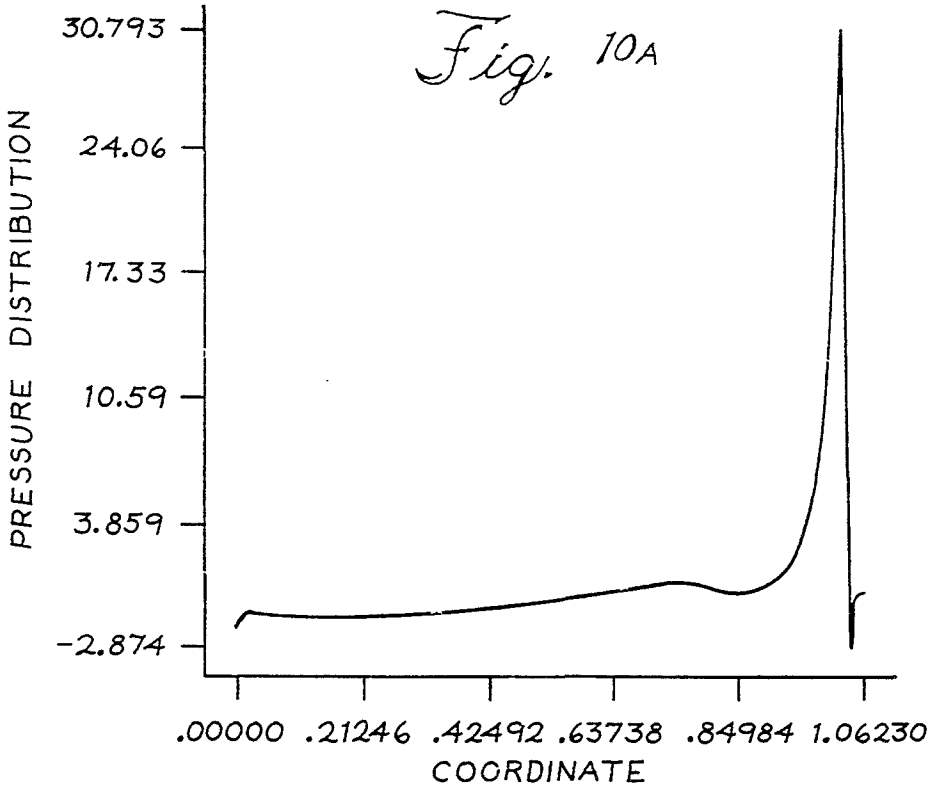

Fig. 10A

Fig. 10B

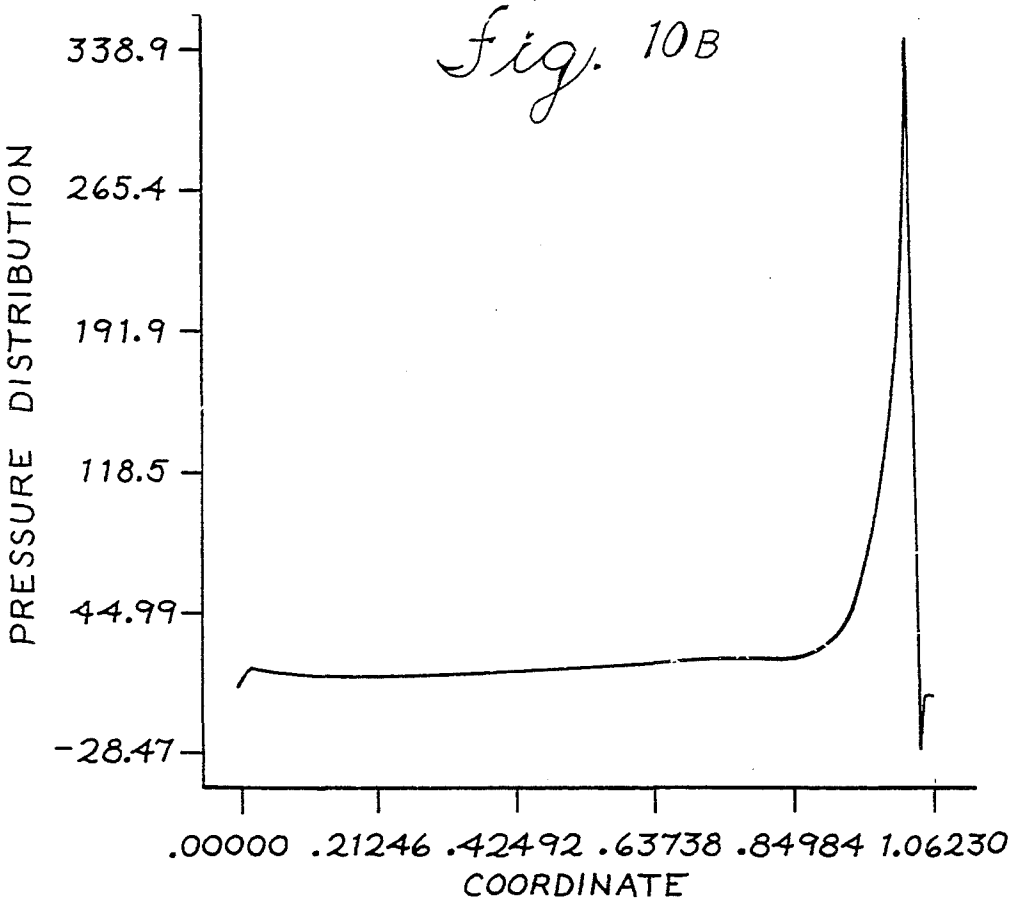

Fig. 10C

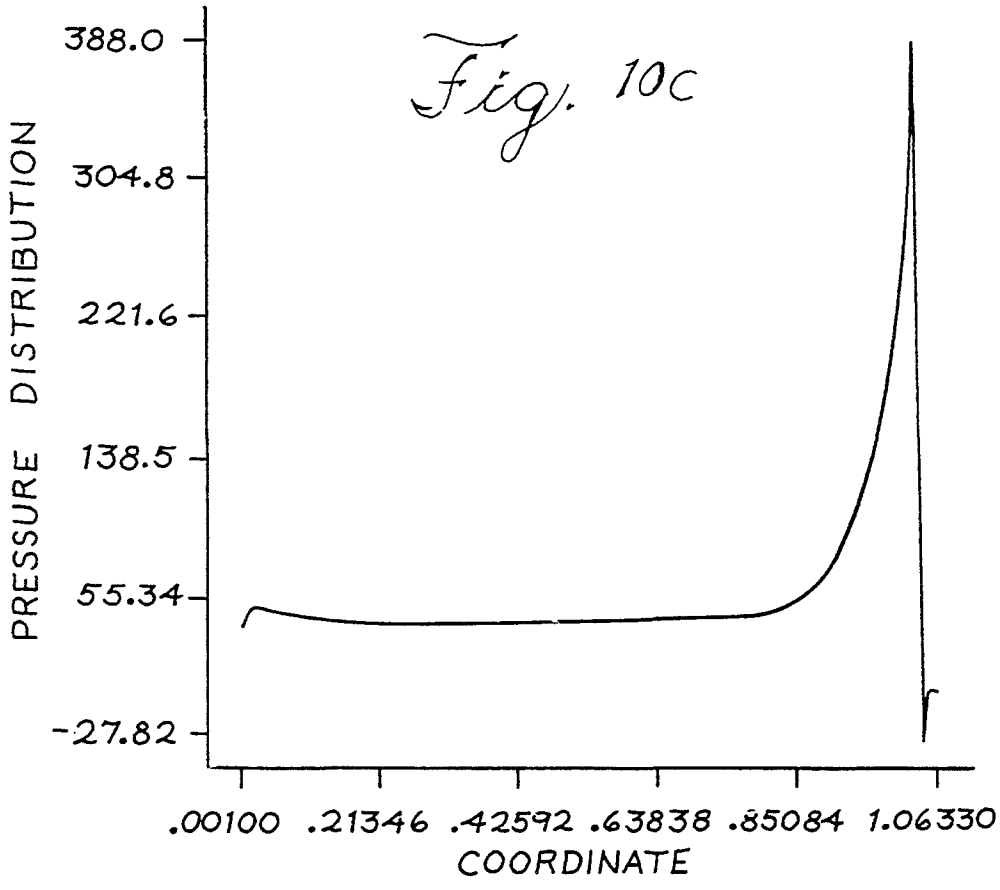

Fig. 10D

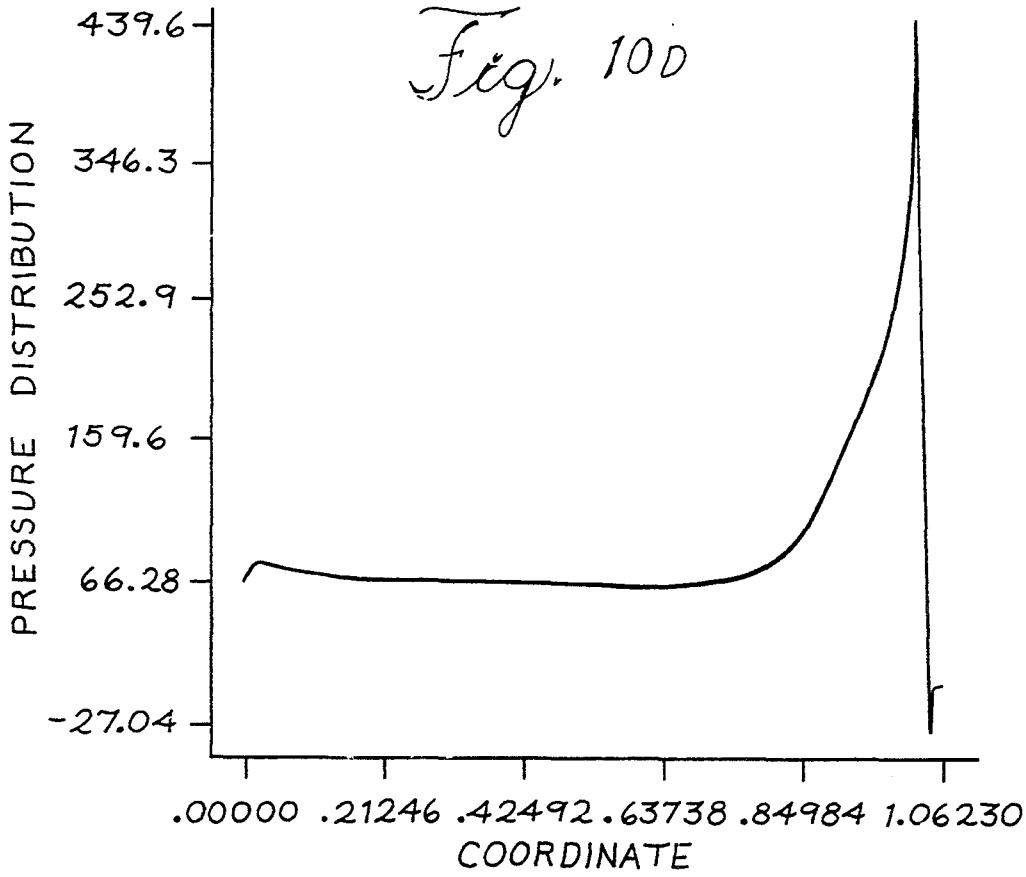

Fig. 10E

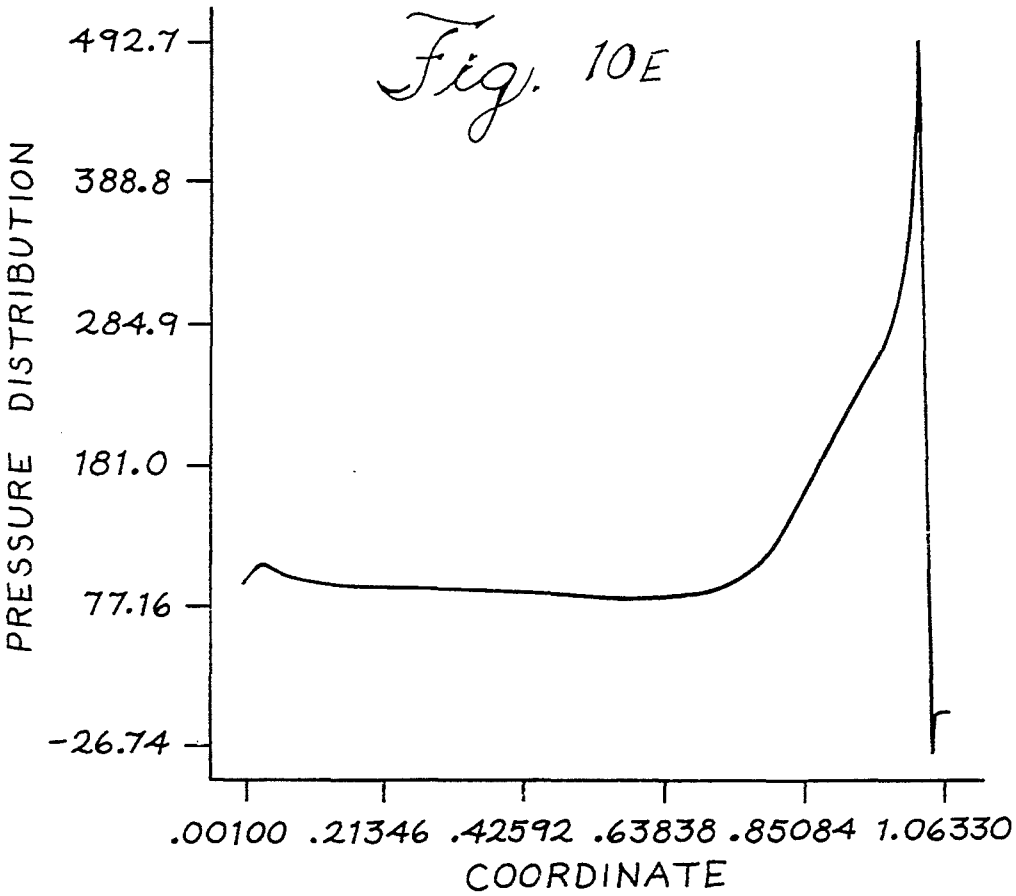

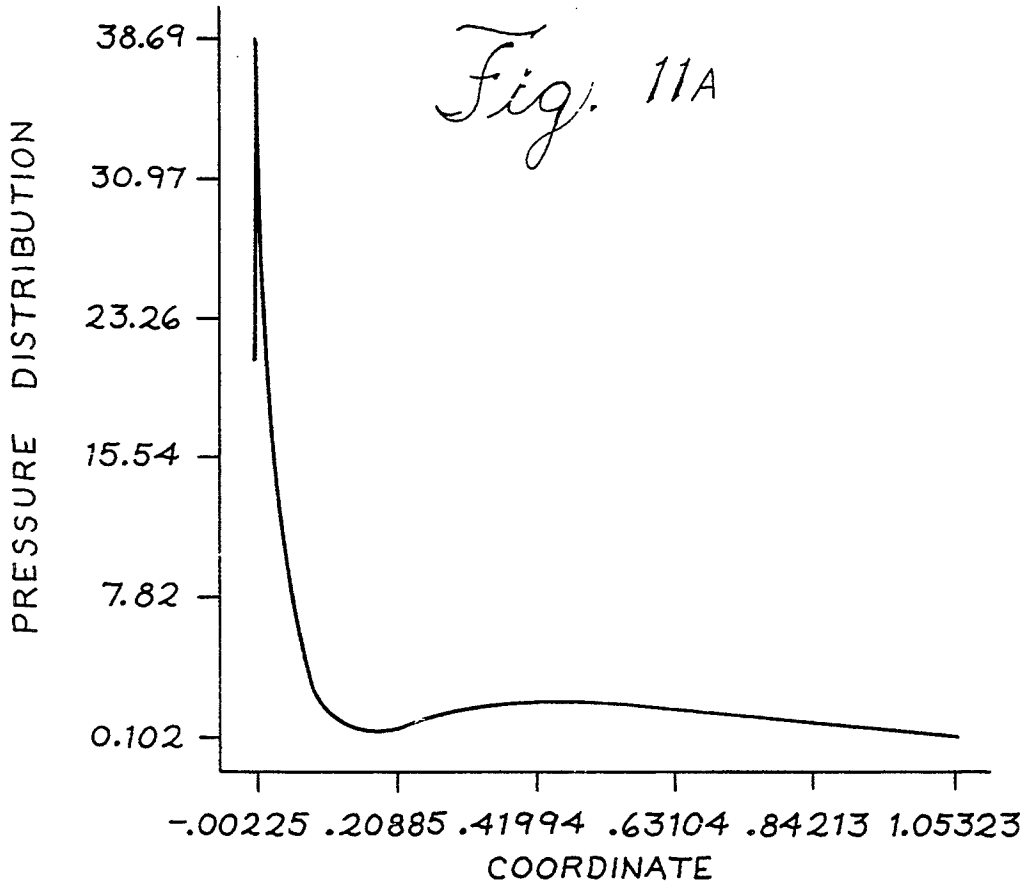

Fig. 11A

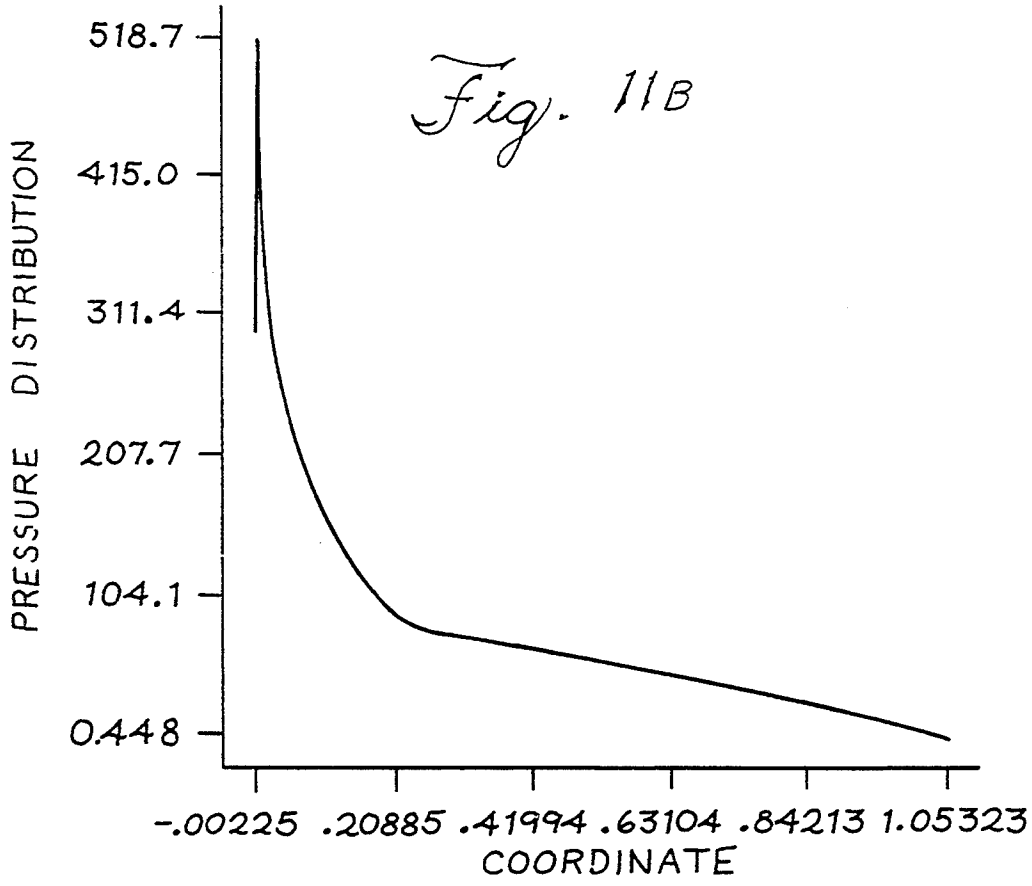

Fig. 11B

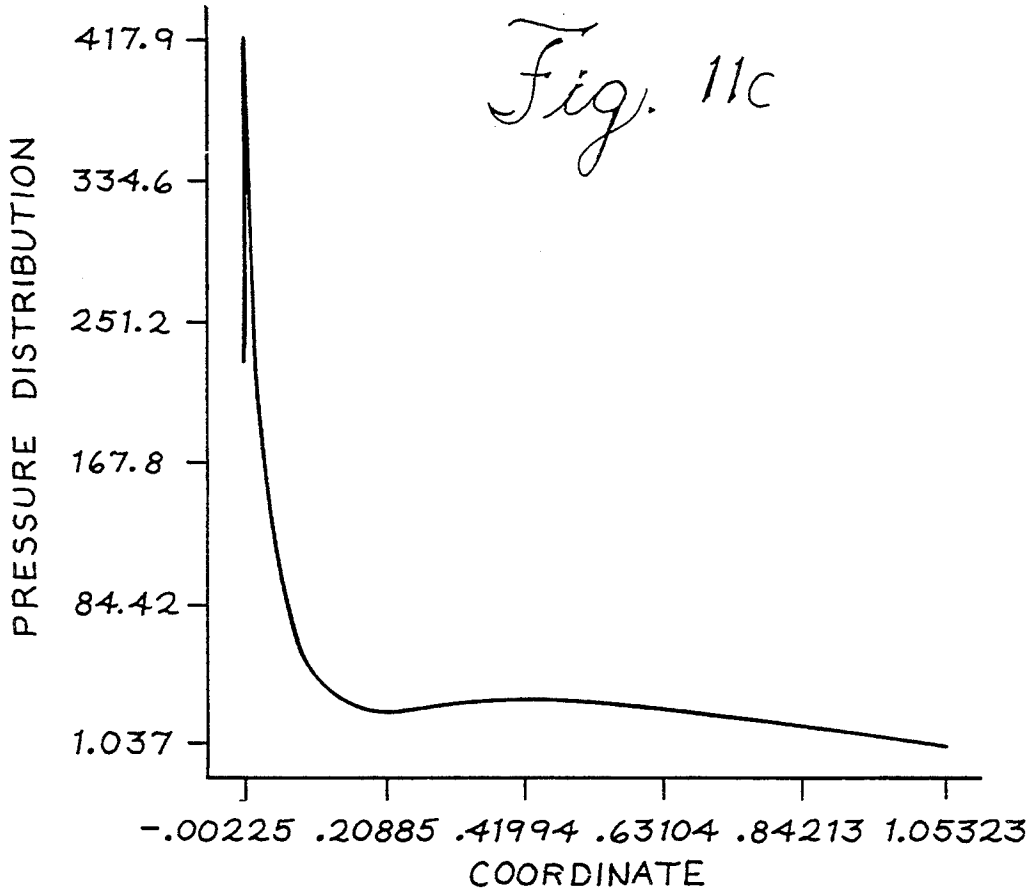

Fig. 11C

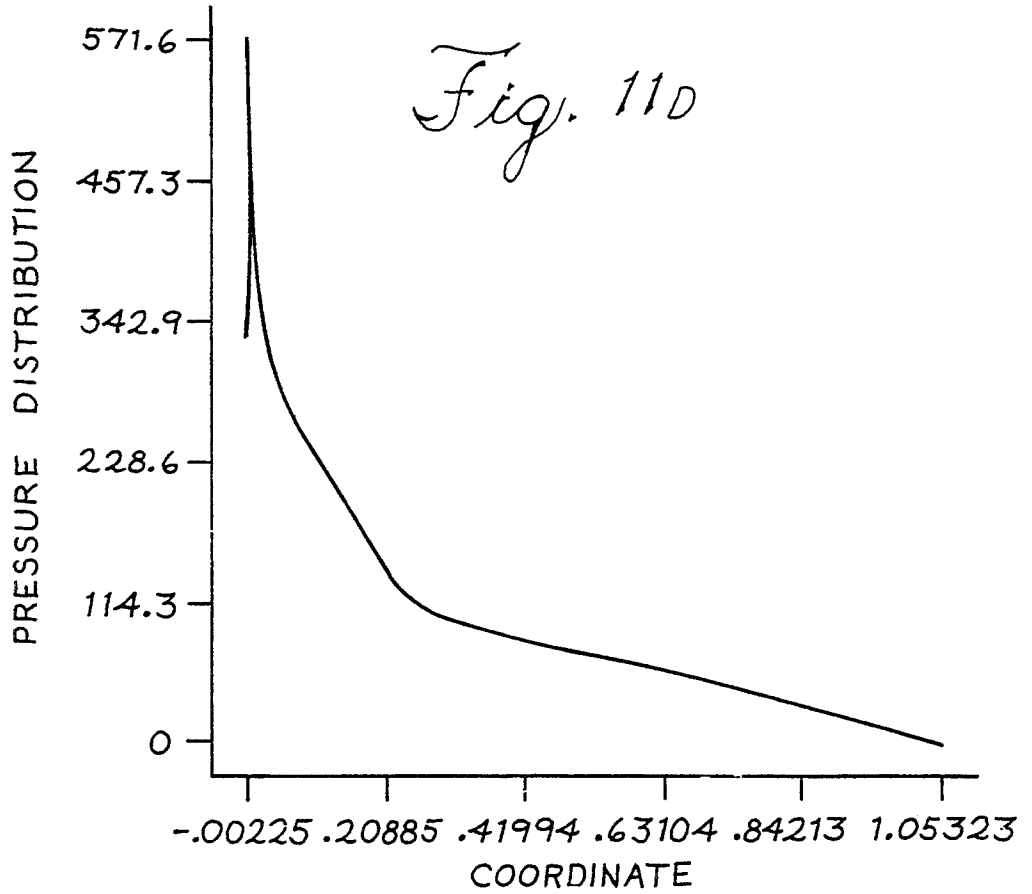

Fig. 11D

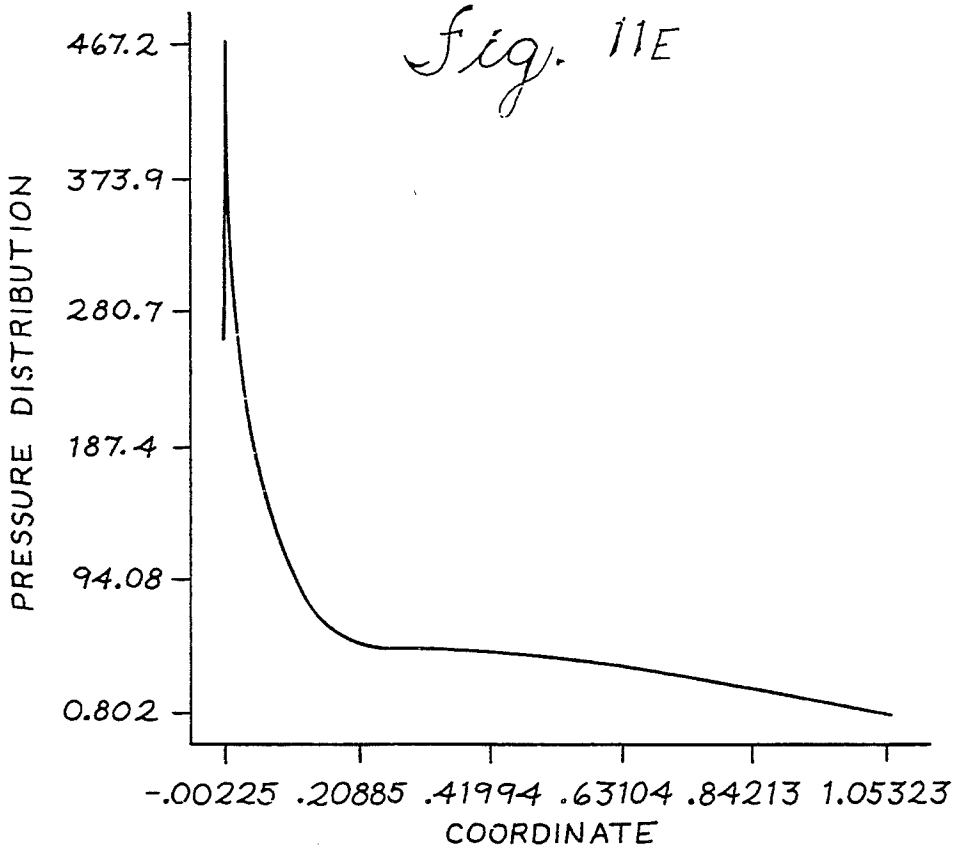

Fig. 11E

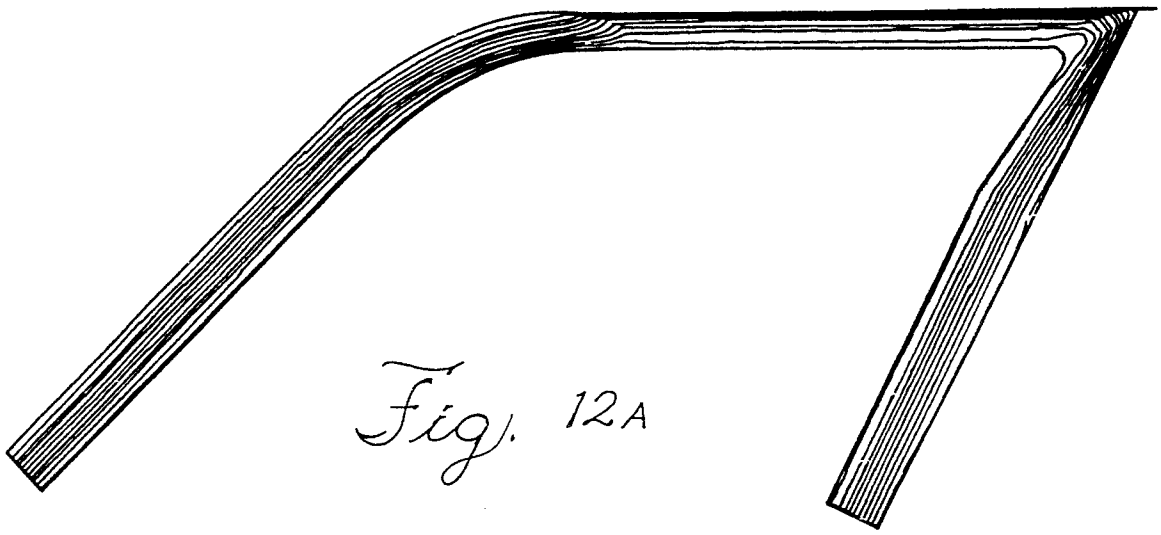

Fig. 12A

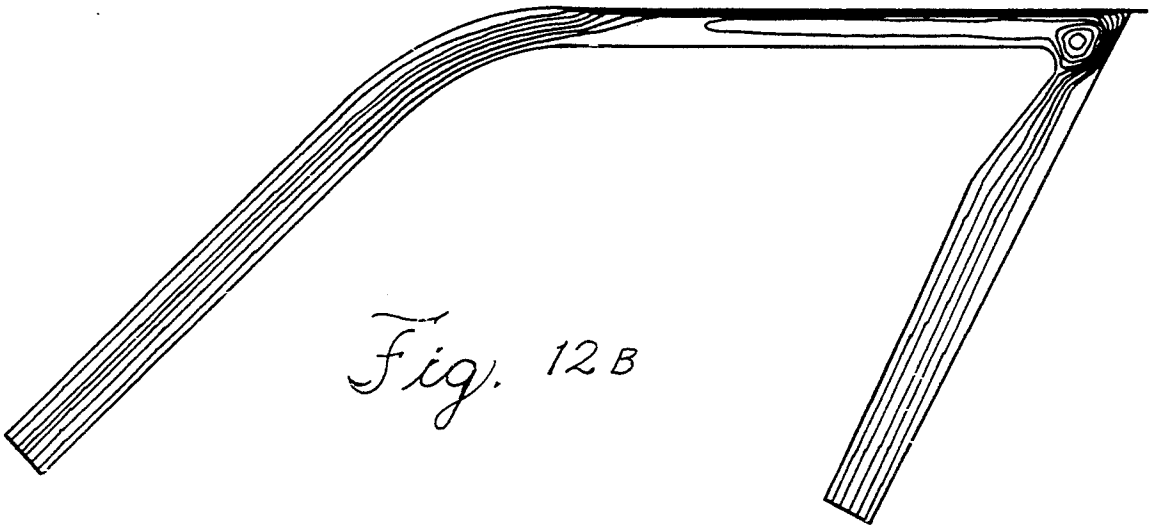

Fig. 12B

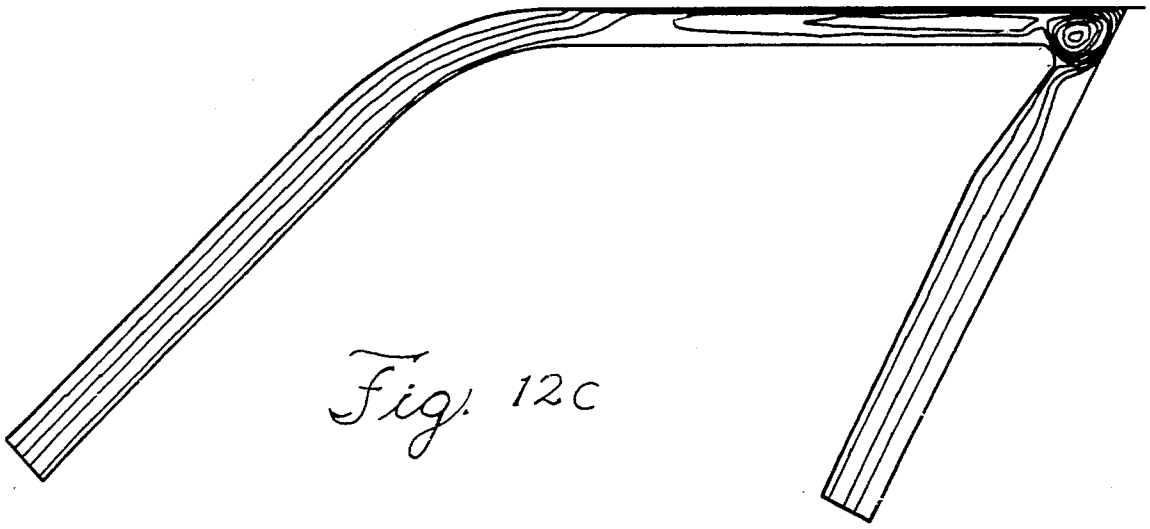

Fig. 12C

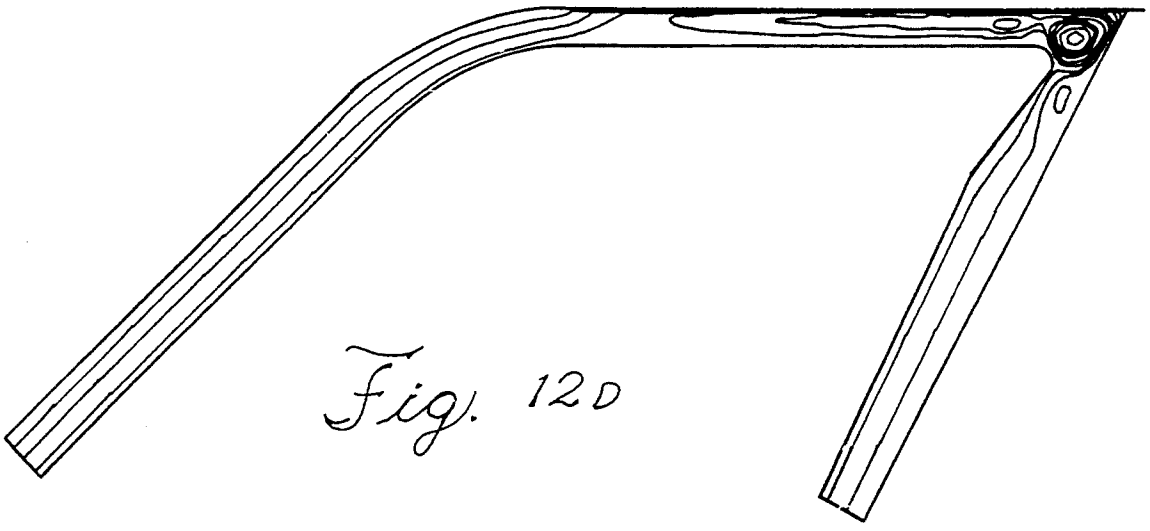

Fig. 12D

Fig. 13A

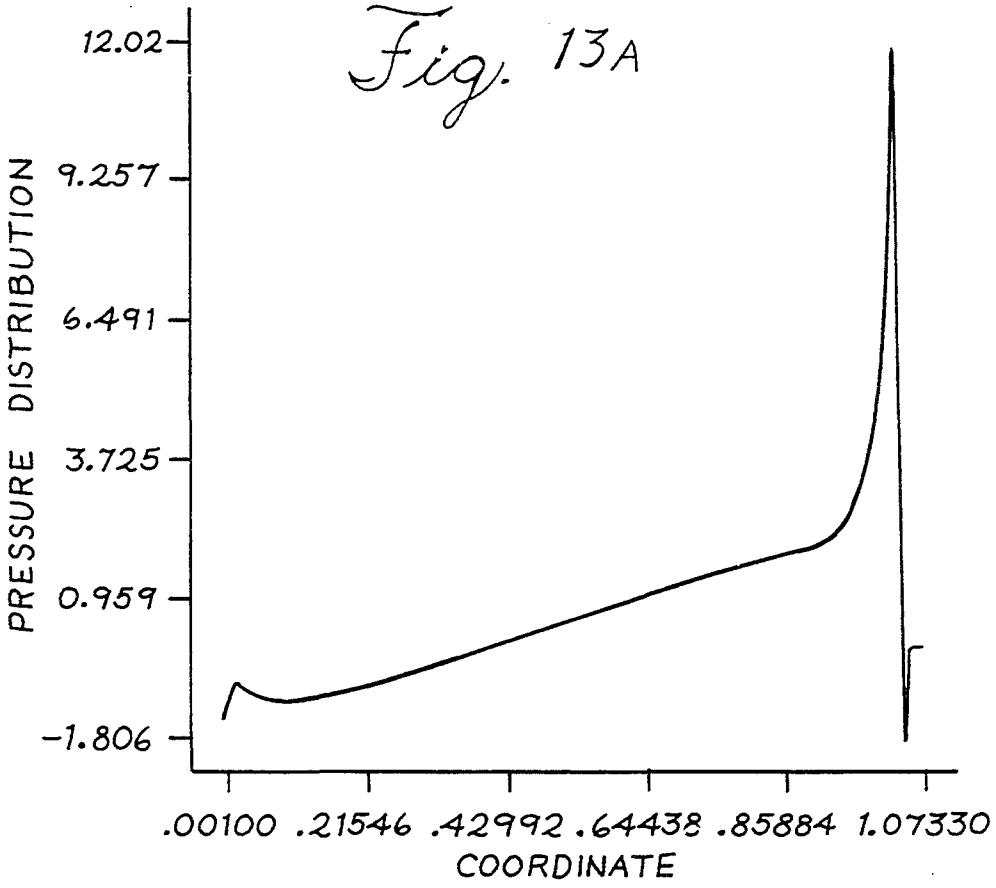

Fig. 13B

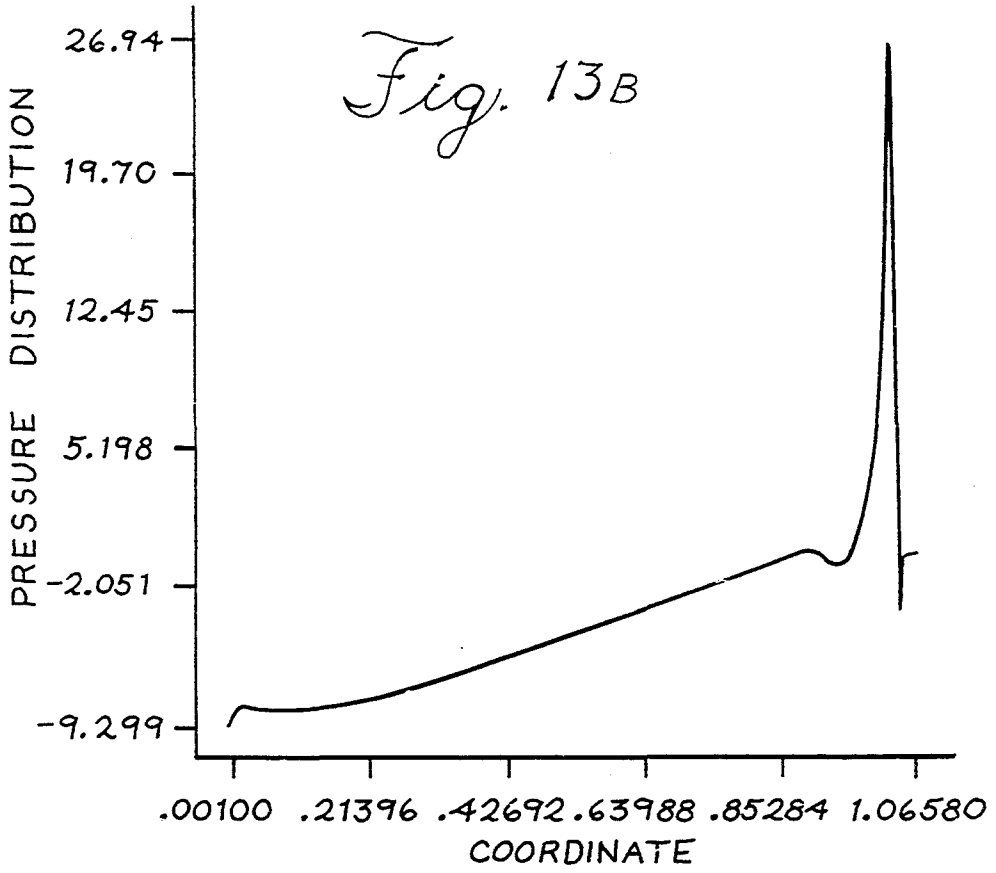

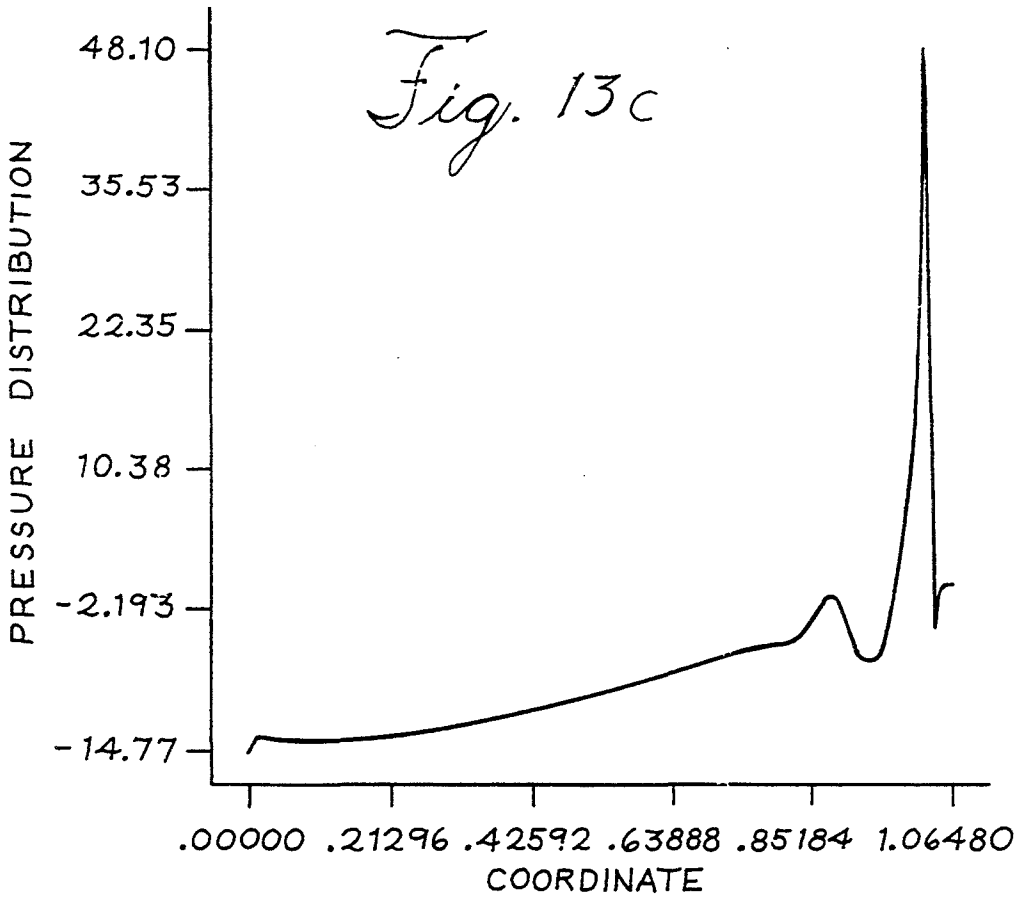

Fig. 13C

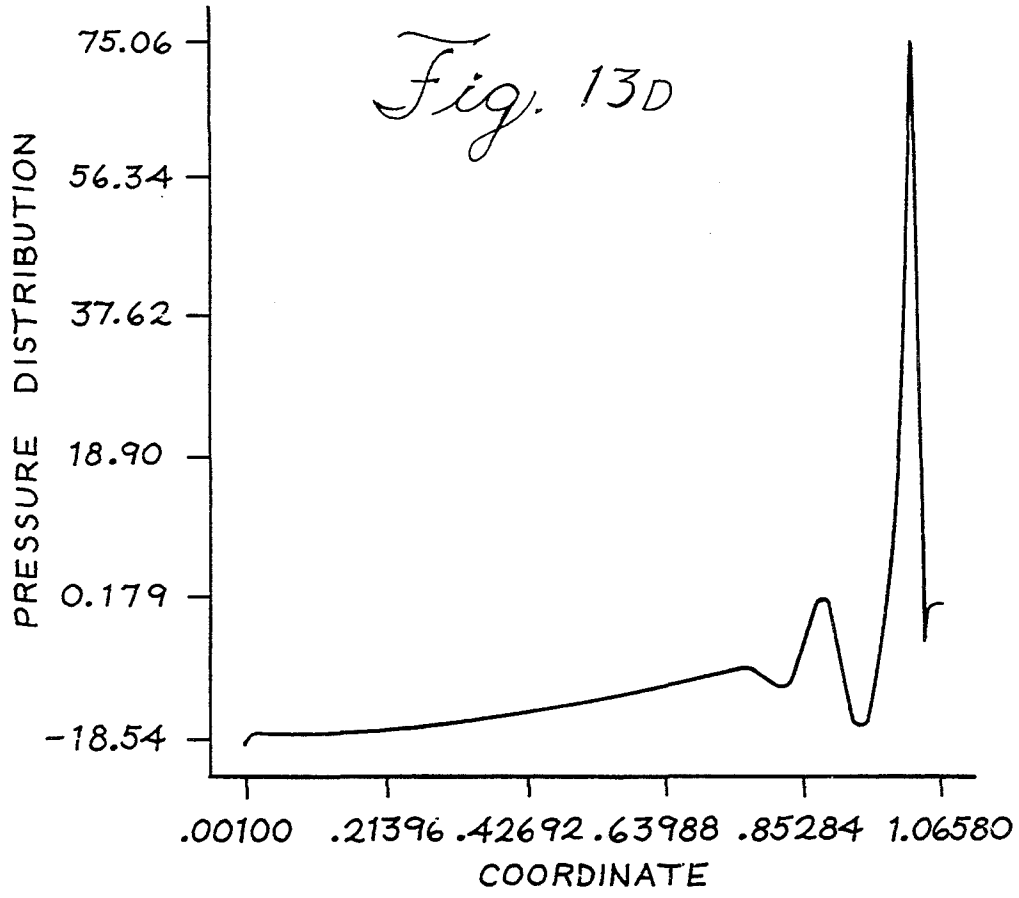

Fig. 13D

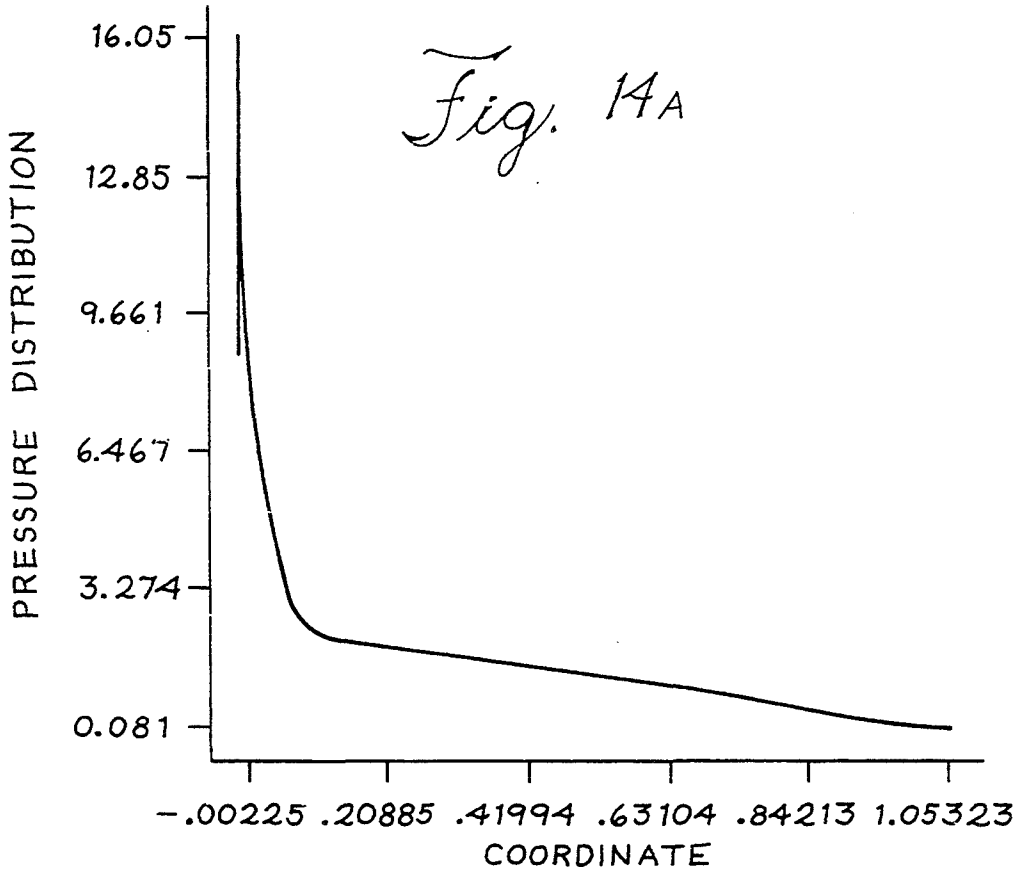

Fig. 14A

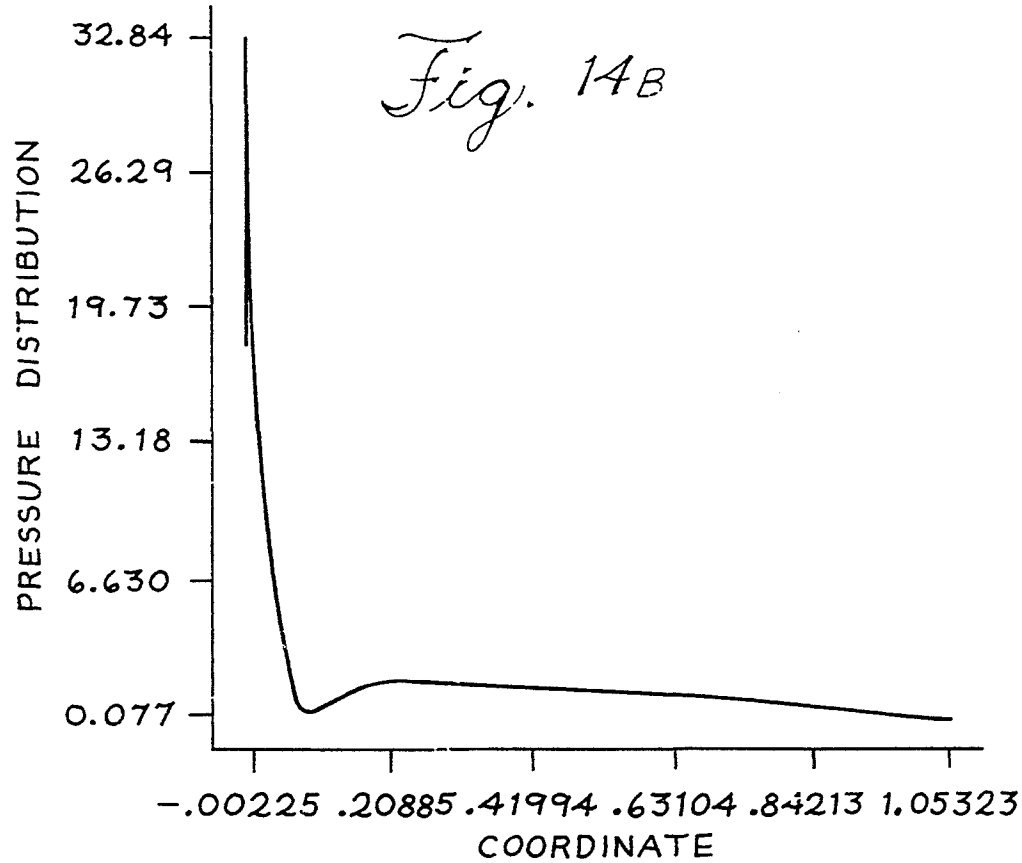

Fig. 14B

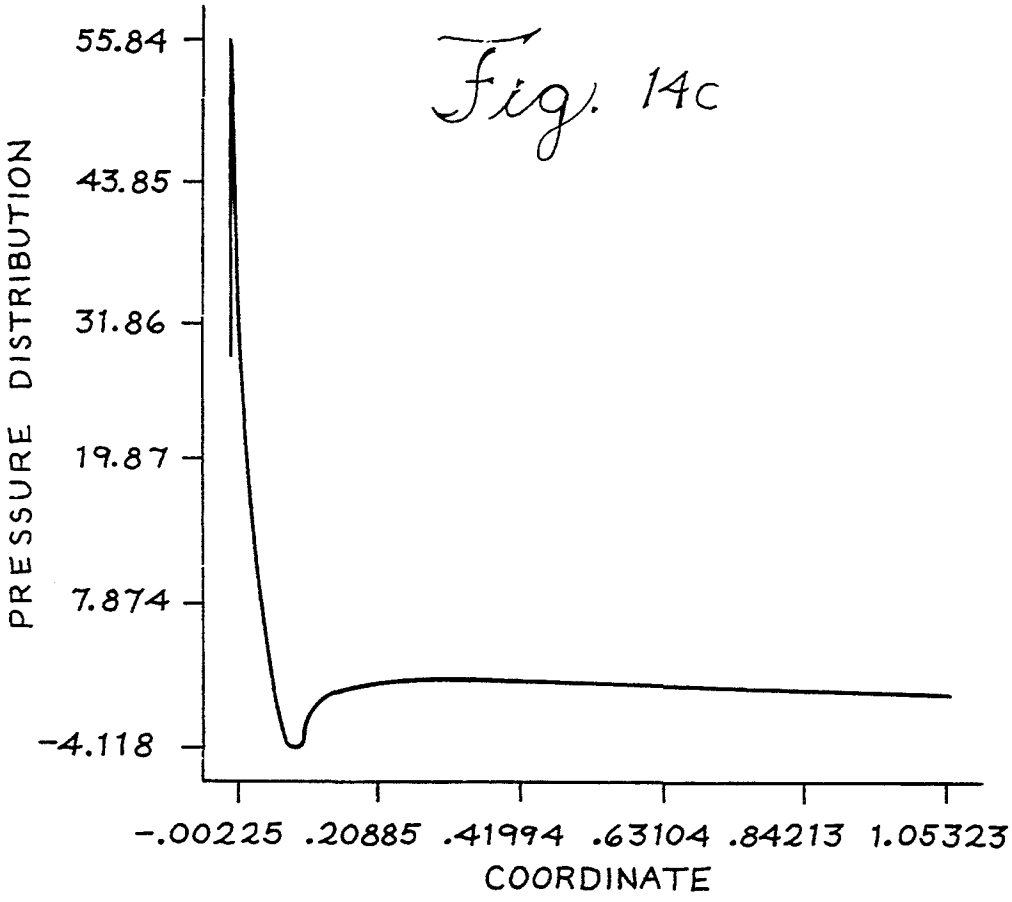

Fig. 14C

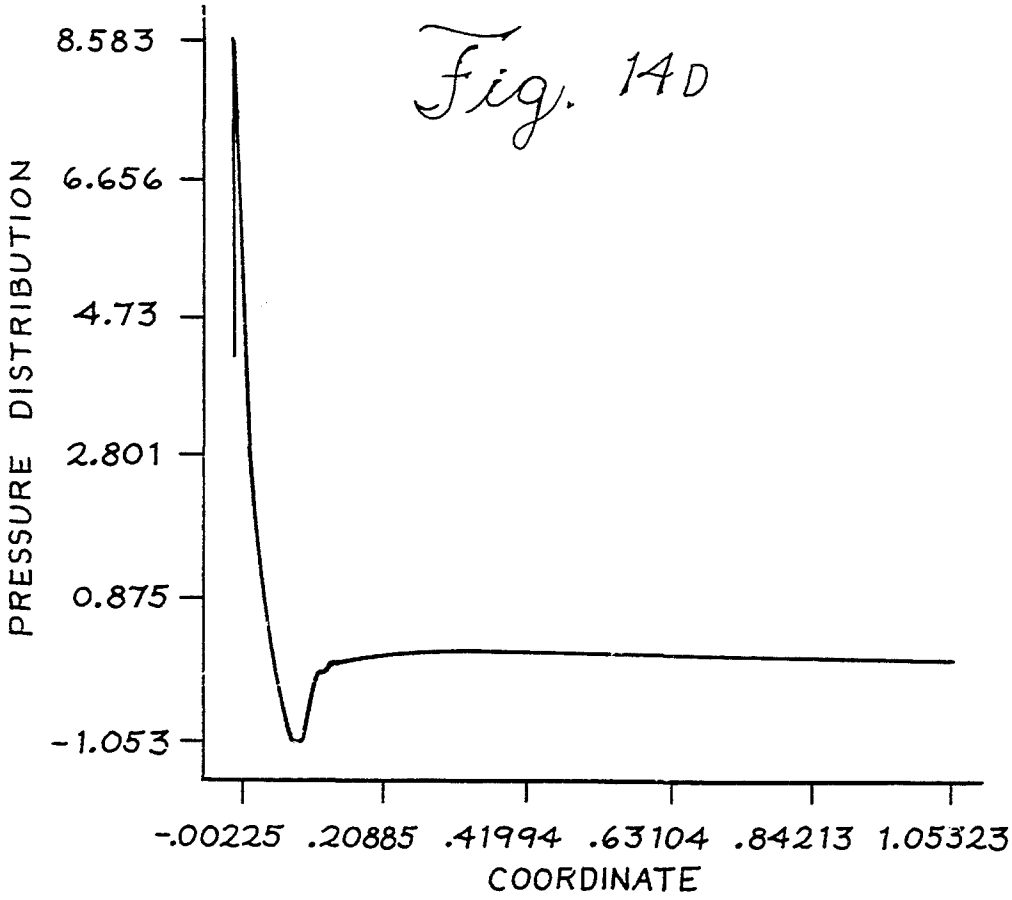

Fig. 14D

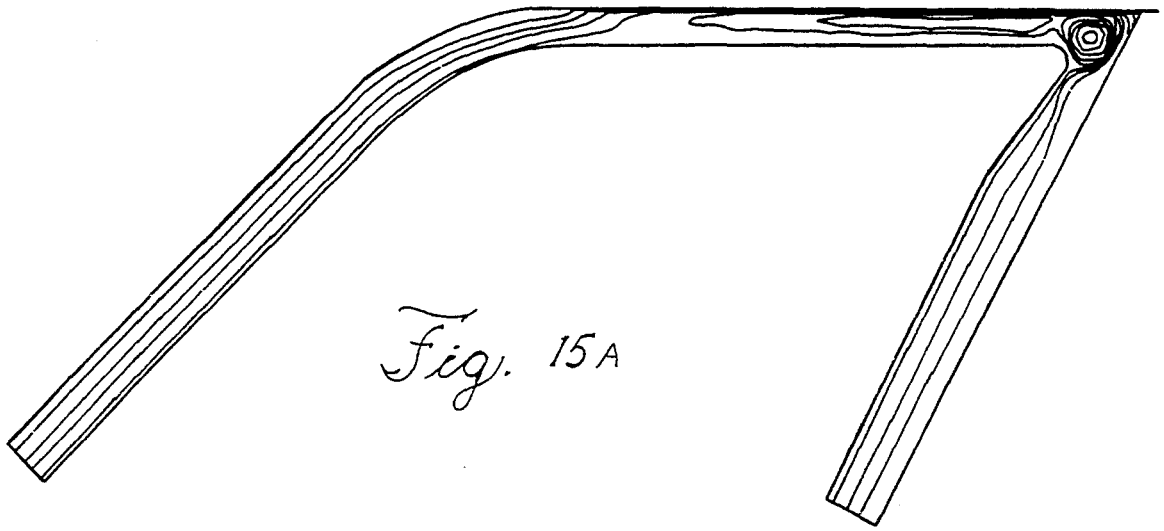

Fig. 15A

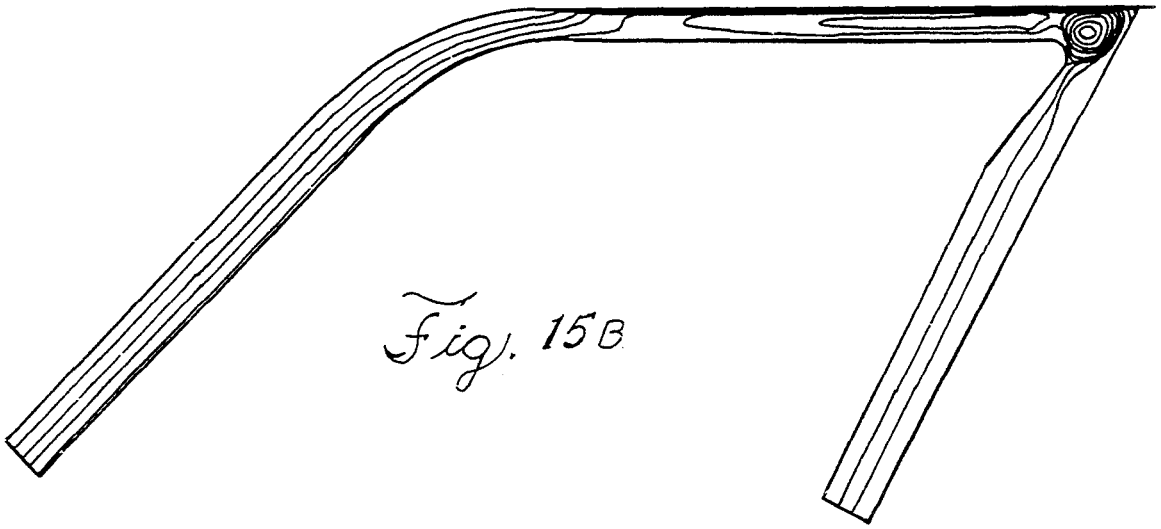

Fig. 15B

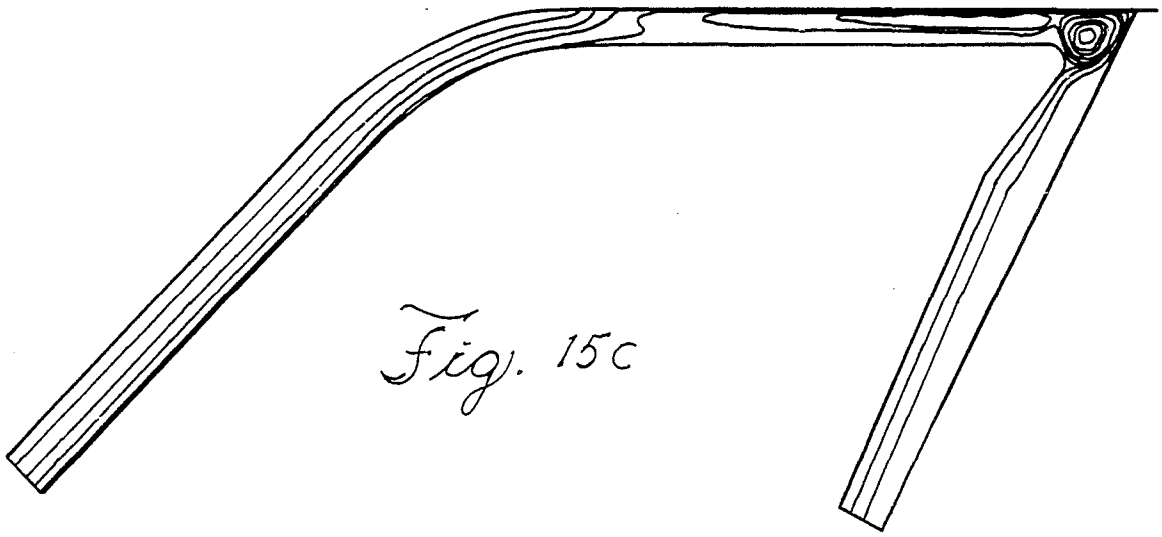

Fig. 15C

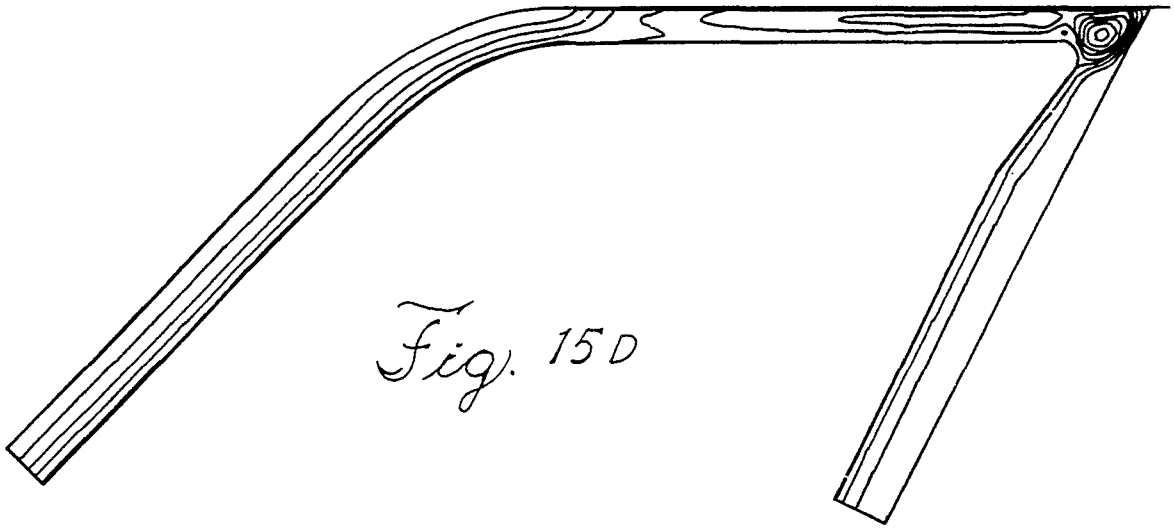

Fig. 15D

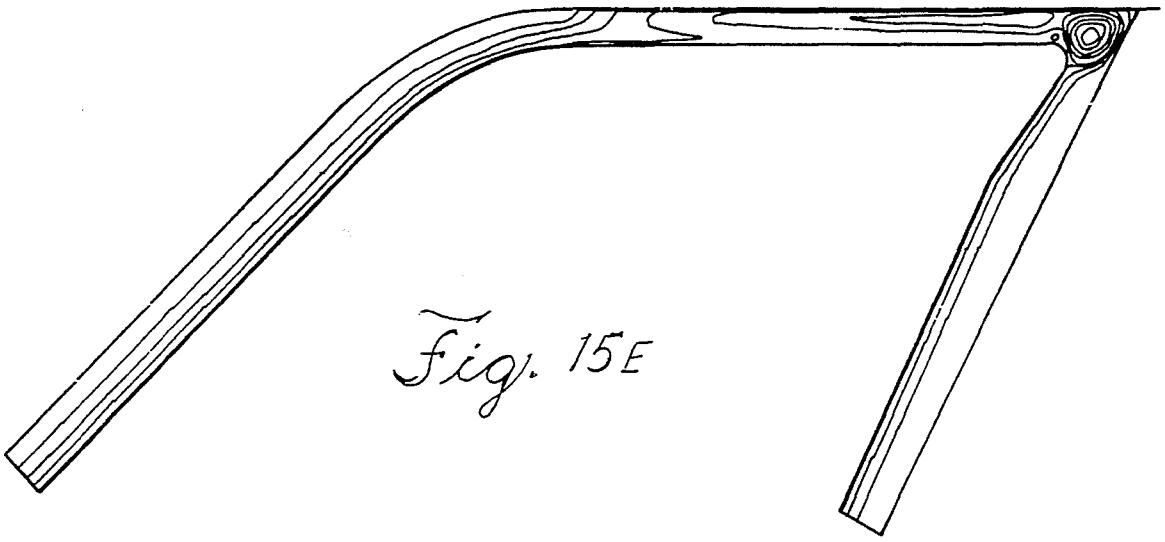

Fig. 15E

Fig. 16A

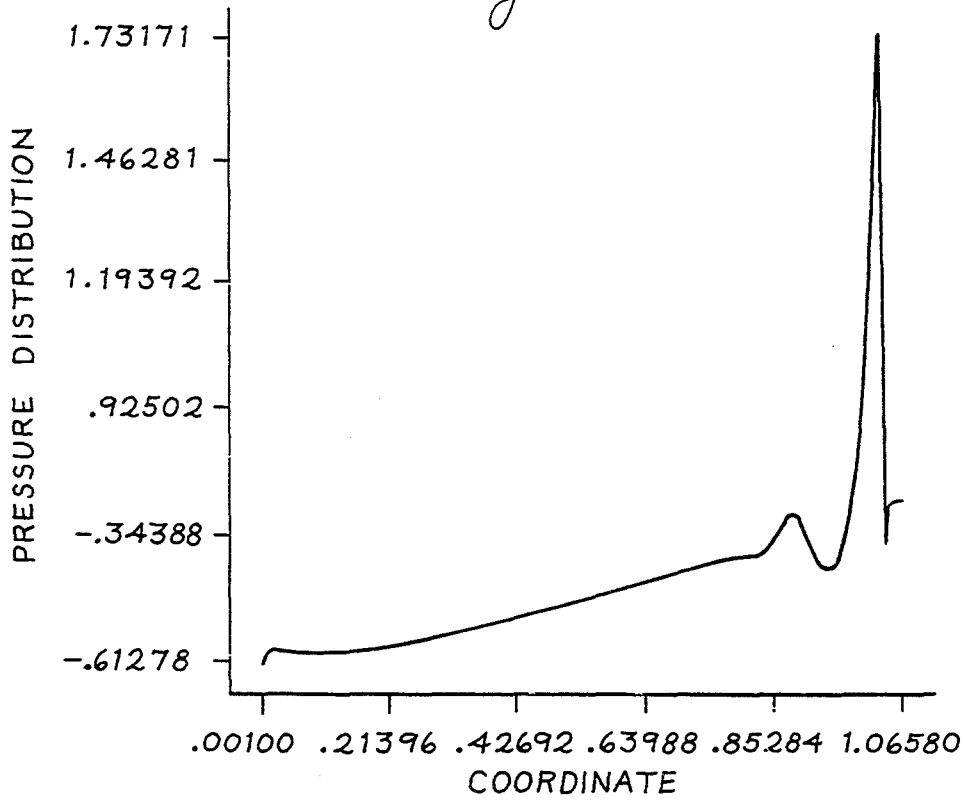

Fig. 16B

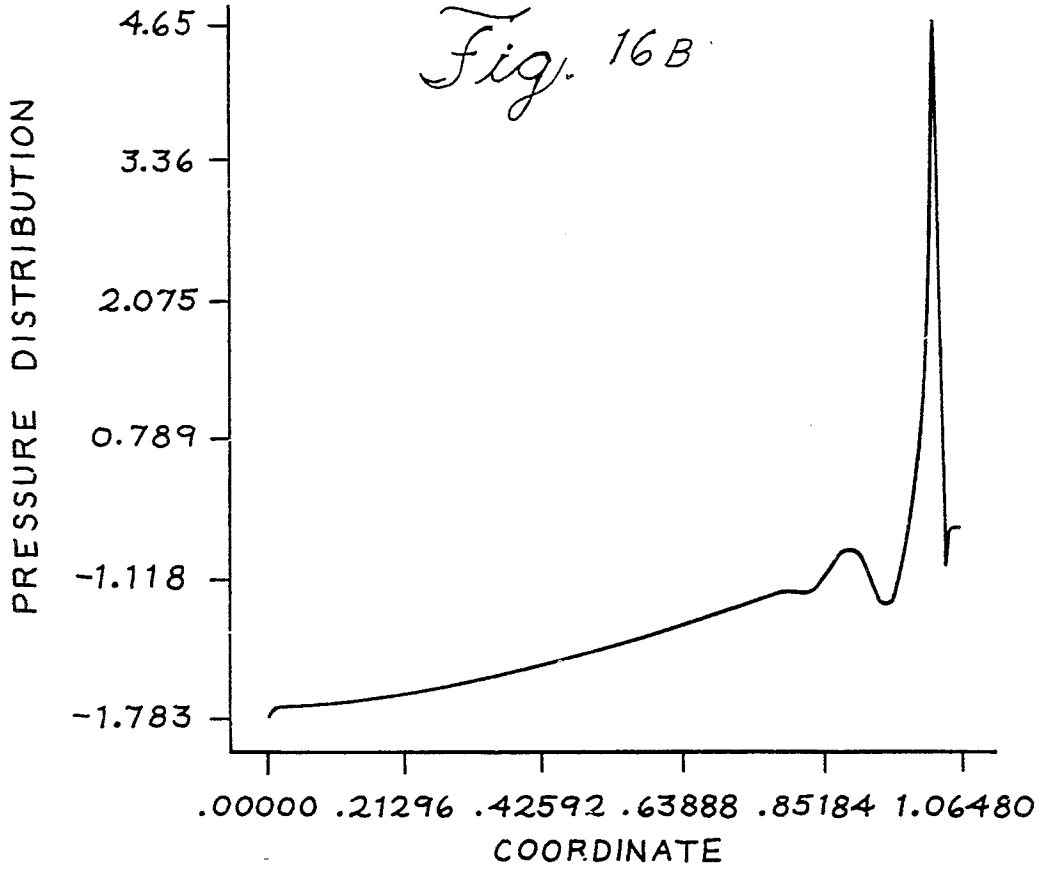

Fig. 16C

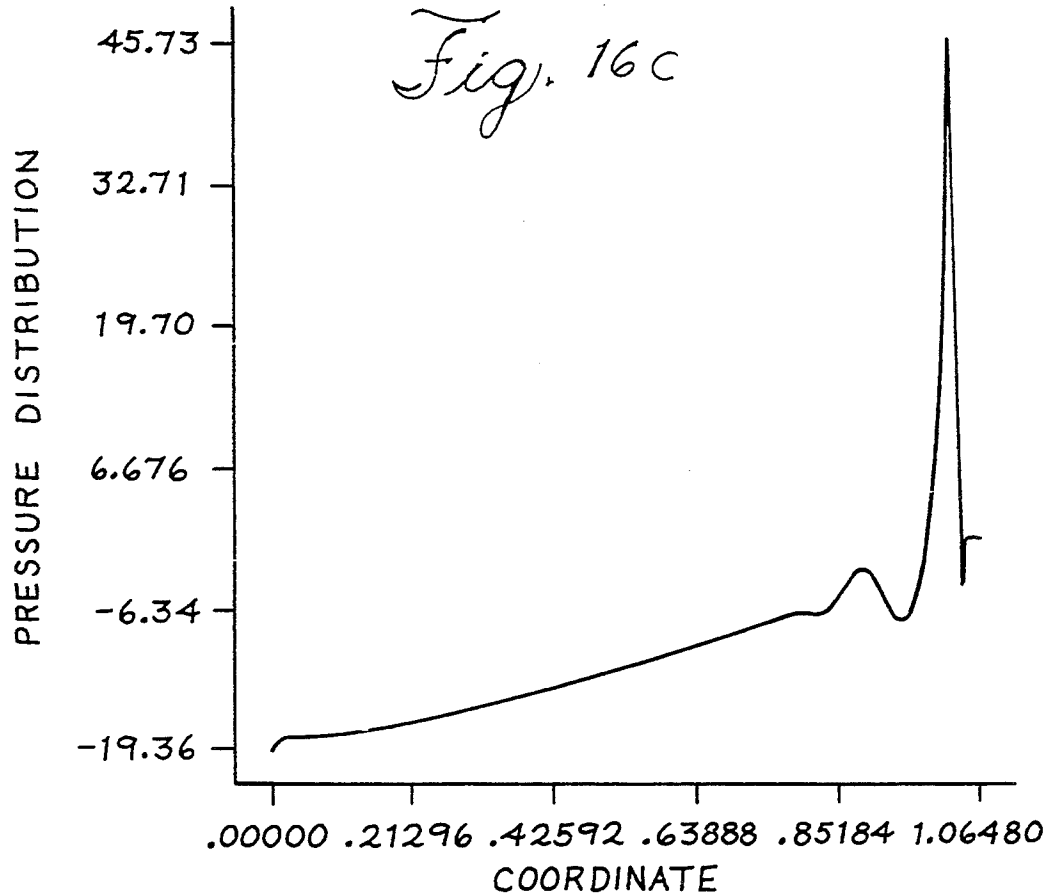

Fig. 16D

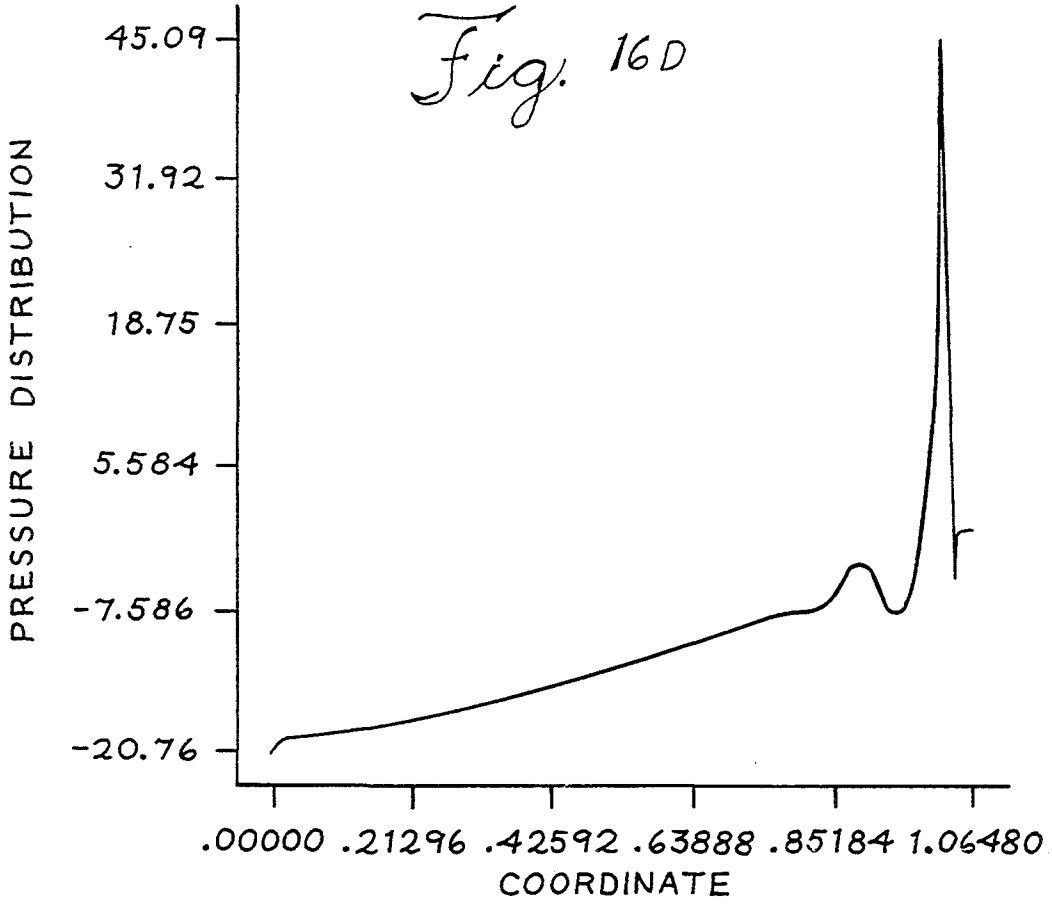

Fig. 16E

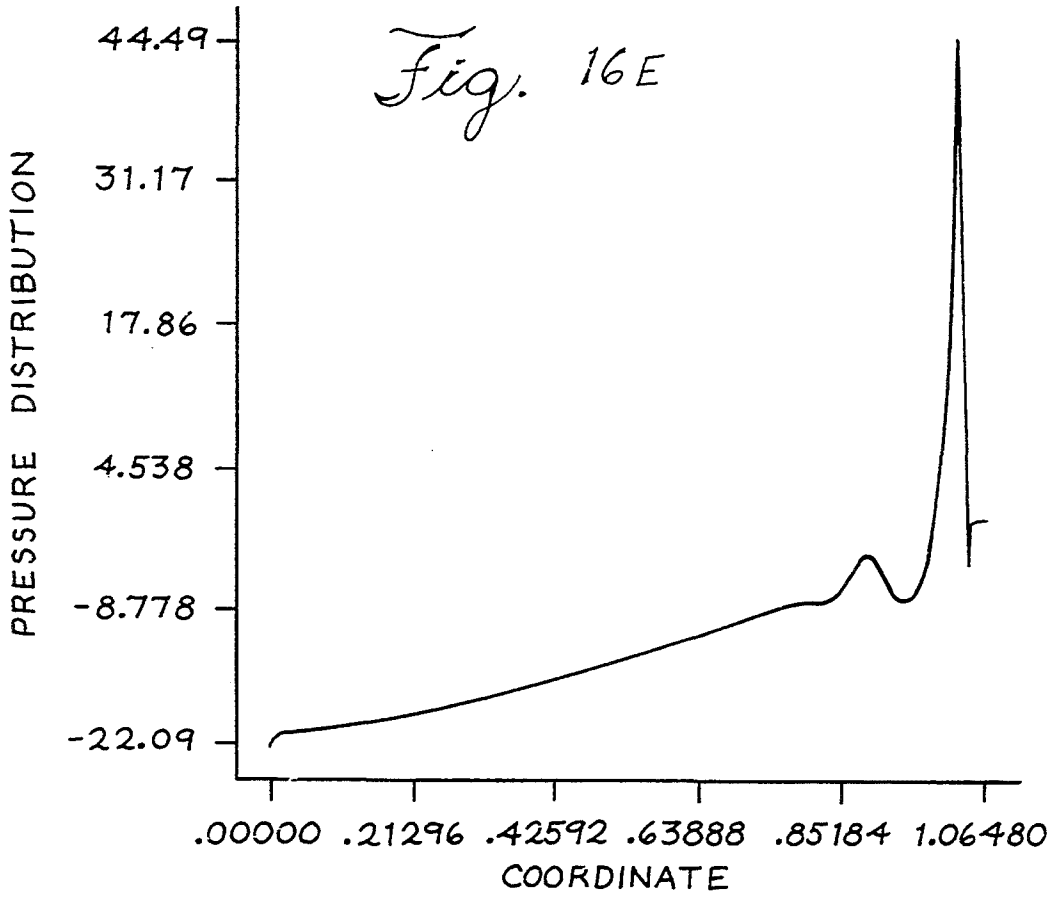

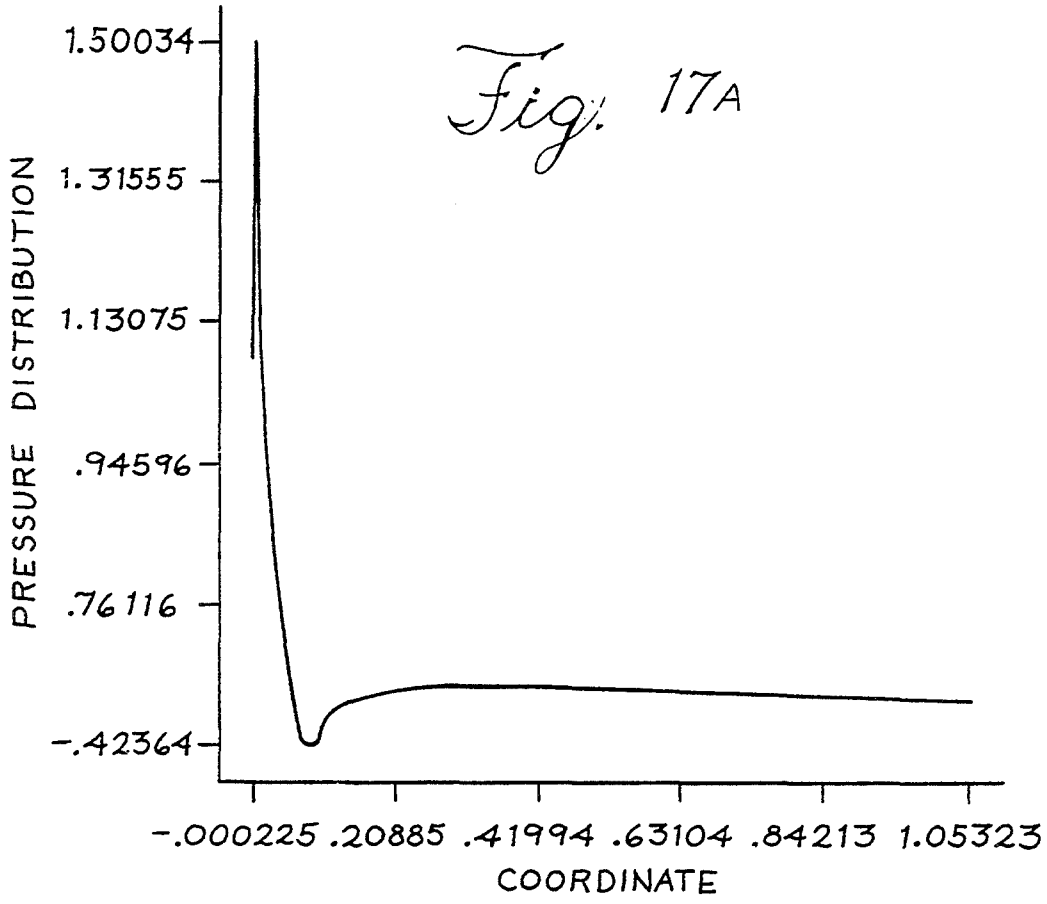

Fig. 17A

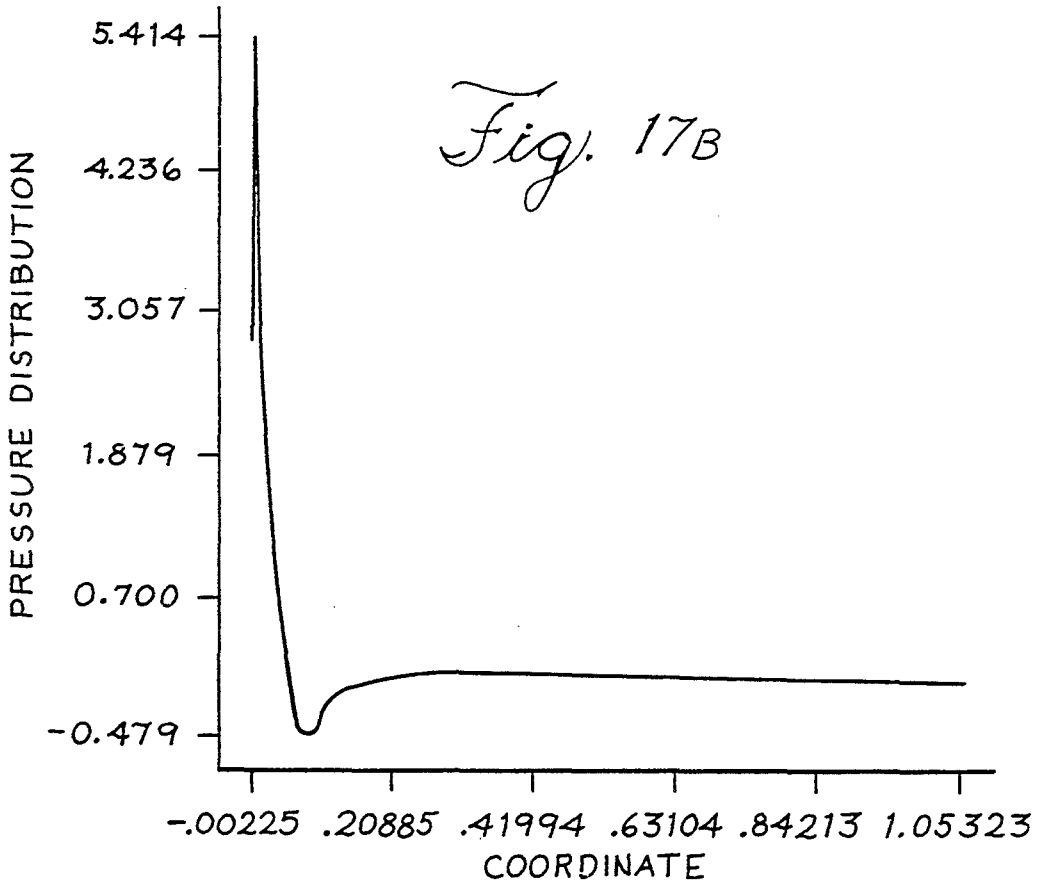

Fig. 17B

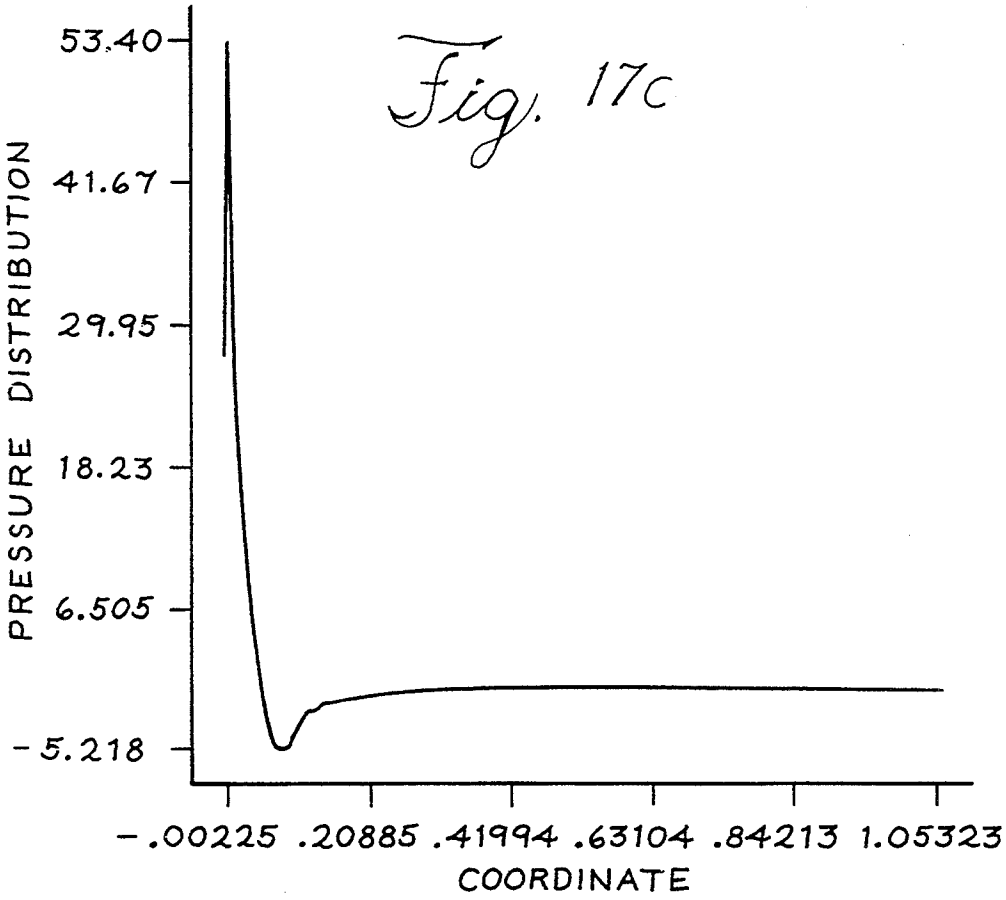

Fig. 17C

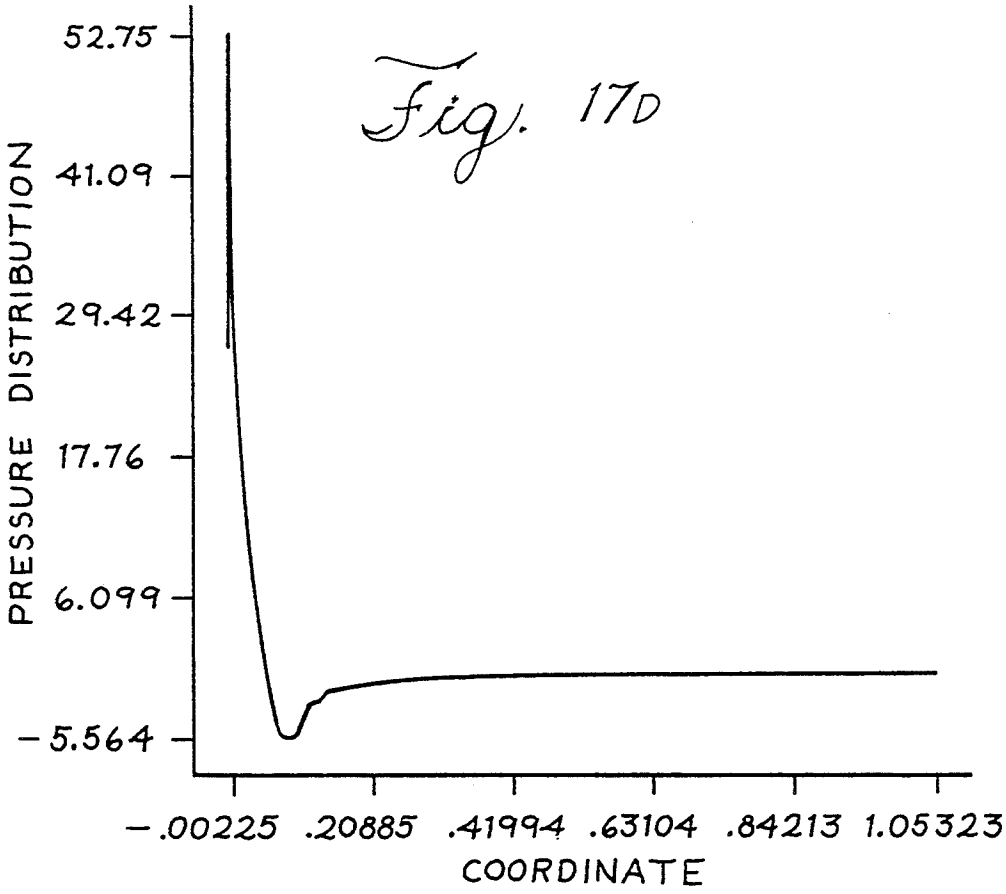

Fig. 17D

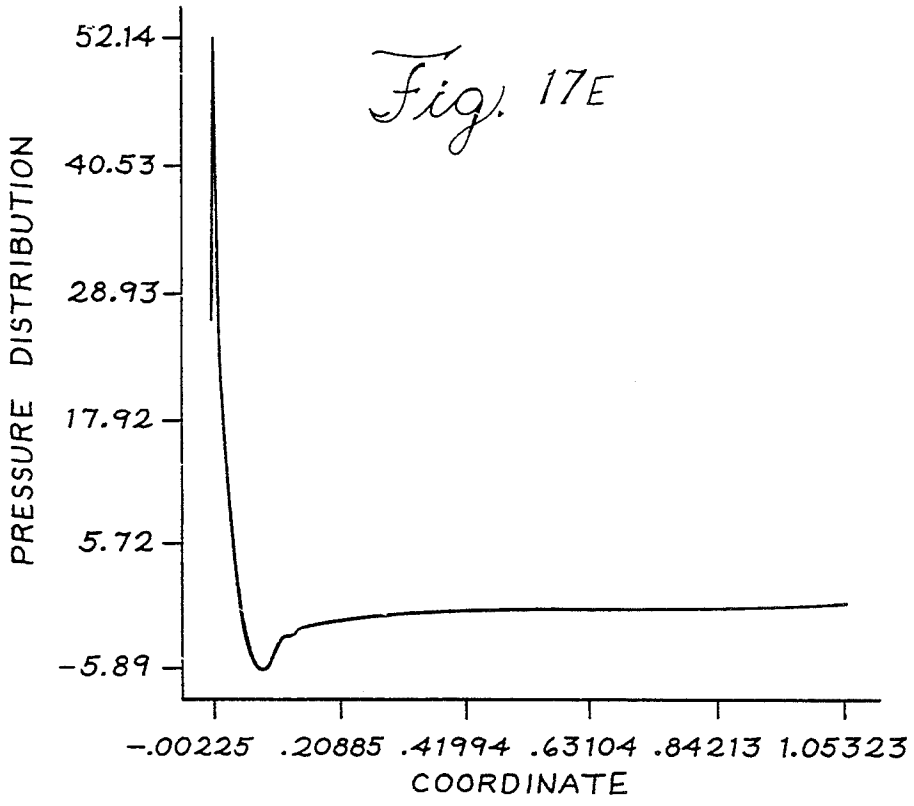

Fig. 17E

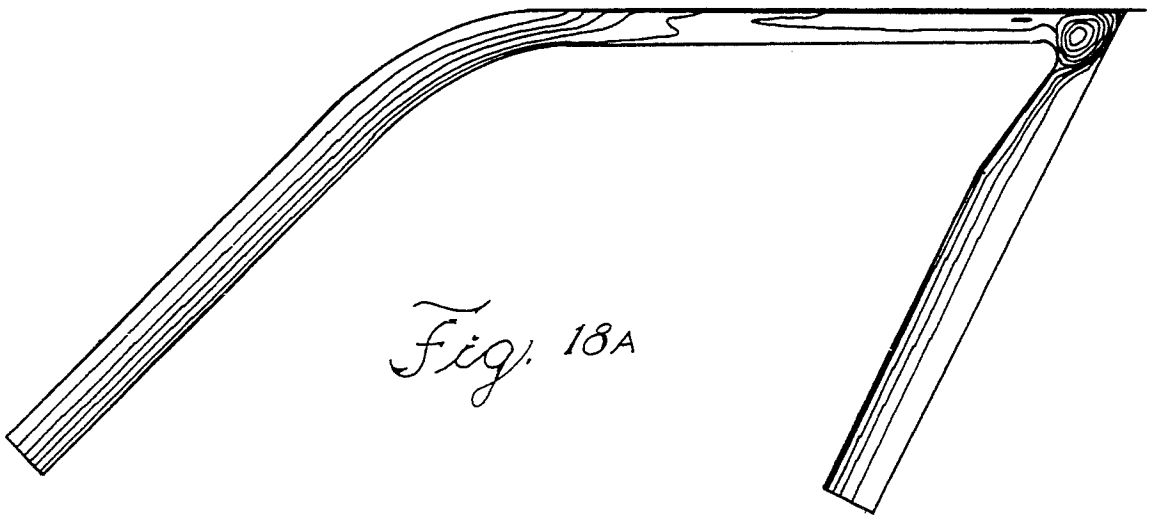

Fig. 18A

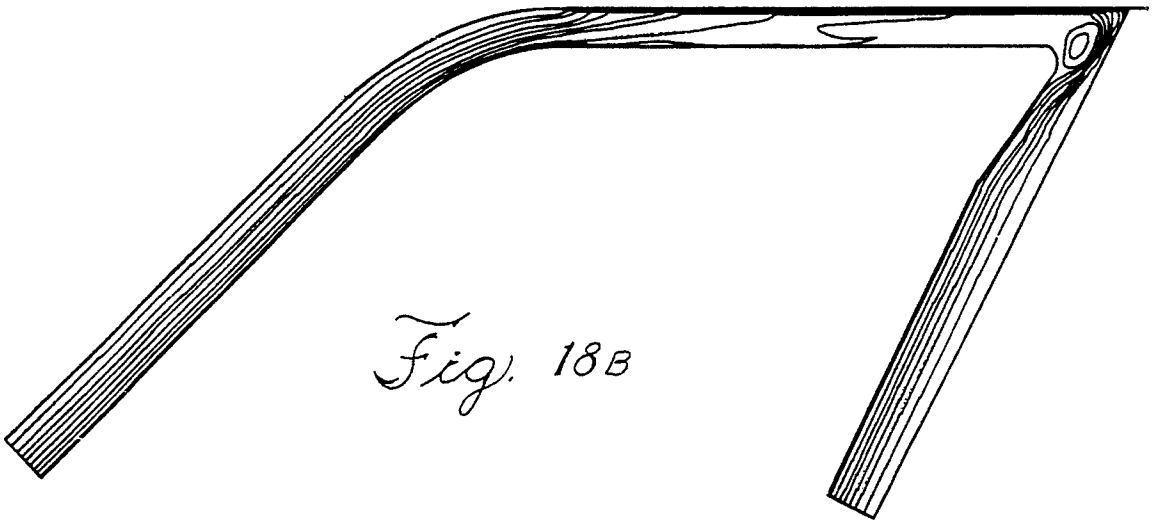

Fig. 18B

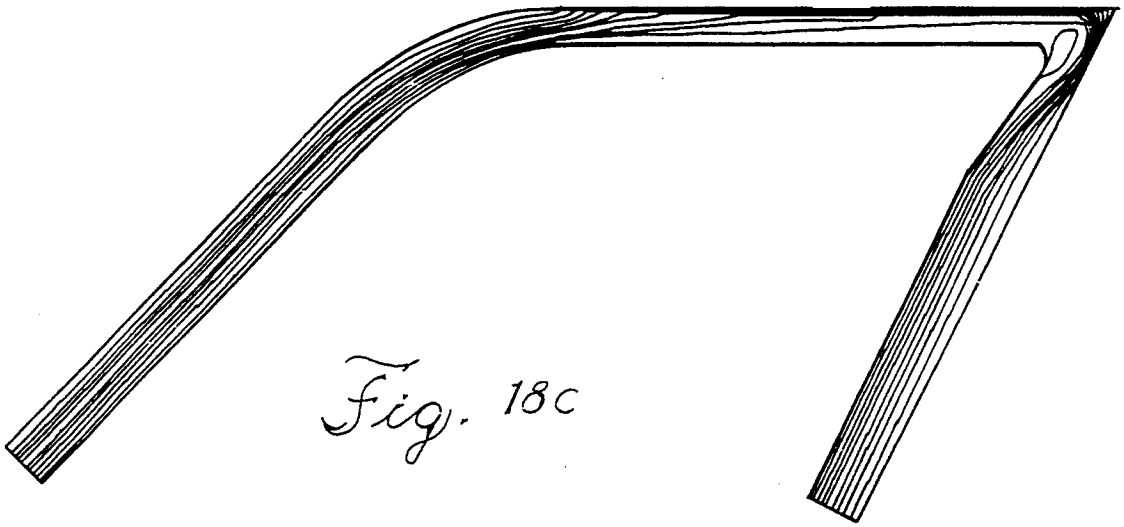

Fig. 18C

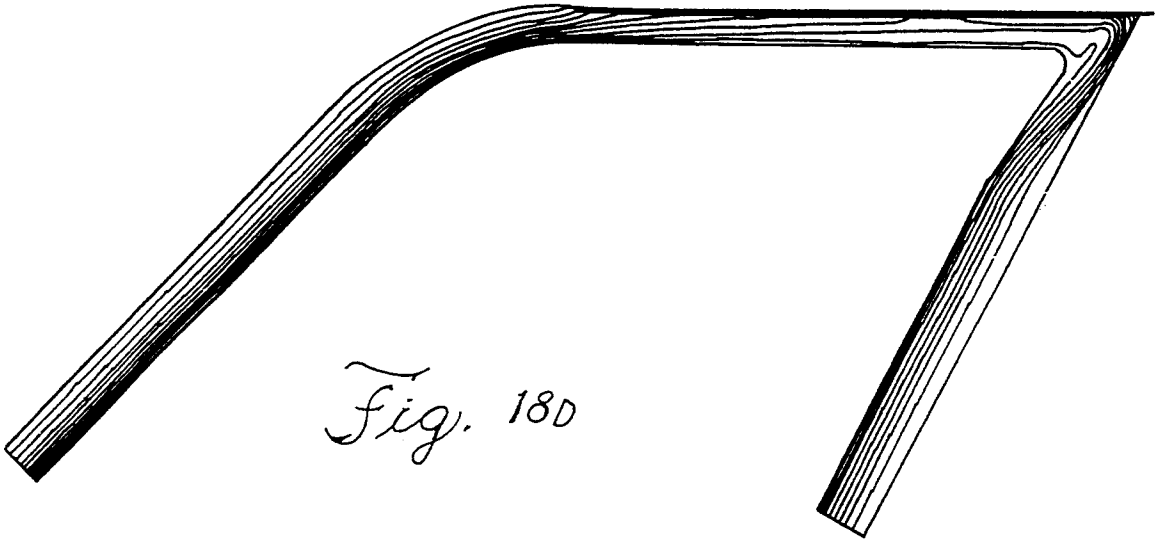

Fig. 18D

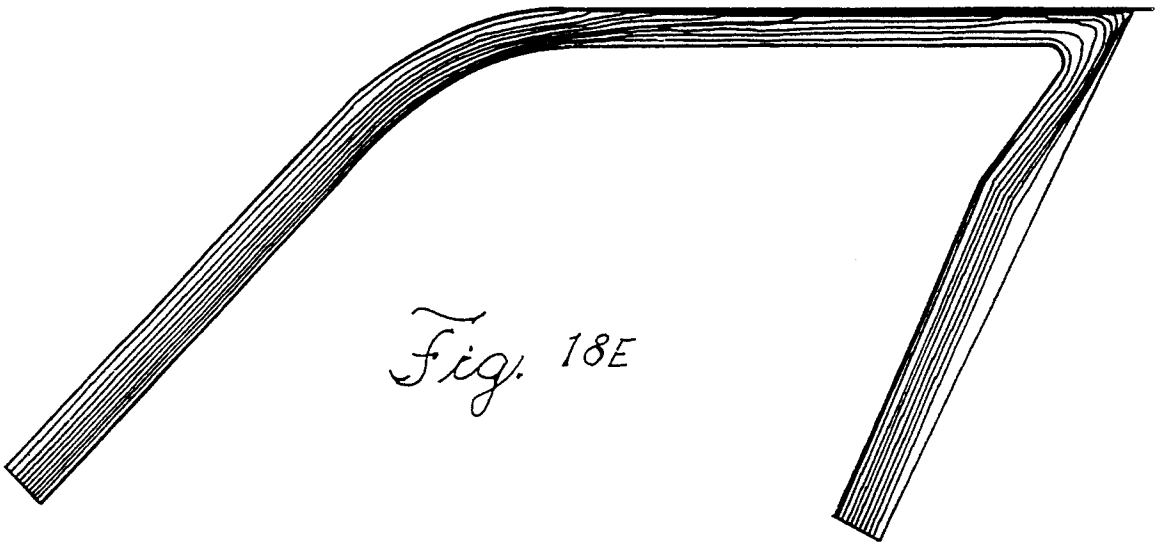

Fig. 18E

Fig. 19A

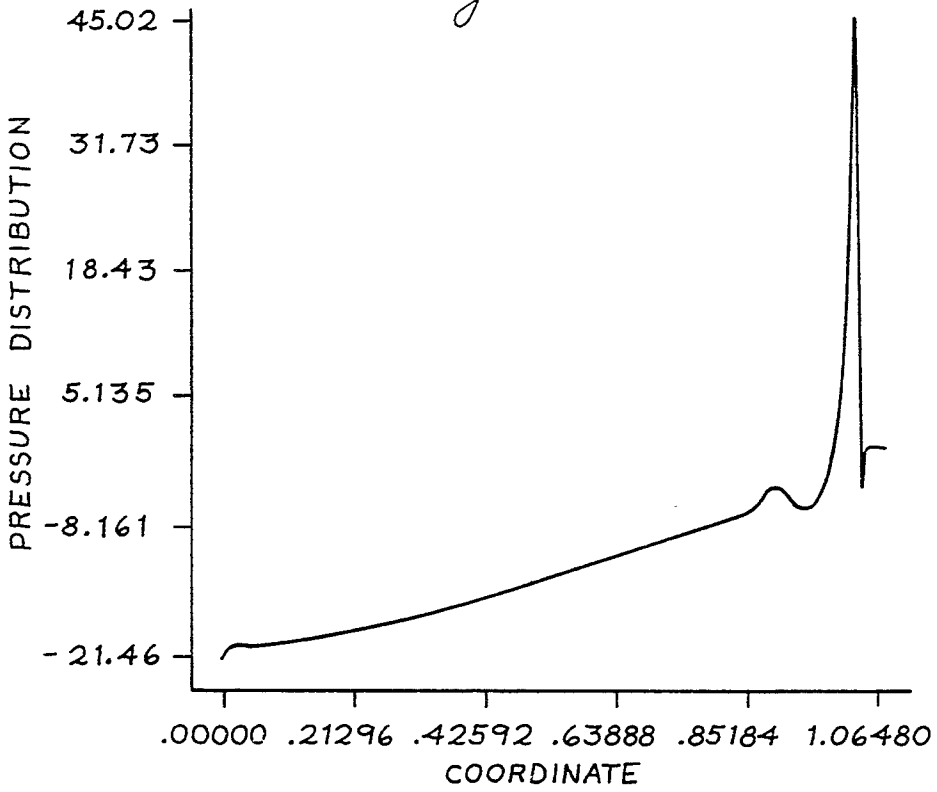

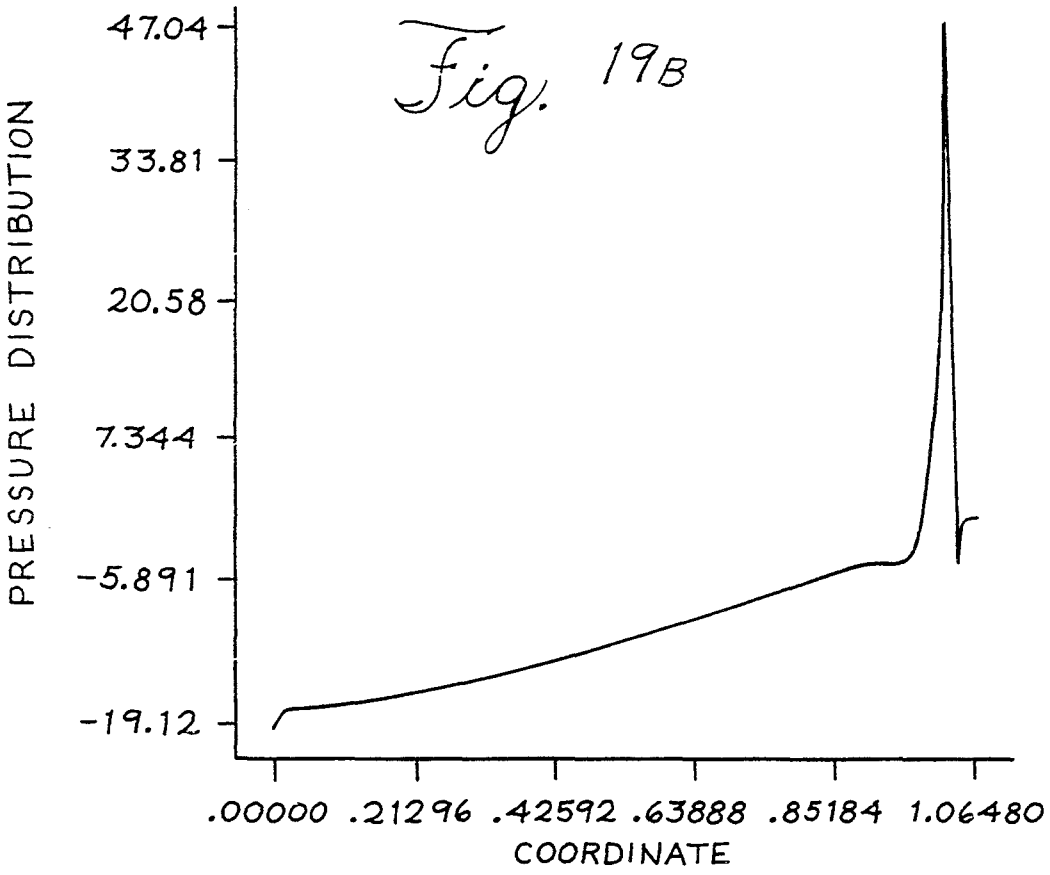

Fig. 19B

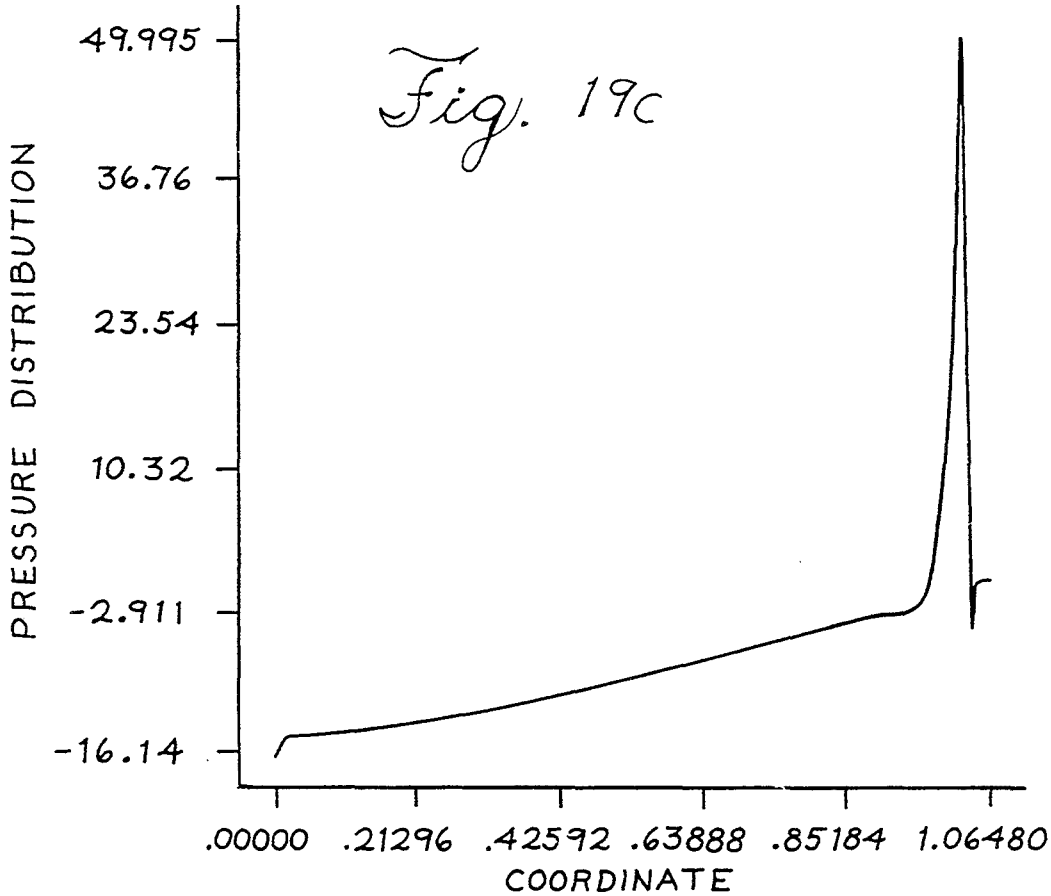

Fig. 19C

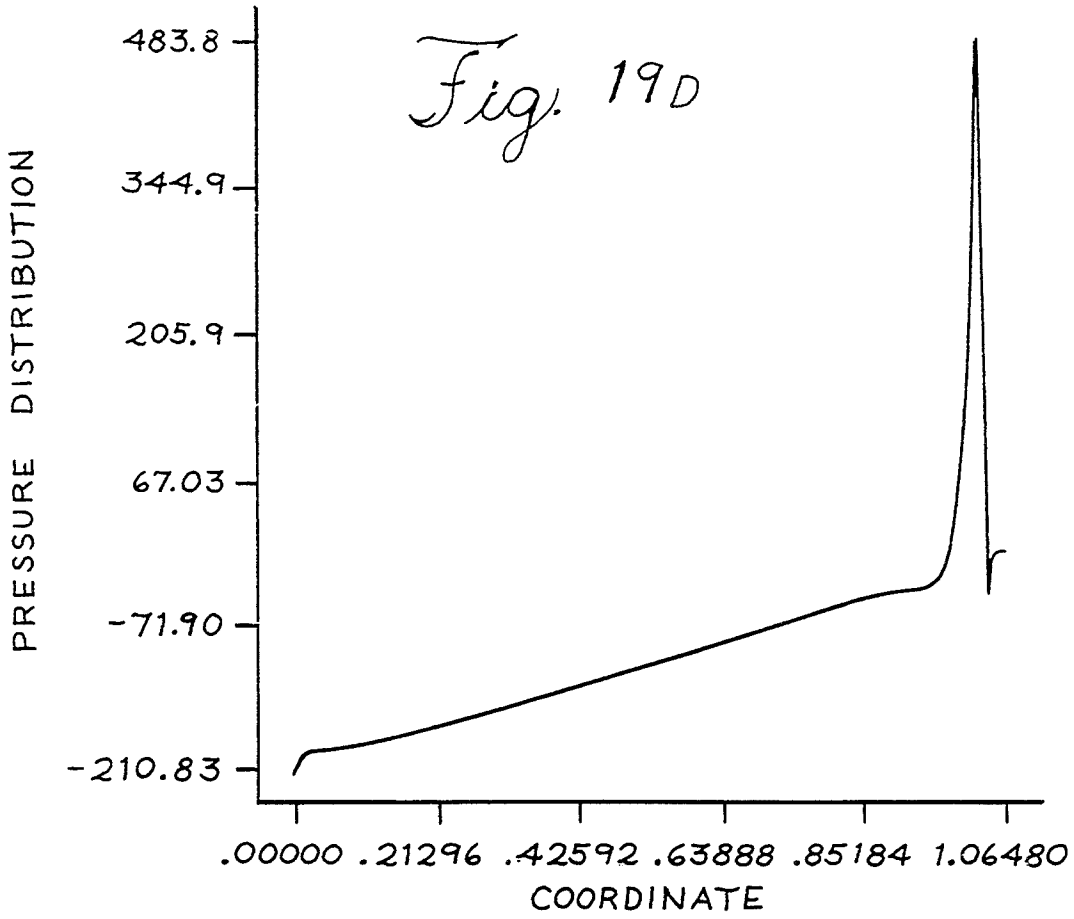

Fig. 19D

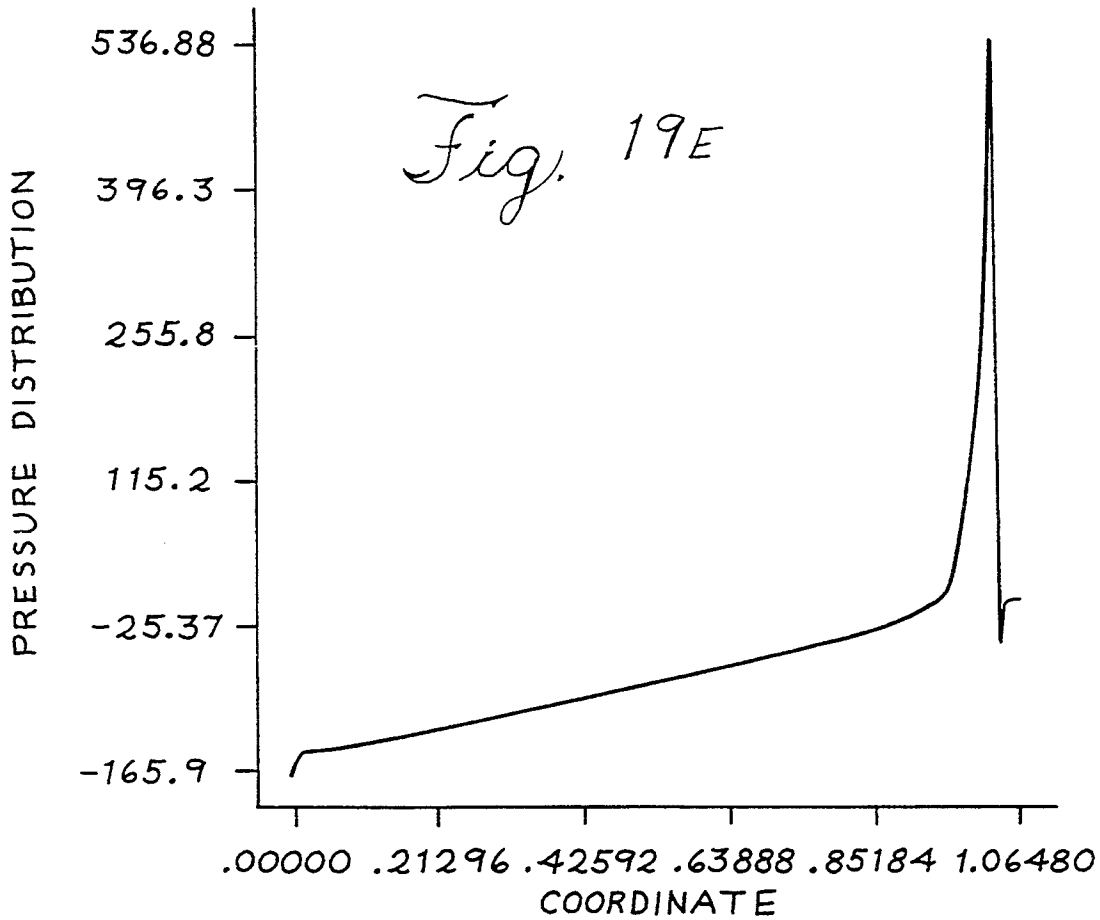

Fig. 19E

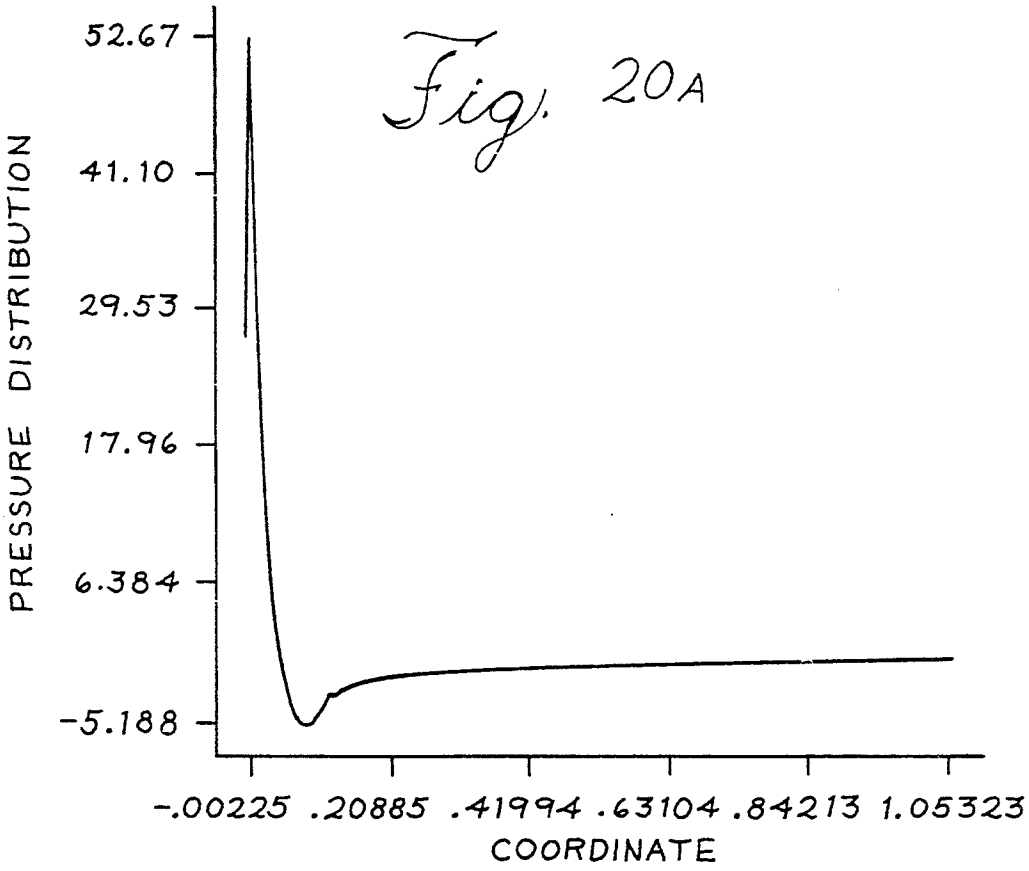

Fig. 20A

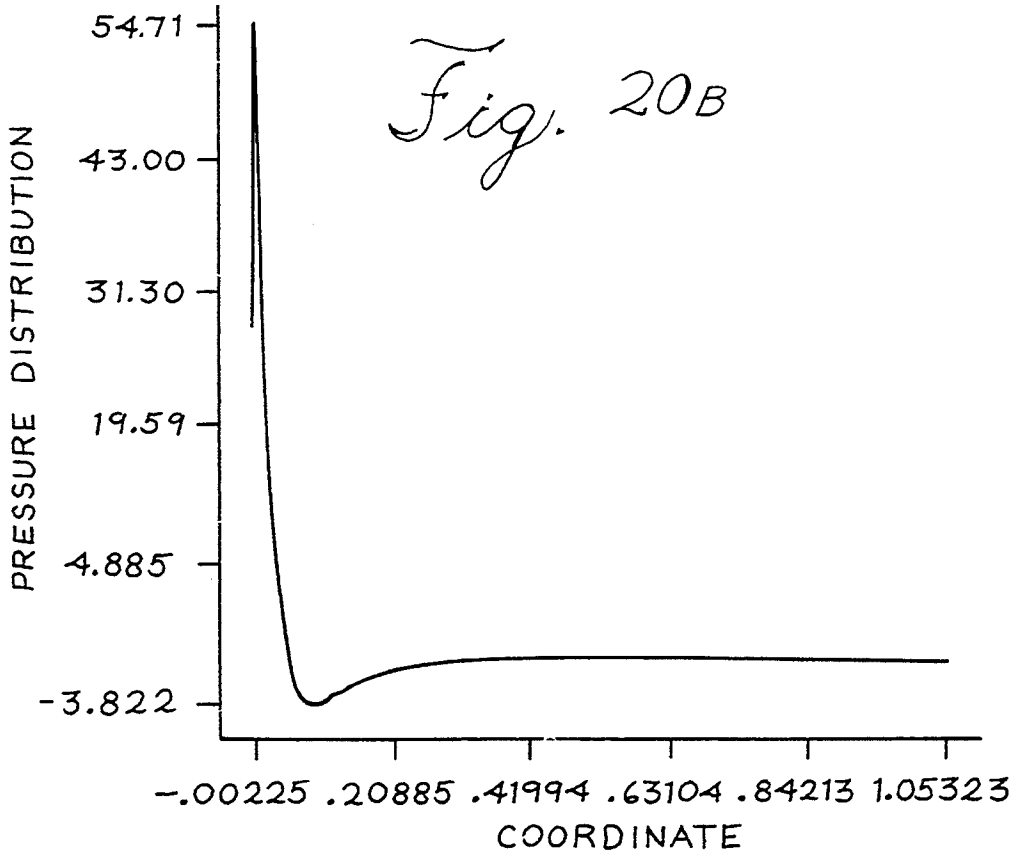

Fig. 20B

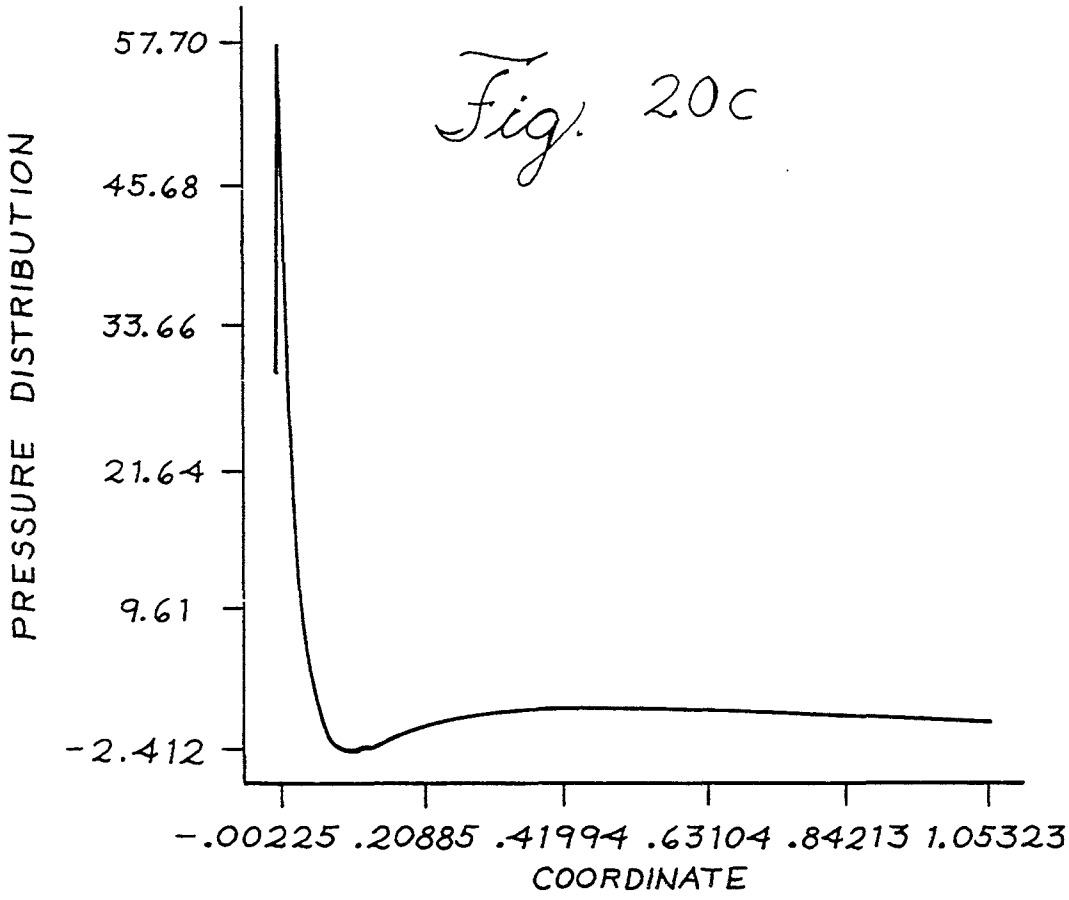

Fig. 20C

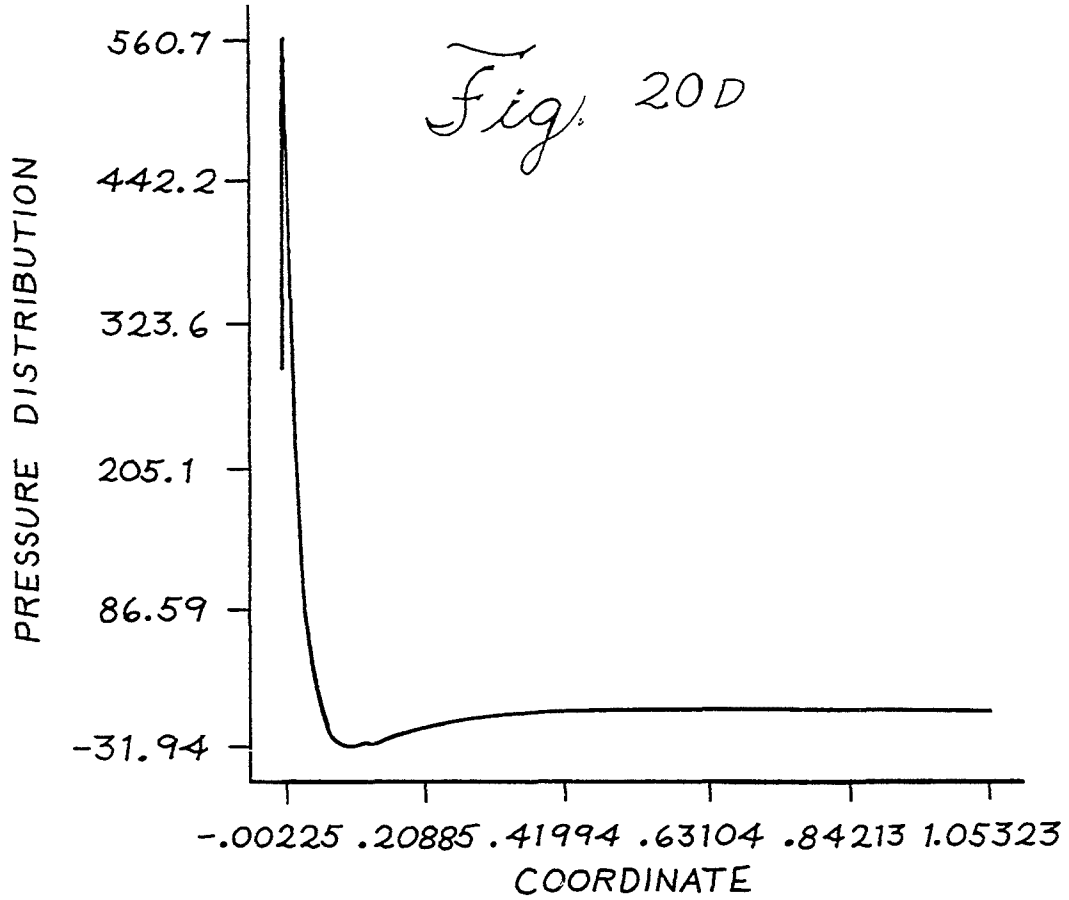

Fig. 20D

Fig. 20E

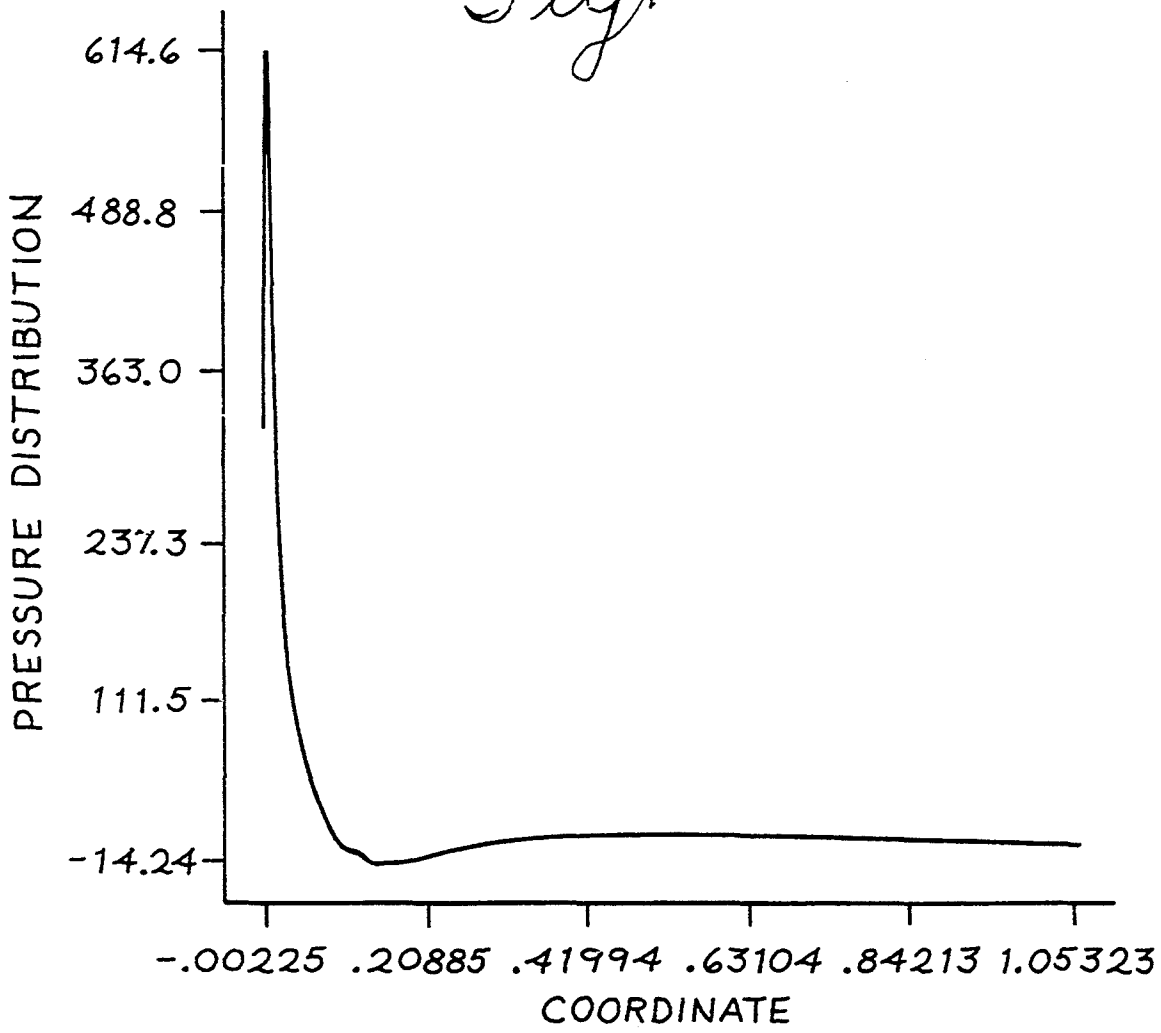
614.6
488.8
363.0
237.3
111.5
-14.24
PRESSURE DISTRIBUTION
-.00225 .20885 .41994 .63104 .84213 1.05323
COORDINATE

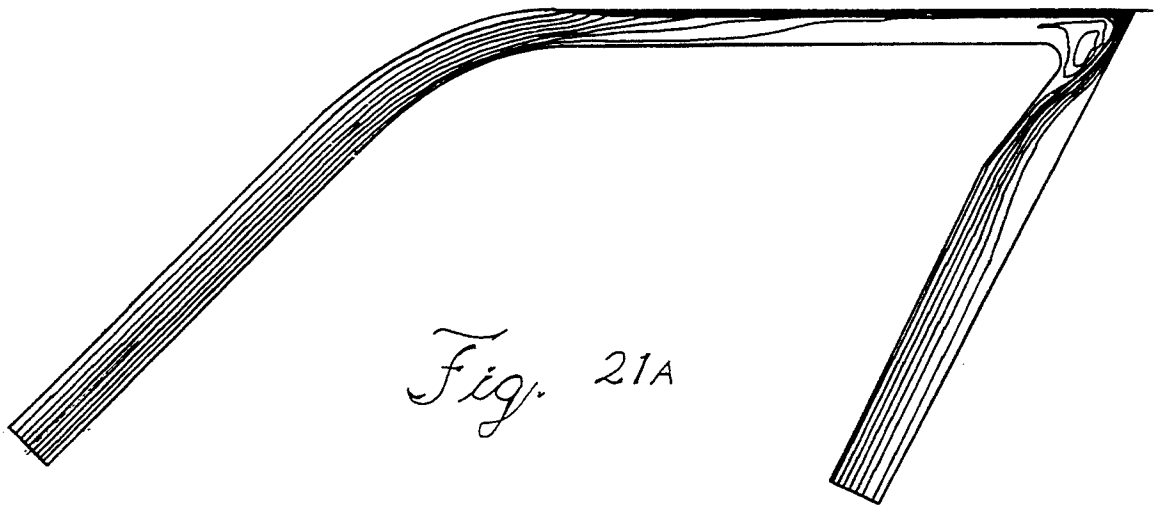

Fig. 21A

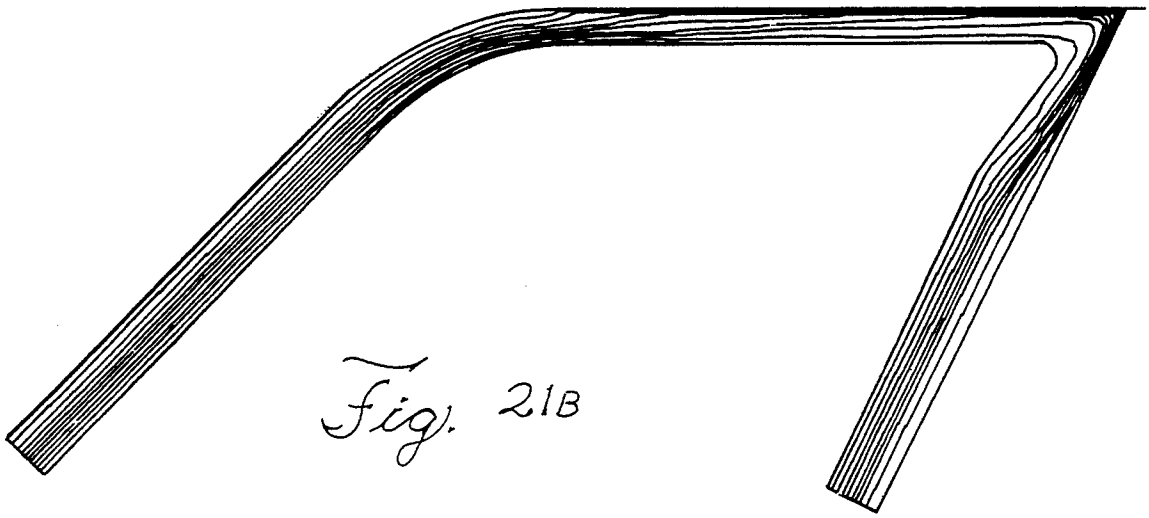

Fig. 21B

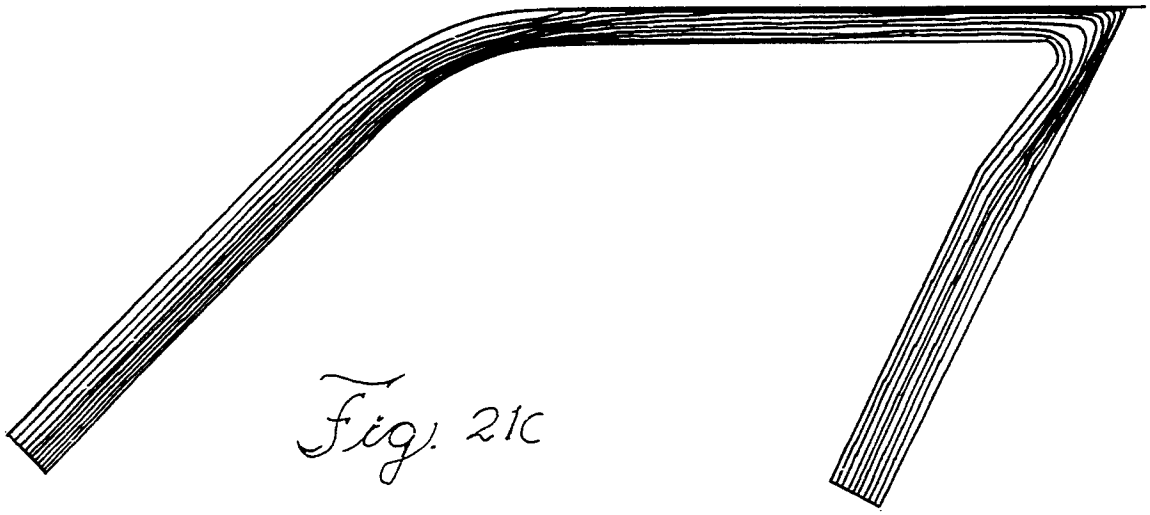

Fig. 21C

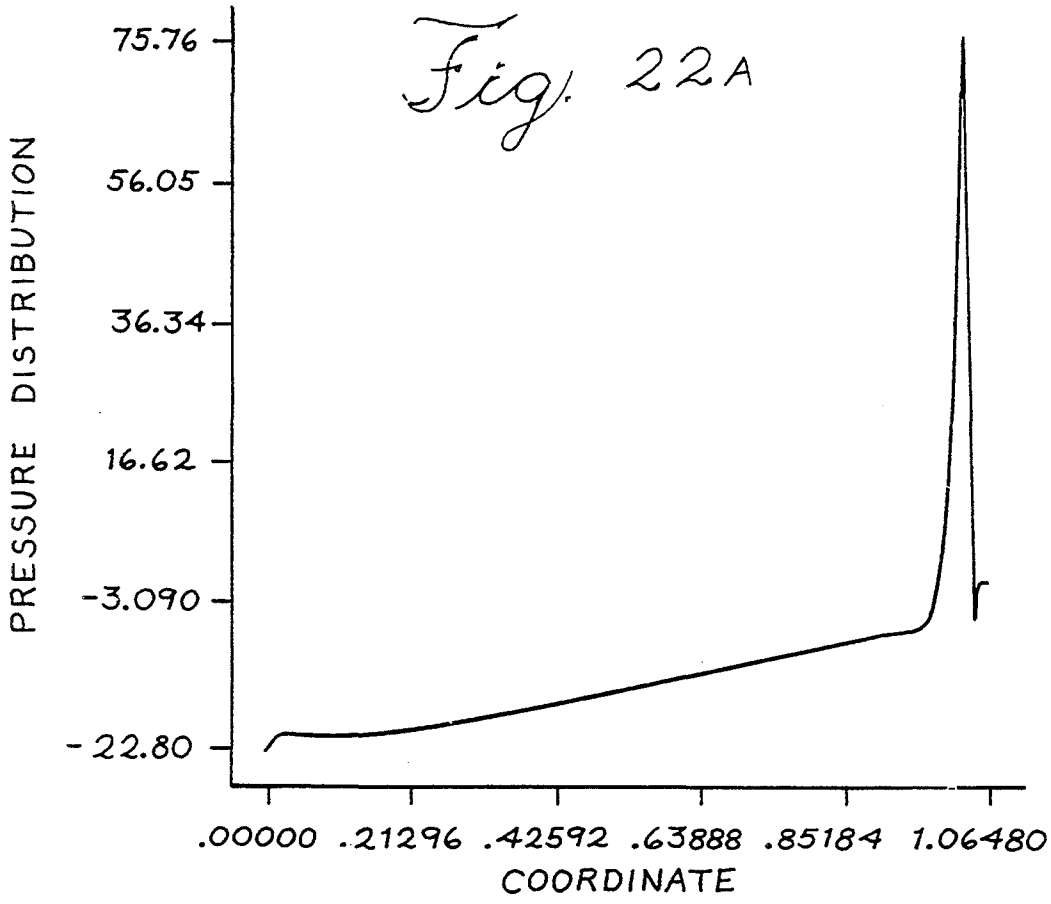

Fig. 22A

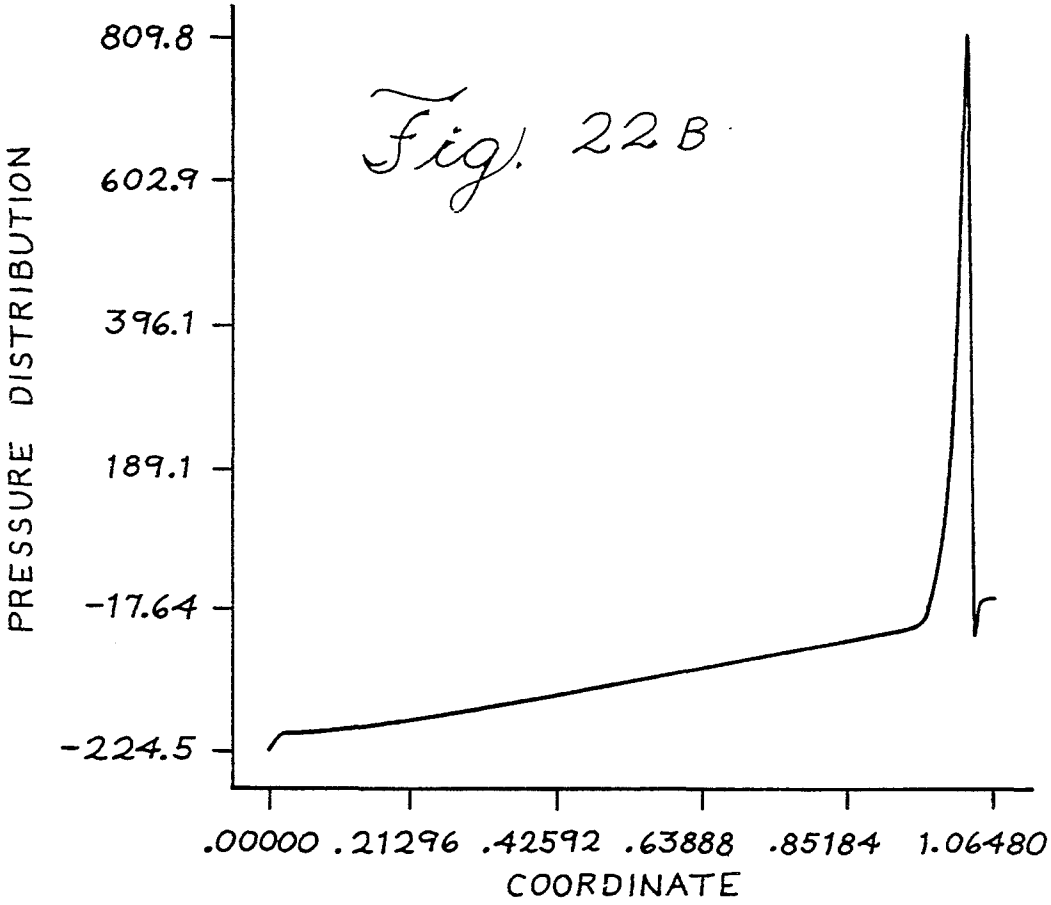

Fig. 22B

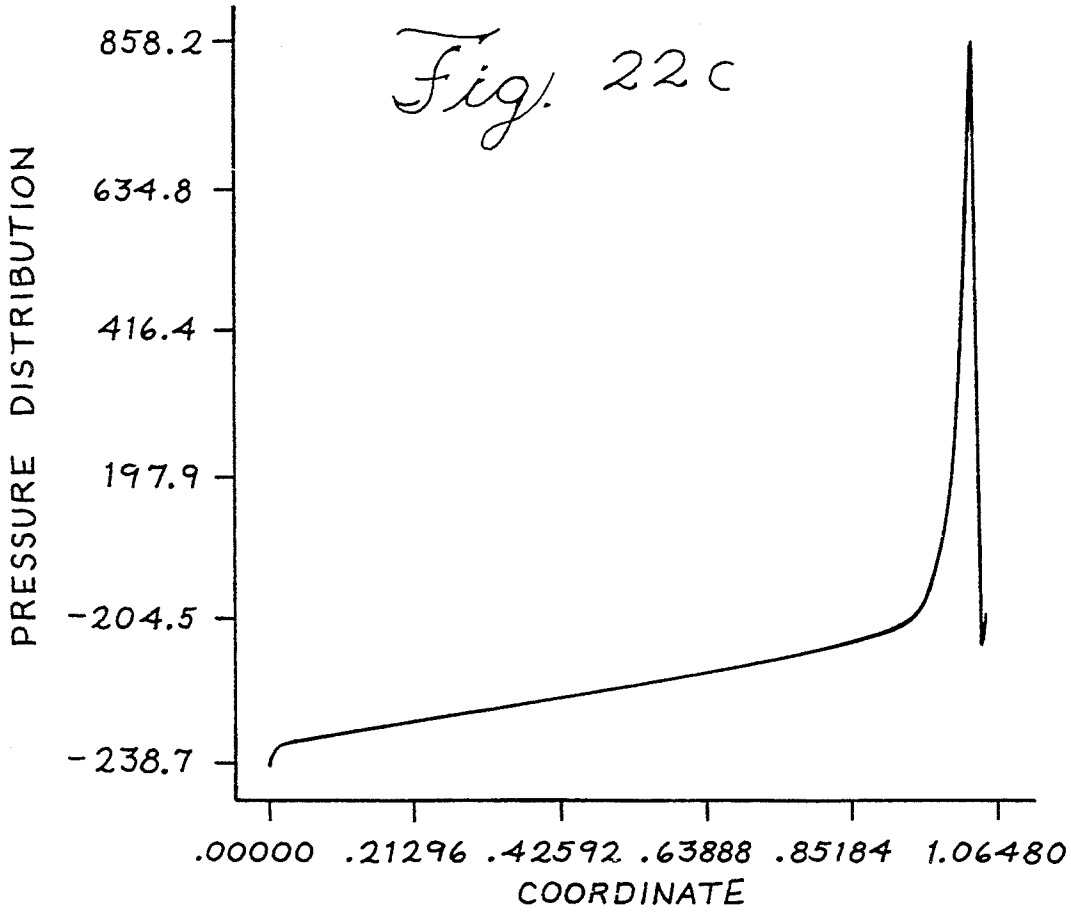

Fig. 22C

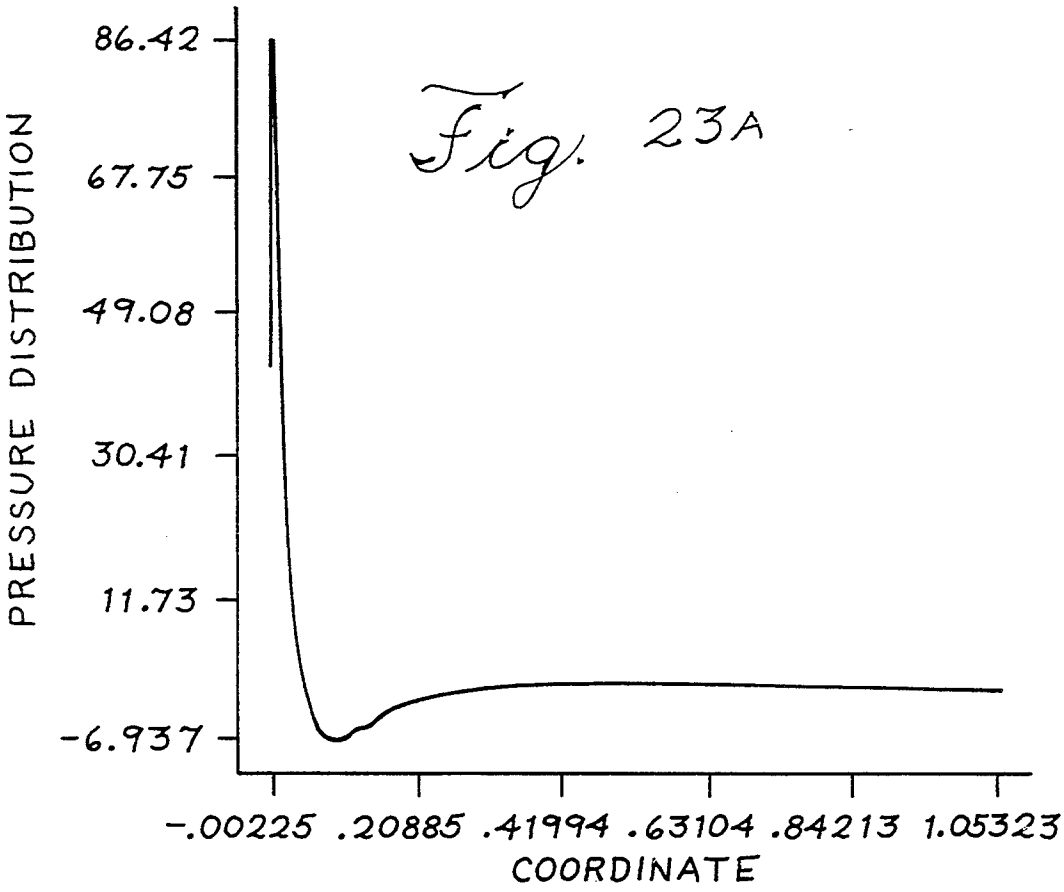

Fig. 23A

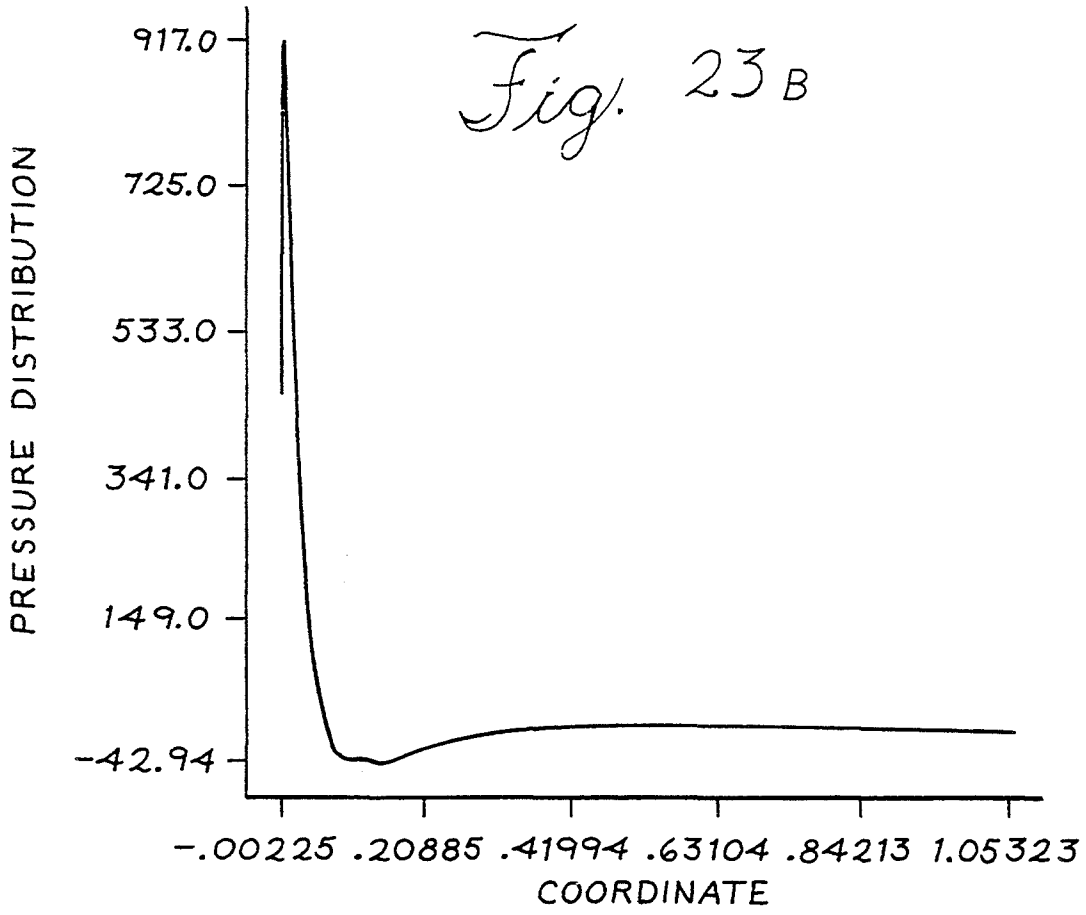

Fig. 23B

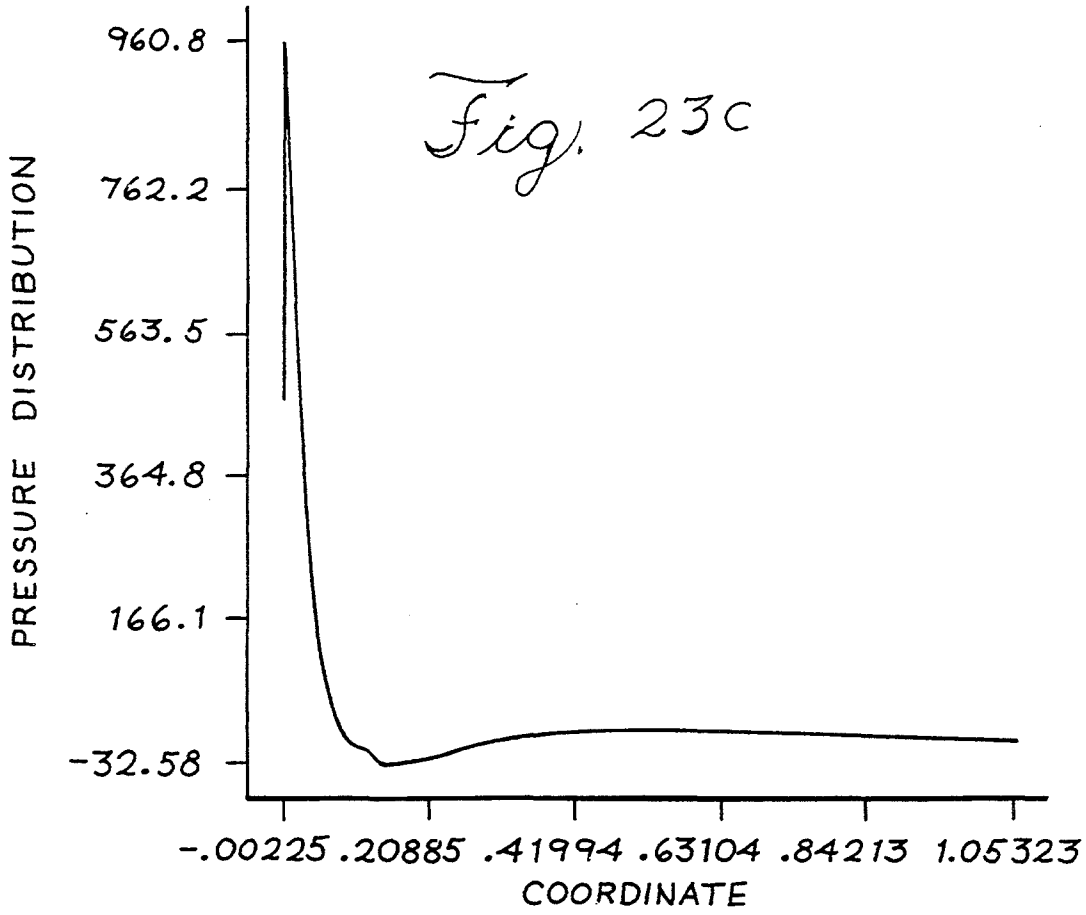

Fig. 23C

FLOTATION COATING DEVICE FOR TRAVELING WEBS

CROSS-REFERENCE TO RELATED APPLICATION

This application is a continuation-in-part of application Ser. No. 881,512, filed May 12, 1992, which is a continuation-in-part of application Ser. No. 849,530 filed Mar. 11, 1992, now abandoned.

FIELD OF THE INVENTION

The present invention relates generally to a coating device for uniform coating of a traveling web of material. More particularly, the present invention relates to a short-dwell coater which eliminates the captive pond associated with short dwell coaters and provides the coating material in the form of a flowing stream of coating material which flows in the same direction as the web movement.

BACKGROUND OF THE INVENTION

One of the most significant changes in light weight coated (LWC) paper production is the use of the short-dwell coater. The short-dwell coater has enabled the paper maker to improve productivity while maintaining coated paper quality. The term "short-dwell" refers to the relatively short period of time that the coating is in contact with a web of paper material before the excess is metered off by a trailing doctor blade. As shown in FIG. **1**, prior art short-dwell coaters consist of a captive pond **21** just prior to the doctor blade **23**. The pond is approximately 5 cm in length and is slightly pressurized to promote adhesion of the coating to the paper web **25**. The excess coating supplied to the sheet creates a backflow of coating **27**. This coating backflow excludes to some extent the boundary layer of air entering with the sheet and eliminates skip coating. The excess coating is channeled over an overflow baffle **29** and collected in a return pan before returning to tanks to be screened.

While short-dwell coaters are extensively used in coating paper webs, such coaters suffer from a major problem. The flow in the coating chamber of the pond upstream of the doctor blade contains recirculating eddies or vortices which can result in coat-weight nonuniformities and wet streaks or striations in several ways. For example, these eddies can become unstable due to centrifugal forces and result in the generation of unsteady flow and rapidly fluctuating vortices, which deteriorate the coating uniformity and its quality. Also, the vortices tend to entrap small air bubbles which result in the buildup of relatively large air inclusions in the coating liquid which tend to accumulate in the core region of the eddies. Vortex fluctuations tend to force these air inclusions into the blade gap. This adversely affects the coating quality. Usually, the presence of air inclusions results in regions of lower coat weight which are 2–4 cm wide and about 10–100 cm long, known in the industry as "wet streaks". These problems are discussed in an article "*Principles of Hydrodynamic Instability: Application in Coating Systems*", C. K. Aidun, Tappi Journal, Vol. 74, No. 3, March, 1991.

It would be desirable to provide a coating device which has the coating advantages of a short-dwell coater, but which did not have the problems associated with recirculating eddies or vortices and the entrapment of air pockets or air bubbles in the core of the vortices.

Accordingly, it is a principal object of the present invention to provide a vortex free short-dwell coating device.

These and other objects will become more apparent from the following description and the appended claims.

BRIEF DESCRIPTION OF THE DRAWINGS

FIG. **1** is a schematic cross-sectional view of a prior art short-dwell coating device;

FIG. **2** is a schematic cross-sectional view of an embodiment of a short-dwell coating device;

FIG. **3** is a schematic cross-sectional view of another embodiment of the short-dwell coating device;

FIG. **4** is a schematic cross-section of a further embodiment of the short-dwell coating device;

FIGS. **5A**, **5B**, **5C** and **5D** are sketches of an embodiment of a blade coating apparatus having a moving applicator wall in accordance with the present invention;

FIGS. **6A–6G** illustrate flow characteristics for cases **B1** to **B7** of Table 2;

FIGS. **7A–7G** illustrate pressure distribution along the substrate for cases **B1** to **B7** of Table 2;

FIGS. **8A–8G** illustrate pressure distribution along the blade for cases **B1** to **B7** of Table 2;

FIGS. **9A–9E** illustrate flow characteristics for cases **C11** to **C15** of Table 3;

FIGS. **10A–10E** illustrate pressure distribution along the substrate for cases **C11** to **C15** of Table 3;

FIGS. **11A–11E** illustrate pressure distribution along the blade for cases **C11** to **C15** of Table 3;

FIGS. **12A–12D** illustrate flow characteristics for cases **N1** to **N4** of Table 4;

FIGS. **13A–13D** illustrate pressure distribution along the substrate for cases **N1** to **N4** of Table 4.

FIGS. **14A–14D** illustrate pressure distribution along the blade for cases **N1** to **N4** of Table 4.

FIGS. **15A–15E** illustrate flow characteristics for cases **NB31** to **NB35** of Table 5.

FIGS. **16A–16E** illustrate pressure distribution along the substrate for cases **NB31** to **NB35** of Table 5.

FIGS. **17A–17E** illustrate pressure distribution along the blade for cases **NB31** to **NB35** of Table 5.

FIGS. **18A–18E** illustrate flow characteristics for cases **NB51** to **NB55** of Table 6.

FIGS. **19A–19E** illustrate pressure distribution along the substrate for cases **NB51** to **NB55** of Table 6;

FIGS. **20A–20E** illustrate pressure distribution along the blade for cases **NB51** to **NB55** of Table 6;

FIGS. **21A–21C** illustrate flow characteristics for cases **NB61** to **NB63** of Table 6;

FIGS. **22A–22C** illustrate pressure distribution along the substrate for cases **NB61** to **NB63** of Table 6; and

FIGS. **23A–23C** illustrate pressure distribution along the blade for cases **NB61** to **NB63** of Table 6.

SUMMARY OF THE INVENTION

The present invention is directed to a coating device for application of coating material to the surface of a web or a flexible substrate. The coating device contains a pressurized channel where a flowing stream of the coating liquid first comes into contact with the substrate. The coating liquid enters the channel at the upstream side and wets the substrate as it flows in the same direction as the substrate. A doctor element is posi-

tioned at the downstream side of the channel where the excess coating in the channel follows the contour of the boundary formed by the doctor element and leaves the channel. The geometry of the streamlined boundaries of the coating device eliminate the formation of recirculating eddies or vortices. The elimination of vortices eliminates flow instability due to centrifugal forces and removes harmful pressure fluctuations which could result in coat-weight nonuniformities. The elimination of recirculating eddies or vortices also removes the possibility of entrapping air pockets or air bubbles in the core of the vortices which could reach the blade gap and could result in coat-weight nonuniformities and wet streaks.

The present invention is further directed toward the study of flow patterns in blade coating to develop high-speed coaters. The walls of the applicator are considered rigid, i.e. they do not deform under the effect of hydrodynamic pressure and shear stress exerted by the flow on the boundaries. One of the applicator walls is designed to be a floating or moving wall or belt. The effect of the floating applicator wall is that recirculating eddies and vortices are reduced.

DETAILED DESCRIPTION OF THE PREFERRED EMBODIMENT

As shown in FIG. **2**, the short-dwell coating device of the present invention consists of a continuous channel of coating material which passes through a coating chamber **51** which is in contact with a web **53** of material which is to be coated. The coating device comprises straight and curvilinear wall sections. For purposes of orientation and discussion, the coating chamber has an upstream side and a downstream side with respect to movement of the web with the upstream side being to the left of FIG. **1**. The use of the terms "horizontal" and "vertical" are with respect to a horizontal orientation of the web. The web, however, is usually supported on a counter roll and has a slight curvature in the region of the coating chamber.

The coating device includes a doctor element **55** which is spaced from the web for defining the thickness of the coating on the web. The doctor element **55** extends across the web transversely to the direction of the web motion. The doctor element also forms a downstream boundary wall of the coating chamber **51** and extends downwardly for a further distance to define the downstream wall of an exit plenum **57**.

An upstream boundary wall **59** defines the upstream side of the coating chamber **51**. The upstream boundary wall **59** extends downwardly for a further distance to define the upstream side of an entrance plenum **61**. The upstream boundary wall **59** terminates at its uppermost end in contact with the web **53**. As shown in FIG. **2**, the terminal end of the upstream boundary wall **59** preferably has a curvilinear shape so that the terminus of the upstream boundary wall **59** is substantially tangential to the web **53**. The upstream boundary wall **59** also extends across the web transversely to the direction of the web motion.

A continuous interior wall which also extends across the web transversely to the direction of web motion, has discrete sections, which in combination with the upstream boundary wall **59**, the web **53** and the doctor element **55**, define the entrance plenum **61**, the coating chamber **51** and the exit plenum **57**, respectively. The first section **65** of the interior wall defines the downstream side of the entrance plenum **61**. The first interior wall section **65** is preferably substantially parallel to the upstream boundary wall **59**. The first interior wall section **65** preferably undergoes a curvilinear transition to a second interior wall section **67**. The second interior wall section **67** defines the bottom wall of the coating chamber **51**. The second interior wall section **67** proceeds to a third interior wall section **69**, preferably through a curvilinear transition section. The third interior wall section **69** defines the upstream side of the exit plenum **57**. Both the second interior wall section **67** and the third interior wall section **69** are preferably substantially parallel to the web and the doctor element **55**, respectively.

The upstream boundary wall **59** preferably terminates in a curvilinear section which is substantially parallel to the curvilinear transition section between first interior wall section **65** and second interior wall section **67**. The terminal end of the upstream boundary wall **59** is also preferably biased against the web **53** to prevent any coating material from being forced between the terminal end of the upstream boundary wall and the web **53** and to prevent air from entering into the coating material. The biasing may be accomplished through the use of any suitable means, such as by use of a spring or a flexible material.

As shown in FIG. **4**, a vacuum box **60** can be provided to further ensure that no air will become entrained in the coating material. When a vacuum is established in vacuum box **60**, the air pressure near the wetting line is reduced, thereby increasing the biasing effect on the boundary wall **59** and preventing any air inclusion at high speeds. The vacuum box **60** is defined by the web **53**, the upstream boundary wall and by walls **62** and **64** which extend across the web transversely to the direction of web motion. The outward ends of the vacuum box are capped and one of these ends is fitted to a vacuum source (not shown).

The walls forming the entrance plenum **61** may be vertical at a right angle to web **53**. The entrance plenum walls, however, are preferably upwardly inclined in a direction toward the downstream side. The angle A of inclination of the entrance plenum is preferably in the range of from about 10° to about 90°, most preferably about 45°. The walls forming the exit plenum **57** may also be vertical, but are preferably inclined downwardly in a direction toward or away from the upstream side of the exit plenum. The angle B of inclination of the exit plenum is preferably in the range of from about 20° to about 175°, most preferably about 63°.

As an example of construction of the coating device of the present invention, various spatial nodes have been designated in the various walls of the coating device with the numbers 1 through 16. These nodes are identified in the table below with spatial displacements from node **1** in terms of X and Y coordinates. Curve points a through i have also been designated with X and Y coordinates.

TABLE 1

Node #	X(mm)	Y(mm)	Curve Points	X(mm)	Y(mm)
1	0	0	a	32	32
2	3.536	−3.536	b	35	34
3	34	27	c	45	39
4	52	35	d	36	29
5	85	35	e	40	31.5
6	91	25	f	47	34
7	76.555	−4.7	g	88	34
8	81	−7	h	91	30
9	105	40	i	91.5	27
10	52	40			

TABLE 1-continued

Node #	X(mm)	Y(mm)	Curve Points	X(mm)	Y(mm)
11	30	30			
12	85	40			
13	98	26			
14	90	32			
15	43	33			
16	40	37			

In another embodiment of the invention, as shown in FIG. 3, a pre-coating chamber **71** is provided on the upstream side of the short-dwell coating device of the invention. The downstream boundary wall of the pre-coating chamber is formed from the upstream boundary wall **59** of the coating device **10**. A downstream wall **73** is spaced from web **53** by a distance of from about 1 to about 5 mm to provide an overflow baffle for coating material to prevent entrance of air in the manner used by prior art short-dwell coaters. The continuous interior wall **75** is used to define an entrance plenum **77**, the pre-coating chamber **71** and an exit plenum **79** in the same fashion and with the same parameters as previously described for the coating device.

The embodiment of the present invention utilizing a floating applicator wall and analysis thereof is set forth in detail in the discussion that follows.

The basic geometrical configuration a blade coating apparatus is shown in FIGS. **5A–5D**. The apparatus illustrated has stationary walls with the exception of the substrate which moves with a given speed. The coating fluid is pumped into a channel that leads the fluid flow to the moving web. The fluid flow considered is a steady, viscous free surface flow that is governed by the equations of momentum and mass conservation. Near the web the liquid accelerates through viscous drag while near the stationary wall it decelerates with a commensurate amount.

The system illustrated in FIG. **5A** and more particularly in FIGS. **5B** and **5C**, is an extension of the coating apparatus previously discussed. The difference, which is best appreciated in FIG. **5B**, is that the applicator's interior wall **80**, which comprises a floating belt or plate, represents a moving surface which is in a state of flotation typically either magnetically or via air pressure or lubricating fluid. The moving parts in the device are the web (or substrate) as depicted and the floating flexible belt or interior wall **80** which rotates in the indicated direction over the flotation device **82**, i.e., the shoe portion in the interior surface of the interior wall **80**. A thin air layer or lubricating fluid layer **84** is created between the floating flexible belt of the interior wall **80** and the flotation device **82**. On the other side of the interior wall **80** the coating fluid moves in the same direction as the interior wall **80**. Therefore, the interior wall **80** contacts the coating fluid at the outside surface and an air layer or lubricating liquid of any kind at the interior surface. The flotation device for levitation of the interior wall **80** can either be an air bar or thin air layer as already described, or a magnetic device or any other flotation means including lubricating fluids. The floating belt can either move primarily by the shear or drag from the coating fluid itself and/or an external force may be utilized to control the floating device and the floating belt.

FIG. **5C** illustrates that the flotation device **82** may be made to comprise an air bar wherein a high pressure air source is provided at **86** and narrow slots **88** are placed on the surface of the flotation device **82** such that air is forced through the slots **88** to keep the interior wall **80** in flotation over the thin air layer **84**. In such an air flotation system the flotation device **82** would typically be manufactured to have a porous surface.

Another mechanism for keeping the interior wall **80** in a flotation state is through magnetic force. In this case the belt should be metallic. By placing magnetic cells inside the flotation device **82** which would then comprise a shoe for housing the magnetic cells, the belt is kept in a flotation state as it rotates with the coating fluid. Since the flotation speed of the belt can be very high, the flotation system would prevent wear and tear of the belt and make the system practical for commercial applications.

The advantage of having the interior surface rotate with the liquid is that it prevents flow separation and recirculation inside the coating chamber, even at the low flow rates. As will be illustrated in Tables 2–6 following, attached flow is desired and avoids problems of eddies associated with flow separation. Without the rotating inner surface, the recirculating eddies can be removed if the flow rate through the channel is sufficiently large. It is very important in coating systems, however, to minimize the flow rate and reduce the demand on the pumping facilities. The flow of the coating fluid will be more stable and uniform in the above-described system. The following extensive computational flow provides visual results which verify the advantage of maintaining attached flow of the coating fluid and thus preventing flow separation resulting in eddies.

In sum, the flotation discussed thus far may be achieved in two ways: (1) fluid fixed in a flotation device or shoe in some form as to levitate the belt such that the fluid acts as a lubricant controlling friction and speed which may be altered by changing pressure, viscosity or temperature of the fluid in the fixed shoe of the flotation device **82**; alternatively (2) air between the floating service and the shoe may be used to keep the floating belt of the interior wall **80** suspended over the porous surface of the flotation device **82**.

In a fluid system, temperature sensitive viscous fluid would work well to control friction in the system. Such fluids might include silicon or glycerine where viscosity is proportional to temperature. Other fluids having molecules loosely oriented might also be advantageous where viscosity is proportional to an electromagnetic field which may be applied to alter viscosity. Electromagnetic fields may also be applied to the approach using air for flotation to that the extent that an electromagnetic field may be used to exert force on the surface of the floating belt **82** to control its flotation and/or rotation.

Materials which work well in the shoe portion of the flotation device **82** include stainless steel and aluminum; however, other metals or even rigid plastics may also work well. The flotation belt of the applicator's interior wall **80** may comprise any flexible material including fabric, plastics or thin metallic sheets such as copper or aluminum.

In operation, the floating belt may be brought up to speed through drag that is exerted upon it by the coating fluid. This will have the effect of pumping additional fluid through the coating system and thus it may be desirable to add friction to maintain a desirable maximum speed for the belt at some fraction of the web rate.

By using friction, the belt rate may be altered to be anything from about 10% to 90% of the web rate.

As the liquid moves toward the applicator's blade, a part of it exits through the narrow gap between the blade and the substrate. The flow entering the gap between the blade and the substrate has a nearly Poiseuille flow distribution. This velocity distribution influences the coating thickness and is determined by the operating parameters. In the wedge-like region formed by the blade and the substrate the pressure sharply increases and has a maximum value near the stagnation point located right under the tip of the blade. The rest of the flow, which could not exit at the gap, is forced to change direction and accelerated by a favorable pressure gradient it leaves the system via another channel along the blade face. Far downstream from the blade the free surface coating fluid moves with uniform velocity together with the substrate. Near the blade tip the shape of the free surface is determined by the ambient pressure and the surface tension effects. The deformation of the blade is considered by e.g. Pranckh (1989).

In the above described coating system the fluid is accelerated by viscous drag near the web and by favorable pressure gradient along the blade face. In other parts of the flow domain the flow decelerates and large recirculation zones, i.e. eddies can form as a result of flow instability. The hydrodynamic characteristics of this coating system have an effect on the quality of the manufactured product. Aidun et al. (1991), and Benson et al. (1992) investigate with the help of flow visualization the behavior of flow in a lid driven cavity and describe a possible mechanism to time periodic flow in such a system. The appearance of a time periodic flow can generate wet film thickness variations across the machine direction and/or longitudinal streaks. The following relates to how flow recirculation can be avoided in the high speed blade coating system through design and process optimization.

GOVERNING EQUATIONS AND BOUNDARY CONDITIONS

With reference to the boundary conditions represented in FIG. 5A, the equations governing the motion of a viscous incompressible fluid are the fluid momentum and the continuity equations. These are,

$$\rho\left(\frac{\partial u_i}{\partial t}+u_j\frac{\partial u_i}{\partial x_j}\right)=\frac{\partial \sigma_{ij}}{\partial x_j}+\rho f_i \tag{1}$$

and

$$\frac{\partial u_j}{\partial x_j}=0 \tag{2}$$

respectively where i,j=1,2 for two-dimensional flow. u_i or u is the velocity, ρ is the fluid density, σ_{ij} is the stress tensor. t denotes time and for steady flow calculations $\partial u_i/\partial t$ is equal to zero. ρf_i is the force due to gravity. In the present two-dimensional study $u_1=u$ and $u_2=v$ are the horizontal and vertical components of velocity, respectively.

The stress tensor can be written as

$$\sigma_{ij}=-p\delta_{ij}+\tau_{ij} \tag{3}$$

where ρ is the pressure, τ_{ij} is the deviatoric stress tensor and δ_{ij} is the Kronecker delta. In the present study the constitutive relation has the following form

$$\tau_{ij}=2\mu\epsilon_{ij} \tag{4}$$

In (4) μ denotes the dynamic viscosity and ϵ_{ij} stands for the strain tensor. ϵ_{ij} is defined by

$$\epsilon_{ij}=\frac{1}{2}\left(\frac{\partial u_i}{\partial x_j}\ \frac{\partial u_j}{\partial x_i}\right) \tag{5}$$

For Newtonian fluid μ is taken to be a constant. For non-Newtonian fluid μ is calculated with the help of the Carreau model;

$$\mu=\mu_\infty+(\mu_o-\mu_\infty)(1+K^2\epsilon_{ij}\epsilon_{ij})^{(n-1)/2} \tag{6}$$

In the above equation μ_o and μ_∞ are the zero and infinite shear rate viscosities, respectively, and K is the time constant. In the case of n=1 the Carreau model gives the Newtonian viscosity, i.e. $\mu=\mu_o$.

Equations (1) to (6) are non-dimensionalized with respect to a characteristic velocity U, and length L. U is chosen to be the maximum inflow velocity (U_ρ) if the applicator has stationary walls, otherwise it is chosen to be the applicator wall velocity (U_b). L is the width of the inlet channel, as illustrated in FIG. 5. The non-dimensional equations to be solved in the present study are

$$\frac{\partial u_i^*}{\partial t^*}+u_j^*\frac{\partial u_i^*}{\partial x_j^*}=\frac{\partial \sigma_{ij}^*}{\partial x_j^*}+f_i^* \tag{7}$$

$$\frac{\partial u_j^*}{\partial x_j^*}=0 \tag{8}$$

$$\sigma_{ij}^*=-p^*\delta_{ij}+{}^*_{ij} \tag{9}$$

$$\tau_{ij}^*=2\epsilon_{ij}^*\frac{\mu}{\rho UL}=2\epsilon_{ij}^*\frac{1}{Re} \tag{10}$$

$$\epsilon_{ij}^*=1/2\left(\frac{\partial u_i^*}{\partial x_j^*}+\frac{\partial u_j^*}{\partial x_i^*}\right) \tag{11}$$

$$\frac{1}{Re}=\frac{\mu_\infty}{\rho UL}+\left[\frac{\mu_o}{\rho UL}-\frac{\mu_\infty}{\rho UL}\right]\left[1+\left(\frac{KU}{L}\right)^2\epsilon_{ij}^*\epsilon_{ij}^*\right]^{(n-1)/2} \tag{12}$$

$$=\frac{1}{Re_\infty}+\left[\frac{1}{Re_o}-\frac{1}{Re_\infty}\right][1+K^2\epsilon_{ij}^*\epsilon_{ij}^*]^{(n-1)/2}$$

corresponding to equations (1) to (6), respectively. In the above equations the non-dimensional unknowns are

$$u_i^*=\frac{u_i}{U},\ p^*=\frac{p}{\rho U^2} \tag{13}$$

The non-dimensional independent variables are

$$x_i^*=\frac{x_i}{L},\ t^*=t\frac{U}{L} \tag{14}$$

The non-dimensional body force due to gravity is

$$f_i^* = f_i \frac{L}{U^2} \tag{15}$$

The important parameters in equations (7)–(12) are the Reynolds number Re ($=\mu UL/\rho$) and the non-dimensional time constant K* ($=KU/L$).

The boundary conditions for the coating system, illustrated on FIG. 5, are given by prescribing the inflow velocity distribution;

$$u_i = U_{in} \text{ on } \Gamma_1 \tag{16a}$$

the substrate velocity;
and the applicator wall velocity;

$$u_i = U_{wi} \text{ on } \Gamma_2 \tag{16b}$$

$$u_i = U_{bi} \text{ on } \Gamma_3 \tag{16c}$$

and

$$u_i = o \text{ on } \Gamma_4 \tag{16d}$$

At the outflow channel of the applicator the normal component of the stress vector is assumed to be vanishing, i.e.

$$\sigma_n = 0 \text{ on } \Gamma_5 \tag{17}$$

On the free surface of the coating liquid the kinematic boundary condition is given as

$$\frac{d\eta}{dt} = \frac{\partial \eta}{\partial t} + u_i \frac{\partial \eta}{\partial x_i} \tag{18}$$

$$\text{on } \eta = \eta(x_i, t)$$

where η denotes the height of the free surface above a horizontal reference plane and x_i is the horizontal coordinate of a point on the free surface. For two-dimensional steady free surface flow $\partial\eta/\partial x$ is equal to v/u in other words the fluid velocity at the gas-liquid interface is tangential to the free surface. η is a priori unknown.

The dynamic boundary condition on the free surface states that the stress is continuous across the gas-liquid interface

$$\sigma_n = 2\gamma H - p_a \tag{19a}$$

and

$$\text{on } \eta = \eta(x_i, t)$$

$$\sigma_t = 0 \tag{19b}$$

In (19a, 19b) σ_n, σ_t are respectively the normal and tangential components of stress at the interface, γ is the surface tension coefficient and H denotes the mean Gaussian curvature of the surface; p_a stands for the ambient pressure.

Far away enough from the blade the liquid film is assumed to move as a plug flow together with the substrate (i.e. $U_{film} = U_w$ and $\partial\eta/\partial x = 0$). The static contact line of the free surface is pinned at the sharp corner of the blade, thus its location is prescribed.

As with the governing equations, the boundary conditions are also non-dimensionalized. The non-dimensionalization of (19a) yields,

$$\sigma_n^* = 2H^* \frac{1}{ReCa} - p_a^* \tag{20}$$

$$\text{on } \eta^* = \eta(x_i, t)/L$$

where H* ($=HL$) is the dimensionless Gaussian mean curvature and Ca ($=\mu U/\gamma$) is the capillary number.

For brevity, the asterisks indicating non-dimensional values will be dropped in the Figures and the text from here on.

SOLUTION PROCEDURE

The governing equations detailed in the previous section together with the prescribed boundary conditions are to be solved. The solution involves two steps. In the first step, the governing equations are solved assuming a fixed shape for the free surface. In the second step, the limitation of fixed free surface is relaxed and the shape of the free surface is calculated. As the governing equations and boundary conditions are highly non-linear the solution is obtained via an iterative method.

The computation in the present study is based on the application of the FIDAP (1991) software package by Fluid Dynamics International, Inc., Evanston, Ill. The discretization of the domain in space is carried out with the finite element method employing nine node isoparametric quadrilaterals. Over these elements the velocity is approximated with a continuous elementwise biquadratic function while the pressure is represented by a discontinuous elementwise linear function. The obtained nonlinear algebraic system of equations is then solved with a strategy based on the application of successive substitutions and then the Newton-Raphson method.

Further description of the numerical solution can be found in the FIDAP (1991) Users Manual.

NUMERICAL EXPERIMENTS

A) Applicator with stationary walls

Tables 2 through 4 show the input parameters for the numerical runs. Table 2 presents the computational experiments carried out assuming Newtonian fluid, while Tables 3 and 4 consider the non-Newtonian behavior of the fluid. In the second column U_p, the maximum inflow velocity, is used as the characteristic velocity, i.e. U. It is assumed that the inflow velocity has a parabolic distribution. The characteristic length, $L = L_{in}$ the width of the inlet channel, can be found in the third column. Furthermore L_{gap} denotes the width of the gap between the blade and the substrate and q is the flowrate per unit width entering the applicator.

TABLE 2

INPUT PARAMETERS FOR THE SIMULATION OF NEWTONIAN FLOW
(S = Flow separation, A = Attached flow)

Run	U_p m/s	L_{in} m	L_{gap} m	q = $2U_pL_{in}/3$ l/s/m	U_w m/s	γ surf.tens kg/s^2	μ viscosity kg/(m s)	ρ density kg/m^3	Re = $U_pL_{in}\rho/\mu$ —	Ca = $\mu U_p/\gamma$ —	COMMENT ON THE RESULT
B1	1.00	0.0025	50 10^{-6}	1.667	1.0	0.05	1.00	1200	3.0	20.0	A

TABLE 2-continued

Run	U_p m/s	L_{in} m	L_{gap} m	$q = 2U_pL_{in}/3$ l/s/m	U_w m/s	γ surf.tens kg/s^2	μ viscosity kg/(m s)	ρ density kg/m^3	$Re = U_pL_{in}\rho/\mu$ —	$Ca = \mu U_p/\gamma$ —	COMMENT ON THE RESULT
				INPUT PARAMETERS FOR THE SIMULATION OF NEWTONIAN FLOW (S = Flow separation, A = Attached flow)							
B2	1.50	"	"	2.500	2.5	"	"	"	4.5	30.0	A
B3	2.00	"	"	3.333	5.0	"	"	"	6.0	40.0	S
B4	2.50	"	"	4.166	10.0	"	"	"	7.5	50.0	S
B5	3.00	"	"	5.000	20.0	"	"	"	9.0	60.0	S
B6	3.00	"	"	5.000	30.0	"	"	"	9.0	60.0	S
B7	3.00	"	"	5.000	40.0	"	"	"	9.0	60.0	S

TABLE 3

Run	U_p m/s	L_{in} m	L_{gap} m	$q = 2U_pL_{in}/3$ l/s/m	U_{web} m/s	γ surf.tens kg/s^2	μ_∞ viscosity kg/(m s)	μ_o viscosity kg/(m s)	K	ρ density kg/m^3	n	COMMENT ON THE RESULT
				INPUT PARAMETERS FOR THE SIMULATION OF NON-NEWTONIAN FLOW (Carreau model) (S = Flow separation, A = Attached flow)								
C1	3.0	0.0025	$50\ 10^{-6}$	5.00	20.0	0.05	0.05	1.00	0.01	1200	0.65	S
C2	"	"	"	"	30.0	"	"	"	"	"	"	S
C3	"	"	"	"	40.0	"	"	"	"	"	"	S
C11	5.0	0.0025	$50\ 10^{-6}$	8.33	20.0	0.05	0.05	1.00	0.01	1200	0.65	S
C12	8.0	"	"	13.33	"	"	"	"	"	"	"	S
C13	12.0	"	"	20.0	"	"	"	"	"	"	"	S
C14	16.0	"	"	26.67	"	"	"	"	"	"	"	A
C15	20.0	"	"	33.33	"	"	"	"	"	"	"	A

TABLE 4

Run	U_p m/s	L_{in} m	L_{gap} m	$q = 2U_pL_{in}/3$ l/s/m	U_{web} m/s	γ surf.tens kg/s^2	μ_∞ viscosity kg/(m s)	μ_o viscosity kg/(m s)	K	ρ density kg/m^3	n	COMMENT ON THE RESULT
				INPUT PARAMETERS FOR THE SIMULATION OF NON-NEWTONIAN FLOW (Carreau model) (S = Flow separation, A = Attached flow)								
N1	3.0	0.0025	$50\ 10^{-6}$	5.0	10.0	0.05	0.05	1.00	0.01	1200	0.65	A
N2	"	"	"	"	20.0	"	"	"	"	"	"	S
N3	"	"	"	"	30.0	"	"	"	"	"	"	S
N4	"	"	"	"	40.0	"	"	"	"	"	"	S

In the first numerical experiments, shown in Table 2, the web velocity (U_{web}) is gradually increased from 1 m/s to 40 m/s. At the same time the fluid discharge (q) is also increased. In FIGS. **6A–6G** respectively show the flow pattern corresponding to the runs **B1** to **B7**. A weak eddy appears at the second curve of the applicator wall in case of **B2**. This eddy gets stronger in the rest of the cases; **B3** to **B7**. Parallel to the evolution of this eddy a second elongated eddy becomes distinguishable and the separation point moves closer to the first curve of the applicator wall. In cases of **B6** and **B7** a third small eddy is also noticeable located close to the blade, right under the first strong eddy. The pressure distribution along the substrate is illustrated in FIGS. **7A–7G** for these cases. In the case of **B5**, for example, near the strong eddy the pressure exerted by the fluid on the substrate experiences a slight drop.

Under the blade the pressure distribution reaches its maximum then its minimum before the ambient pressure becomes dominant for the free surface flow. FIGS. **8A–8G** illustrate the pressure distribution along the blade. Right under the sharp edge of the blade the pressure reaches its maximum then it sharply drops and from there on slowly decreases. The pressure increases approximately forty times from case **B1** to **B7**.

Note that the Figures show $p^*U^2p^*U^2$ values for the pressure distributions. These pressure values are the differences between the local pressure and the ambient pressure.

The numerical experiments denoted by **C1, C2, C3** in Table 3 are investigating the same geometry as experiments **B1** to **B7** for the case of a non-Newtonian fluid. It is observed that the three eddies described earlier again appear and in fact they are stronger for the non-Newtonian case. This is the result of the reduction in viscosity due to large velocity gradients (see eq. (6) of the Carreau model). To see when the eddies disappear for the case of U_{web}=20 m/s the discharge q is gradually increased in the runs **C11** to **C15**. FIGS. **9A–9E** illustrates the change in the streamline pattern for these cases.

In the case of run **C13** there is only one weak eddy attached to the second curve of the applicator wall, in other words the discharge has to be increased from 5 l/s/m to approximately 20 l/s/m in order to suppress the eddies. It is also interesting to see how the pressure distribution along the substrate and the blade are modified with the increasing discharge as it is shown in FIGS. **10A–10E** and **11A–11E**, respectively. In case of **C11** the pressure gradually increases downstream along the substrate and reaches a local maximum. This local maximum is followed by a local minimum from where the pressure rises to its maximum right under the sharp edge of the blade. Near the static contact line of the free surface the pressure has its minimum then its value adjusts to the ambient pressure. With increasing fluid discharge in the cases of **C11** to **C15** the local minimum and maximum in the pressure in front of the blade disappear. The pressure maximum increases approximately 60% from **C11** to **C13**.

In order to suppress the eddies in the present coating system the experiments denoted by **N1** to **N4** in Table 4 employ a new geometry. In this new configuration the width of the channel under the substrate is reduced to the $\frac{2}{3}$ of the width in the previously described experiments. The streamlines of the flow field for these cases are shown in FIGS. **12A–12D**. It is seen that at $U_w=10$ m/s there is only one weak eddy near the second curve of the applicator wall. At $U_{web}=20$ m/s the second elongated weak eddy appears and at $U_{web}=30$ m/s all the above mentioned three eddies are observable in the system. The new geometry has an effect on the pressure distribution along the substrate as well, as presented in FIGS. **13A–13D**. For example, in case of **N4** there are two local minimums with a local maximum in between in front of the blade. On the blade, as shown in FIGS. **14A–14D**, there is also a local minimum in pressure which is the effect of the formation of the third eddy located close to that point. It is important to see that the new geometry alone does not succeed at removing the eddies from the system.

B) Applicator with a moving wall

For cases **N3** and **N4** a further change in the coating system is investigated. One of the applicator walls is designed to be a moving belt. Table 5 shows the cases as the belt speed U_b is gradually increased from 1 m/s to 5 m/s, while the discharge is kept constant, q=5 l/s/m. In the following cases U_b is chosen to be the characteristic velocity, U. The effect of the moving belt is that the second elongated eddy gets shorter and the separation point on the applicator wall moves downstream. FIGS. **15A–15E** illustrates the flow pattern for these cases. In case of **NB34** and **NB35** a fourth eddy becomes more distinguishable, as shown in FIGS. **15A–15E**. FIGS. **16A–16E** and **17A–17E** present the pressure distribution for theses cases along the substrate and the blade, respectively.

Two cases are investigated with respect to the web velocity. Column 5 in Table 6 shows how much liquid is pumped into the system while column 6 gives the total flowrate entering the applicator. As a result of the combined effects from pumping and the motion of the applicator wall the eddies vanish as shown in FIGS. **18A–18E** for $U_{web}=30$ m/s and in FIGS. **21A–21C** for $U_{web}=40$ m/s. FIGS. **19A–19E** and **20A–20E** illustrate the pressure distribution along the substrate and the blade, respectfully, for $U_{web}=30$ m/s. FIGS. **22A–22C** and **23A–23C** present these pressure distributions for $U_{web}=40$ m/s. In both cases the pressure increases approximately 10–20% while the eddies disappear from the system.

In the present blade coating system with increasing web/substrate speed the eddies in general become stronger. Three ways to suppress these eddies have been investigated. The first one corresponds to the gradual increase of fluid discharge per unit width entering the applicator. The second way employs a modified geometry which results in the downstream motion of the separation point. The last procedure is based on designing a moving applicator wall. In this case the combined effects from pumping, converging geometry and moving belt act to remove the eddies from the coating system.

While various aspects of the invention have been described with particularity, various modifications and alterations to the flotation coating device can be made without departing from the scope of the invention as defined in the appended claims.

APPENDIX

List of Symbols

u and u_i fluid velocity

u,v,w fluid velocity components

t time

TABLE 5

INPUT PARAMETERS FOR THE SIMULATION OF NON-NEWTONIAN FLOW (Carreau model)
(S = Flow separation)

Run	U_b m/s	L_{in} m	L_{gap} m	q l/s/m	U_{web} m/s	γ surf.tens kg/s^2	μ_∞ viscosity kg/(m s)	μ_o viscosity kg/(m s)	K	ρ density kg/m^3	n	COMMENT ON THE RESULT
NB31	1.0	0.0025	50 10^{-6}	5.00	30.0	0.05	0.05	1.00	0.01	1200	0.65	S
NB32	2.0	"	"	"	"	"	"	"	"	"	"	S
NB33	3.0	"	"	"	"	"	"	"	"	"	"	S
NB34	4.0	"	"	"	"	"	"	"	"	"	"	S
NB35	5.0	"	"	"	"	"	"	"	"	"	"	S
NB41	1.0	0.0025	50 10^{-6}	5.00	40.0	0.05	0.05	1.00	0.01	1200	0.65	S
NB42	3.0	"	"	"	"	"	"	"	"	"	"	S
NB43	5.0	"	"	"	"	"	"	"	"	"	"	S

TABLE 6

INPUT PARAMETERS FOR THE SIMULATION OF NON-NEWTONIAN FLOW (Carreau model)
(S = Flow separation, A = Attached flow)

Run	U_b m/s	L_{in} m	L_{gap} m	q pumped l/s/m	Σq l/s/m	U_{web} m/s	γ surf.tens kg/s^2	μ_∞ viscosity kg/m s)	μ_o viscosity kg/(m s)	K	ρ density kg/m^3	n	COMMENT ON THE RESULT
NB51	5.0	0.0025	50 10^{-6}	0.0	6.25	30.0	0.05	0.05	1.00	0.01	1200	0.65	S
NB52	5.0	"	"	2.5	8.75	"	"	"	"	"	"	"	S
NB53	5.0	"	"	5.0	11.25	"	"	"	"	"	"	"	S
NB54	10.0	"	"	5.0	17.50	"	"	"	"	"	"	"	S
NB55	15.0	"	"	5.0	17.50	"	"	"	"	"	"	"	A
NB61	5.0	0.0025	50 10^{-6}	5.0	11.25	40.0	0.05	0.05	1.00	0.01	1200	0.65	S
NB62	10.0	"	"	5.0	17.50	"	"	"	"	"	"	"	A
NB63	15.0	"	"	5.0	23.75	"	"	"	"	"	"	"	A

Table 6 gives the parameters for the numerical runs where the fluid discharge is allowed to increase via pumping and letting the moving belt drag liquid with it.

X_i Cartesian coordinate

ρ fluid density

fi component of the Gravitational acceleration
p pressure
P_a ambient pressure
ij stress tensor
n normal component of the stress vector
t tangential component of the stress vector
τ_{ij} deviatoric stress tensor
δ_{ij} Kronecker delta
ϵ_{ij} shear rate tensor
μ dynamic viscosity
μ_∞ infinite shear rate viscosity (Carreau model)
μ_o zero shear rate viscosity (Carreau model)
n power in the Carreau model
K time constant (Carreau model)
* superscript denoting non-dimensional quantity
U characteristic velocity scale
U_p maximum velocity at the inlet if the inflow has a parabolic velocity distribution
L characteristic length
Lin width of the inflow channel
Lgap width of the gap between the blade and the substrate
$Re=\rho UL/\mu$ Reynolds number
$Ca=\mu U/\gamma$ capillary number
U_{in} inflow velocity distribution
U_w substrate velocity
U_b applicator wall velocity boundary of the domain of computation
η height of the free surface
γ surface tension coefficient
H Gaussian mean curvature of the free surface
q flowrate per unit width entering the applicator

What is claimed is:

1. A flotation coating device for coating a traveling web of material comprising:

a coating composition application chamber having upstream and downstream side walls and an interior bottom wall, said upstream side wall and said interior bottom wall defining an entrance plenum therebetween for receiving a flowing coating composition and said downstream side wall and said interior bottom wall defining an exit plenum therebetween for discharge of said flowing coating composition;

means for guiding a traveling web of material over received flowing composition and said interior bottom wall thereunder; and

flotation means for levitating said interior bottom wall allowing said interior bottom wall to move in the same direction as the received flowing composition.

2. A flotation coating device for coating a traveling web of material comprising:

a coating composition application chamber comprising upstream and downstream side-walls and a loop of material having an outer surface positioned therebetween supporting a flowing coating composition, said upstream sidewall and said loop of material defining an entrance plenum for receiving said coating composition and said downstream side wall and said loop of material defining an exit plenum for discharge of said coating composition;

means for guiding a traveling web of material over the surface of said loop positioning received coating composition therebetween; and

means for suspending said loop in a flotation state providing substantially free movement of said loop about an axis substantially traverse to the direction of movement of the received coating composition allowing said outer surface of said loop to move in the same direction as the received and this charged coating composition.

3. A flotation coating device in accordance with claim **2** further comprising a shoe about which said loop is suspended.

4. A flotation coating device in accordance with claim **3** wherein the outer surface of said shoe is similar in form as said loop.

5. A flotation coating device in accordance with claim **3** wherein said suspending means comprise a fluid positioned between the inner surface of said loop and the outer surface of said shoe.

6. A flotation coating device in accordance with claim **5** wherein said fluid includes air.

7. A flotation coating device in accordance with claim **5** wherein said fluid includes a liquid.

8. A flotation coating device in accordance with claim **7** wherein said liquid has viscosity associated therewith, said viscosity causing friction between said loop and said liquid.

9. A flotation coating device in accordance with claim **8** wherein the viscosity of said liquid may be manipulated externally.

10. A flotation coating device in accordance with claim **9** wherein the viscosity of said liquid is manipulated by varying the temperature of said liquid.

11. A flotation coating device in accordance with claim **9** wherein the viscosity of said liquid is manipulated by changing the pressure on said liquid.

12. A flotation coating device in accordance with claim **9** wherein the viscosity of said liquid is manipulated by the presence or absence of an electromagnetic field.

13. A flotation coating device in accordance with claim **2** further comprising means for controlling the movement of said loop.

14. A flotation coating device in accordance with claim **2** wherein said free movement of said loop is proportional to and limited to some fraction of the movement of said flowing coating composition from the entrance plenum to the exit plenum.

15. A flotation coating device in accordance with claim **2** wherein said loop comprises a flexible material.

16. A flotation coating device in accordance with claim **15** wherein said flexible material comprises a thin metallic foil.

17. A flotation coating device in accordance with claim **3** wherein said shoe comprises a porous material.

18. A flotation coating device in accordance with claim **3** wherein said shoe comprises a metallic material.

* * * * *

UNITED STATES PATENT AND TRADEMARK OFFICE

CERTIFICATE OF CORRECTION

PATENT NO. : 5,354,376

DATED : October 11, 1994

INVENTOR(S) : Cyrus K. Aidun

It is certified that error appears in the above-indentified patent and that said Letters Patent is hereby corrected as shown below:

Column 16, line 11, change "this charged" to -- discharged --.

Signed and Sealed this

Twenty-fourth Day of January, 1995

Attest:

BRUCE LEHMAN

Attesting Officer

Commissioner of Patents and Trademarks

UNITED STATES PATENT AND TRADEMARK OFFICE

CERTIFICATE OF CORRECTION

PATENT NO. : 5,354,376

DATED : October 11, 1994

INVENTOR(S) : Cyrus K. Aidun

It is certified that error appears in the above-indentified patent and that said Letters Patent is hereby corrected as shown below:

Column 1, line 5, insert the following paragraph:

--This invention was made with Government support under National Science Foundation Grant Number CTS-9258667 awarded by the National Science Foundation. The Government has certain rights in this invention.--

Signed and Sealed this

Tenth Day of August, 1999

Attest:

Attesting Officer

Q. TODD DICKINSON

Acting Commissioner of Patents and Trademarks